5-2017

Role of Hormonal and Developmental Signaling in Plant-Cyst Nematode Interaction

Sarbottam Piya
University of Tennessee, Knoxville, spiya@utk.edu

To the Graduate Council:

I am submitting herewith a dissertation written by Sarbottam Piya entitled "Role of Hormonal and Developmental Signaling in Plant-Cyst Nematode Interaction." I have examined the final electronic copy of this dissertation for form and content and recommend that it be accepted in partial fulfillment of the requirements for the degree of Doctor of Philosophy, with a major in Plant, Soil and Environmental Sciences.

Tarek Hewezi, Major Professor

We have read this dissertation and recommend its acceptance:

Brad Binder, Feng Chen, Max Cheng, Neal Stewart

Accepted for the Council:

Dixie L. Thompson

Vice Provost and Dean of the Graduate School

(Original signatures are on file with official student records.)

Role of Hormonal and Developmental Signaling in Plant-Cyst Nematode Interaction

A Dissertation Presented for the

Doctor of Philosophy

Degree

The University of Tennessee, Knoxville

Sarbottam Piya

May 2017

DEDICATION

In the memory of

Sheela Shrestha

ACKNOWLEDGEMENTS

I would like to express my deep gratitude and sincere appreciation to Dr. Tarek Hewezi, for his guidance and constant encouragement during my research and dissertation preparation. I am also thankful to members of my advisory committee, Dr. Brad Binder, Dr. Feng Chen, Dr. Max Cheng and Dr. Neal Stewart for their constructive feedback and helpful suggestion

I would also like to thank the members of Dr. Hewezi's lab: John Hollis Rice, Yin Fang, Aditi Rambani, Valeria Lopes, Jin Yi, Jordan Skeen, Christina Kihm, Kelsey and Bahar for providing technical support. In addition, I would also like acknowledge Sandesh Shrestha, Tyra McCray, Arakadipta Bakshi, and Thomas Lane for their assistance.

I would like to express my deep gratitude and heartfelt respect to all my family members, and friends for their encouragement and, and constant support.

Most of all, I would like to thank my beloved wife Utsala, without whom, this dissertation would not have been possible.

ABSTRACT

Plant-parasitic cyst nematodes are one of the most destructive root parasites that cause severe yield losses in many crop plants. These obligate parasites induce a specialized multi-nucleate feeding site called syncytium. This study was conducted to explore the roles of phytohormones particularly auxin and ethylene, and miRNA-mediated crosstalk between development and defense responses in establishing the compatible interaction between Arabidopsis and *Heterodera schachtii*. Using yeast two-hybrid assay, a complete protein-protein interaction map between Auxin/indole-3-acetic acid (Aux/IAA) proteins and auxin response factors (ARFs) was generated. In addition, gene co-expression profiles of ARFs and Aux/IAAs were incorporated with protein-protein interaction data. Together, these analyses revealed the biological significance of the ARFs and Aux/IAA interactions in the differentiation and development of various plant tissues and organs, including *H. schachtii*–induced syncytium. Our analyses also provided evidence for the roles of ETHYLENE RESPONSE 1 and ETHYLENE INSENSITIVE 3/ETHYLENE INSENSITIVE LIKE 1 in regulating Arabidopsis responses to *H. schachtii* infection. The role of miRNAs in mediating the coordination between developmental signaling and defense response is emerging. Functional characterization of miR858 and its MYB83 target gene pointed into novel cooperative regulatory functions of this regulatory module in syncytium transcriptome reprogramming during cyst nematode parasitism of Arabidopsis. We discovered that miR858-mediated silencing of MYB83 is tightly regulated through a feedback loop that may ensure proper expression levels of more than a thousand of MYB83-regulated genes in the syncytium. Finally, the direct targets of Growth Regulating Factor 1 (GRF1) and 3, master regulators of syncytium differentiation, were identified. Specific and the shared cis-binding elements of GRF1 and GRF3 were identified, providing unprecedented understanding of the mechanism of their functional redundancy. GRF1 and GRF3 directly target genes associated with cell cycle regulation, cytoskeleton organization, phytohormone biosynthesis and signaling, and defense responses, key cellular processes that determine the outcomes of plant-cyst nematode interactions. The analysis also provided intriguing evidence for the involvement of GRF1/3 in mediating the trade-off between plant growth and stress signaling. Understanding the molecular mechanisms underlying the coordinated interactions between plant growth and defense signaling will open new avenues for enhancing plant growth and stress response simultaneously.

Keywords: *Heterodera schachtii*, auxin, ethylene, microRNA, RNA-seq, ChIP-seq

TABLE OF CONTENTS

LIST OF TABLES

LIST OF FIGURES

Chapter 1

General introduction and literature review

1. Introduction

Nematodes are one of the most diverse living organisms with more than 25,000 species and are ubiquitously distributed across various habitats that include different soils types, marine and fresh water (Hugot et al., 2001; Blaxter, 2003; Goverse and Smant, 2014). The large majority of these nematodes are beneficial or free living but there are few notorious species that parasitize human, animals and different crop plants causing devastating yield losses (Jasmer et al., 2003; Neher, 2010).

Plant-parasitic nematodes (PPNs) are among the most serious and widely spread plant pathogens with more than 4100 species (Decraemer and Hunt, 2006). It is estimated that every year these parasites cause agricultural loss worth $157 billion (Abad et al., 2008). Based on their feeding habits, PPNs can be grouped into three major groups: ectoparasites, semi-endoparasites and endoparasites. Ectoparasitic nematodes live outside of the plant and extract nutrients from the plant root using the stylet. The head of the semi-endoparasitic nematode penetrates the root where they establish the feeding site while the remaining body lies in the outer root surface. In the case of endoparasitic nematodes the whole body is infiltrated in the root. The endoparasitic nematodes can be further classified into migratory endoparasites and sedentary endoparasites. Migratory endoparasitic nematodes are mobile throughout their life-cycle and feed on the plant cells as they move, while the sedentary nematodes become immobile once they establish their feeding sites. Sedentary endoparasitic nematodes are the most devastating plant-parasitic nematodes and include two major groups of nematodes: cyst nematodes (*Heterodera* and *Globodera* spp) and root-knot nematodes (*Meloidogyne* spp). Extraction of nutrients and water by the nematodes from the root system reduces availability of water and nutrients, causing stunted plant growth with leaf chlorosis, wilting and ultimately lower yield and hence the loss caused by these nematodes are mistakenly attributed to abiotic stress conditions or unfavorable cultural practices.

Cyst nematodes belong to the family Heteroderidae and are characterized by the formation of feeding site termed syncytium from where they extract all essential nutrients during parasitism. The most economically important species in this family are soybean cyst nematode (*Heterodera glycines*) and potato cyst nematode (*Globodera rostochiensis* and *G. pallida*). The beet cyst

nematode (*Heterodera schachtii*) is another economically important species that infect sugar beet in addition to a significant number of vegetable crops. *H. schachtii* also infects Arabidopsis thaliana and the *H. schachtii* -Arabidopsis interaction has been established as a model system for studying the compatible interactions between host plants and cyst nematodes (Sijmons et al., 1991).

The life cycle of cyst nematode comprises of egg, four juvenile stages, and adult male or female stages. The first stage juvenile (J1) develops within the egg and under favorable conditions, the J1 undergoes molting to develop into second-stage juvenile (J2), which hatches out of the egg. After hatching, the migratory J2s migrate towards the root, penetrate the root mostly near the zone of elongation or near the lateral root initiation with the aid of the stylet and enter the epidermal cells. Once the J2s penetrate epidermal root cells, these juveniles migrate intracellularly via the cortex into the vascular cylinders. The J2 nematode selects a competent cell and injects its stylet into the cell to probe the cell. If the plant activates defense responses such as callose deposition or cytoplasm collapse, the J2 retracts its stylet and target another neighboring cell (Hewezi and Baum, 2017). The J2 may probe several cells before finding a competent cell that becomes initial feeding cell (IFC). Then, the J2 injects effector proteins via their stylet into the host cells to suppress defense responses and drive these cells into specific developmental cell fate. These effectors also target host proteins to reprogram various developmental pathways of the IFC and integrate few hundreds neighboring cells to form functional syncytium (Davis et al., 2008; Hewezi and Baum, 2013). Various cell-wall modifying enzymes such as expansins, cellulases and pecinases facilitate dissolution of neighboring cell wall and incorporation into the syncytium (Bohlmann and Sobczak, 2014). The syncytium undergoes considerable cellular changes that include repeated endoreduplication leading to polyploidy and multinucleate protoplast, vacuole fragmentation, thickened cell wall and increasing metabolic activity (Szakasits et al., 2009; Engler and Gheysen, 2013). After fourth molting, males become mobile and leave the root to mate with the female. Females spend all their life attached to the same syncytium sequestering the essential nutrients from the host plant. Females release a gelatinous matrix from the posterior end of the body where they deposit the eggs. When the females die, the body of the females hardens and becomes the cyst that protects the eggs for several years.

Successful establishment of a functional syncytium during cyst nematode infection is the main characteristic of the compatibility between host plants and cyst nematodes. Therefore, understanding syncytium ontogeny would help exploit the vulnerability of the feeding site to engineer plants resistant to cyst nematodes (Mitchum, 2016). However, the mechanisms by which cyst nematodes induce re-differentiation of normal root cells into syncytial cell type are not well-understood. This massive transformation of undifferentiated root cells into specialized syncytial cell-type involves a substantial change in gene expression (Szakasits et al., 2009; Cabrera et al., 2014). The functions of phytohormones and microRNAs (miRNAs) in regulating differentiation and developmental provided the foundation for their potential implication in syncytium initiation and development. In this context, recent experimental evidence pointed into key role of phytohormones and microRNAs in syncytium ontogeny (Hewezi et al., 2008; Gheysen and Mitchum, 2009; Hewezi et al., 2012; Cabrera et al., 2016).

2. Role of phytohormones in plant nematode interaction

Role of various phytohormones and their signaling during plant-pathogen interactions is well-studied. Particularly, defense-related plant hormones (salicylic acid, jasmonic acid and ethylene) act independently or in conjugation with other phytohormones during plant-pathogen interactions (Figure 1.1). Hormonal signaling associated with both defense and growth are often activated during pathogen attack resulting in their cross-talk to fine-tune the balance between plant growth and defense response (Kazan and Lyons, 2014). This is supported by various studies that demonstrate interfaces of phytohormones associated with plant growth and development (auxin, cytokinin, gibberellins and abscisic acid) with phytohormones associated with plant defense (Wang et al., 2007; Argueso et al., 2012; Song et al., 2014).

Pharmacological and nematode susceptibility assays of mutants defective in various hormone signaling pathways revealed the function of phytohormones such as auxin, ethylene, jasmonic acid, salicylic acid and cytokinin in mediating plant-nematode interactions (Wubben et al., 2001; Gheysen and Mitchum, 2009; Cabrera et al., 2014; Kammerhofer et al., 2015; Shanks et al., 2015). In addition, transcriptome analyses have revealed that genes associated with auxin and ethylene are predominant among the differentially expressed genes in the syncytium (Gheysen and Mitchum, 2009; Cabrera et al., 2014), providing further support for their involvement in syncytium formation and development.

2.1 Auxin

Auxin is a key player of the root development and is involved in various root development processes that includes cell division, and establishing and maintaining root meristem (De Smet et al., 2010). In general, auxin has been implicated for organ primordia initiation in plant (Tanaka et al., 2006). Similarly, auxin levels increase in the initial nematode feeding sites as early as one day post infection and after 2-5 days, auxin response shifts to the neighboring cells (Hutangura et al., 1999; Karczmarek et al., 2004) pointing to the role of auxin in nematode feeding site initiation and development. In addition, the auxin insensitive tomato mutant *diageotropica* (*dgt*) exhibit impaired feeding sites when infected with *Globodera rostochiensis* (Goverse et al., 2000) that provide evidence for the role of auxin in cyst nematode feeding site development.

Molecular and biochemical analyses revealed that the AUXIN RESPONSE FACTOR (ARF)-AUXIN/INDONE-3-ACETIC ACID (Aux/IAA) module regulates the auxin signaling pathway (Chapman and Estelle, 2009). In the presence of auxin, AUXIN F-BOX (AFB) proteins AFB1, AFB2 and AFB3 degrade AUX/IAAs via 26S proteasome and hence Aux/IAAs fail to repress ARF activity. ARFs bind to auxin response elements present in auxin responsive genes and regulate their expression. In contrast, in the absence of auxin, Aux/IAA proteins bind to ARFs and inhibit their function (Chapman and Estelle, 2009). Studies have shown that Aux/IAAs and ARFs play vital roles in plant-nematode interactions. GFP reporters driven by various ARF promoters showed expression of various ARFs at different stages of syncytium initiation and development. The expression patterns revealed distinct and overlapping functions of ARFs during syncytium initiation and formation (Hewezi et al., 2014). In addition, various auxin transcriptional repressor mutants *axr2/iaa7*, *slr/iaa14* and *iaa16* have shown altered susceptibility to *H. schachtii* (Goverse et al., 2000; Grunewald et al., 2008; Hewezi et al., 2015). Hewezi et al. (2015) reported that the 10A07 effector from *H. schachtii* targets IAA16 to interfere with auxin signaling during nematode parasitism of Arabidopsis. IAA16 overexpression lines demonstrated reduced expression of ARF6-8 and 19 under non-infected conditions, while the expression of these ARFs were upregulated under *H. schachtii* infected conditions, suggesting that in response to *H. schachtii* infection IAA16 releases these ARFs which in turn regulate the expression of auxin responsive genes that are required for syncytium initiation and formation. In addition, severak auxin responsive genes have been identified as differentially expressed in response to cyst nematode

infection. For instance, auxin repressed genes such as AUXIN DOWNREGULATED 6 (ADR6), ADR11 and ADR12 are downregulated in the early stage of H. glycine infection (Hermsmeier et al., 1998). Furthermore, several cell wall degrading genes that change the expression in the syncytium contain auxin response elements in their promoters. For example, endo-β-1,4-glucanase genes such as *NtCel7* from tobacco and its homolog *SlCel7* from potato, and *AtCel2* from Arabidopsis contain auxin response element in their promoters and are strongly induced in the syncytium (Wang et al., 2007; Karczmarek et al., 2008; Wieczorek et al., 2008). These results point to a role of auxin signaling in cyst nematode-induced syncytia. Considering the facts that Aux/IAAs bind to ARFs and repress the function of ARFs, and several members of these transcription factor families can modulate plant-nematode interactions, constructing a protein-protein interaction map of the ARFs and Aux/IAAs will elucidate the possible interlinks between ARFs and Aux/IAAs in mediating auxin signaling for syncytium development during plant-nematode interaction.

2.2 Ethylene

Ethylene is a gaseous plant hormone that regulates a wide range of plant metabolic, physiological, and developmental processes including defense against various pathogens (Broekaert et al., 2006; Schaller, 2012). The role of ethylene in syncytium development was implied through the finding that the mutations in Arabidopsis ethylene-overproducing genes such as *ETHYLENE OVERPRODUCER 1* (*ETO1*), *ETO2* and *ETO3* are more susceptible to the cyst nematode (Goverse et al., 2000; Wubben et al., 2001). In addition, *eto2* also exhibited enhanced cell wall breakdown during cyst nematode infection, suggesting that ethylene is a positive regulator of Arabidopsis susceptibility to *H. schachtii* (Goverse et al., 2000; Wubben et al., 2001). However, the role of ethylene in plant-nematode interaction is complex and contradictory (Kyndt et al., 2013). Several ethylene insensitive mutants such as *ethylene response 1-1* (*etr1-1*), *ethylene insensitive 2-1* (*ein2-1*), *ein3-1* and *ethylene insensitive root 1-1* (*eir1-1*) were less susceptible to *H. schachtii*, implying a role of ethylene in the regulation of Arabidopsis susceptibility to *H. schachtii* (Wubben et al., 2001; Wubben et al., 2004). Wubben et al. (2001) also reported that increase attractiveness of *H. schachtii* towards the root exudates of ethylene over-producing mutant *eto3* could be attributed to the observed susceptibility of *eto3* mutant to *H. schachtii*. In contrast, the expression of ethylene responsive ethylene binding protein family

genes- *RAP2.3* and *RAP2.6* that enhance plant basal defense responses, were downregulated in the beet cyst nematode-induced syncytium (Hermsmeier et al., 2000; Ali et al., 2013). Likewise, expression of soybean ethylene responsive element–binding protein gene, *EREBP1* was also downregulated in cyst nematode infected susceptible soybean roots and upregulated in resistant plants suggesting that *EREBP1* is a positive regulator of ethylene-mediated defense response (Mazarei et al., 2002; Mazarei et al., 2007). A plausible explanation for this discrepancy of ethylene function in plant-cyst nematode interactions is that the role of ethylene is dependent on the stage of parasitism. At early stage, ethylene plays positive role in attracting nematode towards the roots, but during sedentary parasitism it seems to have a negative impact on nematode development (Kammerhofer et al., 2015).

Studies have shown cross-talk of ethylene signaling with other stress hormones namely salicylic acid and jasmonic acid. Plants with reduced expression of *EIN3* and *EIL1* showed enhanced pathogen-associated molecular patterns (PAMP) response and reduced susceptibility to *Pseudomonas syringae* (Chen et al., 2009). Further analysis showed that these two ethylene signaling transcription factors directly regulate the expression of *SALICYLIC ACID INDUCTION DEFICEINT 2* (*SID2*) that encode isochorismate synthase. The fact that ISOCHORISMATE SYNTHASE is required for salicylic acid biosynthesis indicates that *EIN3/EIL1* directly target *SID2* to repress PAMP response (Chen et al., 2009). In contrast to the antagonistic interaction between ethylene signaling and salicylic acid biosynthesis, ethylene signaling has synergistic function with jasmonic acid signaling pathway. Zhu et al. (2011) reported that plants lacking *EIN3* and *EIL1* have reduced resistance to *Botrytis cinerea*. They observed that the expression of JA-induced pathogenesis related genes, *PLANT DEFENSIN 1.2* (*PDF1.2*), *ETHYLENE RESPONSE FACTOR 1* (*ERF1*) *and OCTADECANOID-RESPONSIVE ARABIDOPSIS 59* (*ORA59*), was absent in the *ein3/eil1* double mutant in presence of JA, a finding that explains the susceptibility of this mutant to *Botrytis cinerea.*

3. Small RNA

Small RNAs (sRNAs) are non-coding short (21 to 24) nucleotides that play important regulatory roles by controlling the transcriptional activity of their target genes containing complementary sequences. In plants, sRNAs have emerged as an important player that regulate different biological processes such as plant morphogenesis and development, nutrient uptake and

metabolism, hormone signaling, abiotic and biotic stress responses (Weiberg et al., 2014). Based on the origin, sRNAs can be divided into microRNAs (miRNAs), hairpin derived siRNAs (hp siRNAs), natural antisense siRNAs (natsiRNAs), secondary siRNAs, and heterochromatic siRNAs (hetsiRNAs). Despite the difference in the origin, these sRNAs share the following four characteristics; 1) production of double stranded RNA, 2) cleavage of the dsRNA into 21-24 nucleotides, 3) 3'-O-methylation of sRNA, and 4) loading into the RNA-induced silencing complex (RISC) that facilitates association with the targeted genes having complementary sequence (Borges and Martienssen, 2015).

MiRNAs play important regulatory roles by controlling the activity of their target genes containing complementary sequences at post-transcriptional level (Bartel, 2004; Voinnet, 2009). In plants, miRNAs have been identified as one of the vital regulators of plant gene expression. A growing body of experimental evidence demonstrated the involvement of miRNAs in plant developmental processes such as vascular tissue development, root initiation and development, flower development, and seed development as well as plant defense against various pathogens [reviewed in (Kidner and Martienssen, 2005; Chen, 2009; Chuck et al., 2009; Weiberg et al., 2014)].

The biogenesis of miRNA is presented in Figure 1.2. The primary transcripts of miRNAs are encoded from endogenous genes by RNA polymerase II into single stranded molecules that fold into hairpin-like structures. The stem-loop precursor molecules are cleaved by DICER-like 1 (DCL1) and generate miRNA-miRNA* duplex (Voinnet, 2009; Axtell et al., 2011). Upon processing by DCL1, 3′ end of miRNA-miRNA* duplex is 2′-O- methylated by methyltransferase HUA ENHANCER 1 (HEN1) that prevents decay of miRNAs (Yu et al., 2005). This duplex is transported to the cytoplasm where the duplex separates and the passenger miRNA (miRNA*) is degraded. Guide miRNAs (mature miRNAs) are loaded into ARGONAUTE1 (AGO1)-containing RNA-induced silencing complex (RISC). Mature miRNAs in RISC serve as guide to bind the target mRNAs, while the AGO1 protein functions as effector that recruits factors for post-transcriptional gene silencing (PTGS) by endonucleolytic cleavage or translational repression (Huntzinger and Izaurralde, 2011).

Several Arabidopsis mutants such as *dcl1-9, ago1-25* and *ago1-27* with impaired miRNA activity showed compromised basal defense response, implicating miRNAs in plant immunity (Navarro et al., 2008; Li et al., 2010). The activity of miR393 in plant pattern-triggered immunity (PTI) against *Pseudomonas syringae* by regulating auxin-signaling pathway was the first report showing the function of miRNAs in modulating plant immunity (Navarro et al., 2006). Thereafter, an increasing number of studies have reported the role of various miRNAs in plant-pathogen interactions. Recent advancement in the field of deep sequencing and bioinformatics has allowed genome wide identification of differentially expressed miRNAs in response to pathogen infection (Zhang et al., 2011; Li et al., 2014). Despite the large number of miRNAs that are regulated in response to pathogen infection, a limited number of these miRNAs were functionally characterized. Functional characterization of some miRNAs has shown that these miRNAs may positively or negatively regulate plant susceptibility to a large array of pathogens including bacteria, fungi, viruses, and nematodes. These functional characterization studies of various miRNAs and their target have shown that miRNAs regulate genes associated with various PTI responses in plants such as callose deposition, ROS production under pathogen attack (Sunkar et al., 2006; Li et al., 2010). In addition, several recent studies have also shown that miRNA guide cleavage of resistance genes in different plant species, demonstrating the function of miRNAs in plant immunity (Li et al., 2012; Shivaprasad et al., 2012; Boccara et al., 2014).

Several miRNAs that show significant change in their expression in response to infection by plant-parasitic nematodes infection have been identified (Hewezi et al., 2008; Li et al., 2012; Zhang et al., 2016), suggesting a functional role of miRNAs in plant-nematode interactions. In the last few years, the functions of few plant miRNAs in regulating various aspects of plant-nematode interactions have been established (Hewezi and Baum, 2012; Hewezi et al., 2012; Zhao et al., 2015; Cabrera et al., 2016; Hewezi et al., 2016). Arabidopsis miR396-mediated regulation of GROWTH REGULATING FACTOR 1 (GRF1) and GRF3 was found to control the differentiation and development of the syncytia during *H. schachtii* infection of Arabidopsis (Hewezi et al., 2012). It was also reported that this module regulates the expression of a large number of genes that are differentially expressed in the syncytium mostly associated with hormone signaling, defense response and disease resistance (Hewezi and Baum, 2012; Hewezi et al., 2012; Liu et al., 2014). In another study, miR319/TEOSINTE

BRANCHED1/CYCLOIDEA/PRO-LIFERATING CELL FACTOR 4 (TCP4) regulatory module was found to regulate plant susceptibility to the root-knot nematode *Meloidogyne incognita* by regulating jasmonic acid level in tomato (Zhao et al., 2015). Another recent study suggested a regulatory function of Arabidopsis miR390a/TAS3 system in *Meloidogyne javanica*–triggered gall formation, presumably by regulating auxin response factors (Cabrera et al., 2016). More recently, Hewezi et al. (2016) reported a key functional role of the miR827-*NITROGEN LIMITATION ADAPTATION (NLA*) regulatory system in *H. schachtii*–induced syncytium. It was demonstrated that *H. schachtii*–activated miR827 inhibits plant immune response, thereby facilitating the initiation and development of nematode feeding sites. Collectively, these results strongly support a vital regulatory function of miRNAs in establishing the interaction between host plants and plant parasitic nematodes.

4. Role of GRF1/3 in plant-nematode interaction

In Arabidopsis, miR396 is encoded by two loci, miR396a and miR396b, and post-transcriptionally regulates the expression of seven of the nine GRF genes except GRF5 and GRF6 (Jones-Rhoades and Bartel, 2004). GRFs regulate various aspects of plant growth and development, including leaf, stem and root development, floral development, and reproductive competence as well as defense responses (van der Knaap et al., 2000; Kim et al., 2003; Hewezi et al., 2012; Kim et al., 2012; Bao et al., 2014; Liu et al., 2014; Omidbakhshfard et al., 2015). Hewezi et al. (2012) showed that miR396 and its target genes GRF1 and GRF3 play vital role in the differentiation of cyst nematode-induced feeding sites and ultimately affect plant susceptibility to the beet cyst nematode. During the early stage of nematode infection, the expression of miR396 was reduced with concomitant increases in GRF1 and GRF3 expression that facilitate the initiation and formation of the feeding sites. Once the syncytium formation stage is completed, the expression of miR396 was increased leading to a significant reduction in the expression of GRF1 and GRF3, defining the beginning of syncytium maintenance stage. It was also reported that transgenic lines overexpressing miR396-resistant version of GRF1or GRF3 were less susceptible to beet cyst nematode, a phenotype that was associated with reduced syncytium size. Collectively, these results point to the role of miR396-GRF1/3 module in beet cyst nematode parasitism. Furthermore, this study also revealed that miR396-GRF1/3 system regulates 44% of the 7225 genes that are differentially expressed in the syncytium (Szakasits et

al., 2009), suggesting pivotal roles of this regulatory system in the reprogramming of root cells into syncytium cell-type. mRNA expression profiling using microarray, genes associated with developmental pathways and defense signaling were significantly enriched among the differentially expressed genes, suggesting a role GRF1/3 in mediating the trade-off between growth and defense signaling pathways (Hewezi et al., 2012; Liu et al., 2014). However, the mechanisms through which GRF transcription factors control the growth/defense trade-off remain to be determined.

Several recent studies have combined ChIP-seq and RNA-seq approaches to identify gene that are directly regulated by the transcription factors. These analyses provided novel insights into the regulatory mechanisms underlying plant immunity (Liu et al., 2015; Sun et al., 2015; Birkenbihl et al., 2016). For example, Liu et al. (2015) reported that WRKY33 directly regulates the ABA biosynthesis genes NCED3 and NCED5 to negatively regulate ABA biosynthesis, which in turn influences plant immunity. In another study, identification of genome-wide HOMOLOG OF BEE2 INTERACTING WITH IBH 1 (HBI1) binding sites along with transcriptome analysis revealed that HBI1 is the primary node that mediates the trade-off between plant growth and immunity in Arabidopsis (Fan et al., 2014). It was reported that HBI1 is a negative regulator of plant immunity and in response to plant pathogen, the expression of this gene is inhibited leading to increased plant immunity and reduced plant growth (Fan et al., 2014). Since GRF1 and GRF3 regulate the expression of exceptionally large number of genes that are differentially expressed in the syncytium, identification of the genes that are directly regulated by these transcription factors would allow identification of gene expression networks and pathways that control Arabidopsis-cyst nematode interactions. In addition, considering the role of GRF1/3 in plant growth and development as well as defense signaling, identifying direct targets of GRF1and 3 will provide a mechanistic understanding of the growth/defense trade-off; a phenomenon that is poorly understood. Understanding the molecular principals of growth/defense trade-off is expected to open avenues to increase plant growth and defense simultaneously.

5. Dissertation organization

This dissertation is organized into five chapters based on the objective of the project.

i) General introduction on cyst nematode and literature review on current understanding of the role of phytohormones particularly auxin and ethylene, and miRNA in plant-nematode interactions.

ii) Generate protein-protein interaction map of all auxin response factor (ARFs) and auxin/indole-3-acetic acid (Aux/IAAs) and integrate the global gene co-expression network with the protein interaction map to identify tissue-specificity for the various ARF-Aux/IAAs interacting pairs.

iii) Understand the functional roles of various components ethylene signaling pathways in establishing the compatible interactions between *H. schachtii* and Arabidopsis.

iv) Understand the role of miR858-MYB83 module in *H. schachtii*-Arabidopsis interactions.

v) Identify genome-wide direct targets of GRF1 and GRF3 and explore the functional role of the regulatory pathway in plant development and defense**.**

References

Abad P, Gouzy J, Aury JM, Castagnone-Sereno P, Danchin EGJ, Deleury E, Perfus-Barbeoch L, Anthouard V, Artiguenave F, Blok VC, Caillaud MC, Coutinho PM, Dasilva C, De Luca F, Deau F, Esquibet M, Flutre T, Goldstone JV, Hamamouch N, Hewezi T, Jaillon O, Jubin C, Leonetti P, Magliano M, Maier TR, Markov GV, McVeigh P, Pesole G, Poulain J, Robinson-Rechavi M, Sallet E, Segurens B, Steinbach D, Tytgat T, Ugarte E, van Ghelder C, Veronico P, Baum TJ, Blaxter M, Bleve-Zacheo T, Davis EL, Ewbank JJ, Favery B, Grenier E, Henrissat B, Jones JT, Laudet V, Maule AG, Quesneville H, Rosso MN, Schiex T, Smant G, Weissenbach J, Wincker P (2008) Genome sequence of the metazoan plant-parasitic nematode *Meloidogyne incognita*. Nat Biotechnol **26:** 909-915

Ali MA, Abbas A, Kreil DP, Bohlmann H (2013) Overexpression of the transcription factor RAP2.6 leads to enhanced callose deposition in syncytia and enhanced resistance against the beet cyst nematode *Heterodera schachtii* in Arabidopsis roots. BMC Plant Biol **13**

Argueso CT, Ferreira FJ, Epple P, To JP, Hutchison CE, Schaller GE, Dangl JL, Kieber JJ (2012) Two-component elements mediate interactions between cytokinin and salicylic acid in plant immunity. PLoS Genet **8:** e1002448

Axtell MJ, Westholm JO, Lai EC (2011) Vive la difference: biogenesis and evolution of microRNAs in plants and animals. Genome Biol **12:** 221

Bao M, Bian H, Zha Y, Li F, Sun Y, Bai B, Chen Z, Wang J, Zhu M, Han N (2014) miR396a-mediated basic helix-loop-helix transcription factor bHLH74 repression acts as a regulator for root growth in Arabidopsis seedlings. Plant Cell Physiol **55:** 1343-1353

Bartel DP (2004) MicroRNAs: genomics, biogenesis, mechanism, and function. Cell **116:** 281-297

Birkenbihl RP, Kracher B, Somssich IE (2016) Induced genome-wide binding of three Arabidopsis WRKY transcription factors during early MAMP-triggered immunity. Plant Cell **doi: http://dx.doi.org/10.1105/tpc.16.00681**

Blaxter ML (2003) Nematoda: genes, genomes and the evolution of parasitism. Adv Parasit **54:** 101-195

Bohlmann H, Sobczak M (2014) The plant cell wall in the feeding sites of cyst nematodes. Front Plant Sci **5:** 89

Borges F, Martienssen RA (2015) The expanding world of small RNAs in plants. Nat Rev Mol Cell Biol **16:** 727–741

Broekaert WF, Delaure SL, De Bolle MF, Cammue BP (2006) The role of ethylene in host-pathogen interactions. Annu Rev Phytopathol **44:** 393-416

Cabrera J, Barcala M, Fenoll C, Escobar C (2014) Transcriptomic signatures of transfer cells in early developing nematode feeding cells of Arabidopsis focused on auxin and ethylene signaling. Front Plant Sci **5:** 107

Cabrera J, Barcala M, Garcia A, Rio-Machin A, Medina C, Jaubert-Possamai S, Favery B, Maizel A, Ruiz-Ferrer V, Fenoll C, Escobar C (2016) Differentially expressed small RNAs in Arabidopsis galls formed by *Meloidogyne javanica*: a functional role for miR390 and its TAS3-derived tasiRNAs. New Phytol **209:** 1625-1640

Chapman EJ, Estelle M (2009) Mechanism of auxin-regulated gene expression in plants. Annu Rev Genet **43:** 265-285

Chen HM, Xue L, Chintamanani S, Germain H, Lin HQ, Cui HT, Cai R, Zuo JR, Tang XY, Li X, Guo HW, Zhou JM (2009) ETHYLENE INSENSITIVE3 and ETHYLENE INSENSITIVE3-LIKE1 repress SALICYLIC ACID INDUCTION DEFICIENT2 expression to negatively regulate plant innate immunity in Arabidopsis. Plant Cell **21:** 2527-2540

Chen XM (2009) Small RNAs and their roles in plant development. Annu Rev Cell Dev Biol **25:** 21-44

Chuck G, Candela H, Hake S (2009) Big impacts by small RNAs in plant development. Curr Opin Plant Biol **12:** 81-86

Davis EL, Hussey RS, Mitchum MG, Baum TJ (2008) Parasitism proteins in nematode-plant interactions. Curr Opin Plant Biol **11:** 360-366

De Smet I, Lau S, Voss U, Vanneste S, Benjamins R, Rademacher EH, Schlereth A, De Rybel B, Vassileva V, Grunewald W, Naudts M, Levesque MP, Ehrismann JS, Inze D, Luschnig C, Benfey PN, Weijers D, Van Montagu MC, Bennett MJ, Jurgens G, Beeckman T (2010) Bimodular auxin response controls organogenesis in Arabidopsis. Proc Natl Acad Sci USA **107:** 2705-2710

Decraemer W, Hunt DJ (2006) Structure and classification. *In* R Perry, M Moens, eds, Plant nematology. CABI, Wallingford, UK ; Cambridge, MA, USA, pp 3-32

Engler JD, Gheysen G (2013) Nematode-induced endoreduplication in plant host cells: why and how? Mol Plant Microbe Interact **26:** 17-24

Fan M, Bai MY, Kim JG, Wang TN, Oh E, Chen L, Park CH, Son SH, Kim SK, Mudgett MB, Wang ZY (2014) The bHLH transcription factor HBI1 mediates the trade-off between growth and pathogen-associated molecular pattern-triggered immunity in Arabidopsis. Plant Cell **26:** 828-841

Gheysen G, Mitchum MG (2009) Molecular insights in the susceptible plant response to nematode infection. *In* RH Berg, CG Taylor, eds, Cell Biology of Plant Nematode Parasitism. Springer, Verlag Berlin Heidelberg

Goverse A, Overmars H, Engelbertink J, Schots A, Bakker J, Helder J (2000) Both induction and morphogenesis of cyst nematode feeding cells are mediated by auxin. Mol Plant Microbe Interact **13:** 1121-1129

Goverse A, Smant G (2014) The activation and suppression of plant innate immunity by parasitic nematodes. Annu Rev Phytopathol **52:** 243-265

Grunewald W, Karimi M, Wieczorek K, Van de Cappelle E, Wischnitzki E, Grundler F, Inze D, Beeckman T, Gheysen G (2008) A role for AtWRKY23 in feeding site establishment of plant-parasitic nematodes. Plant Physiol **148:** 358-368

Hermsmeier D, Hart JK, Byzova M, Rodermel SR, Baum TJ (2000) Changes in mRNA abundance within *Heterodera schachtii*-infected roots of *Arabidopsis thaliana*. Mol Plant Microbe Interact **13:** 309-315

Hermsmeier D, Mazarei M, Baum TJ (1998) Differential display analysis of the early compatible interaction between soybean and the soybean cyst nematode. Mol Plant Microbe Interact **11:** 1258-1263

Hewezi T, Baum T (2017) Communication of sedentary plant-parasitic nematodes with their host plants. *In* Advances in Botanical Research, Vol http://dx.doi.org/10.1016/bs.abr.2016.11.004. Elsevier

Hewezi T, Baum TJ (2012) Complex feedback regulations govern the expression of miRNA396 and its GRF target genes. Plant Signal Behav **7:** 749-751

Hewezi T, Baum TJ (2013) Manipulation of plant cells by cyst and root-knot nematode effectors. Mol Plant Microbe Interact **26:** 9-16

Hewezi T, Howe P, Maier TR, Baum TJ (2008) Arabidopsis small RNAs and their targets during cyst nematode parasitism. Mol Plant Microbe Interact **21:** 1622-1634

Hewezi T, Juvale PS, Piya S, Maier TR, Rambani A, Rice JH, Mitchum MG, Davis EL, Hussey RS, Baum TJ (2015) The cyst nematode effector protein 10A07 targets and recruits host posttranslational machinery to mediate its nuclear trafficking and to promote parasitism in Arabidopsis. Plant Cell **27:** 891-907

Hewezi T, Maier TR, Nettleton D, Baum TJ (2012) The Arabidopsis microRNA396-GRF1/GRF3 regulatory module acts as a developmental regulator in the reprogramming of root cells during cyst nematode infection. Plant Physiol **159:** 321-335

Hewezi T, Piya S, Qi M, Balasubramaniam M, Rice JH, Baum TJ (2016) Arabidopsis miR827 mediates post-transcriptional gene silencing of its ubiquitin E3 ligase target gene in the syncytium of the cyst nematode *Heterodera schachtii* to enhance susceptibility. Plant J **88:** 179-192

Hewezi T, Piya S, Richard G, Rice JH (2014) Spatial and temporal expression patterns of auxin response transcription factors in the syncytium induced by the beet cyst nematode *Heterodera schachtii* in Arabidopsis. Mol Plant Pathol **15:** 730-736

Hugot JP, Baujard P, Morand S (2001) Biodiversity in helminths and nematodes as a field of study: an overview. Nematology **3:** 199-208

Huntzinger E, Izaurralde E (2011) Gene silencing by microRNAs: contributions of translational repression and mRNA decay. Nat Rev Genet **12:** 99-110

Hutangura P, Mathesius U, Jones MG, Rolfe BG (1999) Auxin induction is a trigger for root gall formation caused by root-knot nematodes in white clover and is associated with the activation of the flavonoid pathway. Funct Plant Biol **26:** 221-231

Jasmer DP, Goverse A, Smart G (2003) Parasitic nematode interactions with mammals and plants. Annu Rev Phytopathol **41:** 245-270

Jones-Rhoades MW, Bartel DP (2004) Computational identification of plant microRNAs and their targets, including a stress-induced miRNA. Mol Cell **14:** 787-799

Kammerhofer N, Radakovic Z, Regis JM, Dobrev P, Vankova R, Grundler FM, Siddique S, Hofmann J, Wieczorek K (2015) Role of stress-related hormones in plant defence during early infection of the cyst nematode *Heterodera schachtii* in Arabidopsis. New Phytol **207:** 778-789

Karczmarek A, Fudali S, Lichocka M, Sobczak M, Kurek W, Janakowski S, Roosien J, Golinowski W, Bakker J, Goverse A, Helder J (2008) Expression of two functionally distinct plant endo-beta-1,4-glucanases is essential for the compatible interaction between potato cyst nematode and its hosts. Mol Plant Microbe Interact **21:** 791-798

Karczmarek A, Overmars H, Helder J, Goverse A (2004) Feeding cell development by cyst and root-knot nematodes involves a similar early, local and transient activation of a specific auxin-inducible promoter element. Mol Plant Pathol **5:** 343-346

Kazan K, Lyons R (2014) Intervention of phytohormone pathways by pathogen effectors. Plant Cell **26:** 2285-2309

Kidner CA, Martienssen RA (2005) The developmental role of microRNA in plants. Curr Opin Plant Biol **8:** 38-44

Kim J-S, Mizoi J, Kidokoro S, Maruyama K, Nakajima J, Nakashima K, Mitsuda N, Takiguchi Y, Ohme-Takagi M, Kondou Y (2012) Arabidopsis GROWTH-REGULATING FACTOR7 functions as a transcriptional repressor of abscisic acid–and osmotic stress–responsive genes, including DREB2A. Plant Cell **24:** 3393-3405

Kim JH, Choi D, Kende H (2003) The AtGRF family of putative transcription factors is involved in leaf and cotyledon growth in Arabidopsis. Plant J **36:** 94-104

Kyndt T, Vieira P, Gheysen G, de Almeida-Engler J (2013) Nematode feeding sites: unique organs in plant roots. Planta **238:** 807-818

Li XY, Wang X, Zhang SP, Liu DW, Duan YX, Dong W (2012) Identification of soybean microRNAs involved in soybean cyst nematode infection by deep sequencing. Plos One **7:** e39650

Li Y, Lu YG, Shi Y, Wu L, Xu YJ, Huang F, Guo XY, Zhang Y, Fan J, Zhao JQ, Zhang HY, Xu PZ, Zhou JM, Wu XJ, Wang PR, Wang WM (2014) Multiple rice microRNAs are involved in immunity against the blast fungus *Magnaporthe oryzae*. Plant Physiol **164:** 1077-1092

Li Y, Zhang Q, Zhang J, Wu L, Qi Y, Zhou JM (2010) Identification of microRNAs involved in pathogen-associated molecular pattern-triggered plant innate immunity. Plant Physiol **152:** 2222-2231

Liu J, Rice JH, Chen N, Baum TJ, Hewezi T (2014) Synchronization of developmental processes and defense signaling by growth regulating transcription factors. Plos One **9:** e98477

Liu SA, Kracher B, Ziegler J, Birkenbihl RP, Somssich IE (2015) Negative regulation of ABA signaling by WRKY33 is critical for Arabidopsis immunity towards *Botrytis cinerea* 2100. Elife **4:** e07295

Mazarei M, Elling AA, Maier TR, Puthoff DP, Baum TJ (2007) GmEREBP1 is a transcription factor activating defense genes in soybean and Arabidopsis. Mol Plant Microbe Interact **20:** 107-119

Mazarei M, Puthoff DP, Hart JK, Rodermel SR, Baum TJ (2002) Identification and characterization of a soybean ethylene-responsive element-binding protein gene whose mRNA expression changes during soybean cyst nematode infection. Mol Plant Microbe Interact **15:** 577-586

Mitchum MG (2016) Soybean resistance to the soybean cyst nematode *Heterodera glycines*: an update. Phytopathology **106:** 1444-1450

Navarro L, Dunoyer P, Jay F, Arnold B, Dharmasiri N, Estelle M, Voinnet O, Jones JDG (2006) A plant miRNA contributes to antibacterial resistance by repressing auxin signaling. Science **312:** 436-439

Navarro L, Jay F, Nomura K, He SY, Voinnet O (2008) Suppression of the microRNA pathway by bacterial effector proteins. Science **321:** 964-967

Neher DA (2010) Ecology of plant and free-living nematodes in natural and agricultural soil. Annu Rev Phytopathol **48:** 371-394

Omidbakhshfard MA, Proost S, Fujikura U, Mueller-Roeber B (2015) Growth-regulating factors (GRFs): a small transcription factor family with important functions in plant biology. Mol Plant **8:** 998-1010

Schaller GE (2012) Ethylene and the regulation of plant development. BMC Biol **10:** 9

Shanks CM, Rice JH, Zubo Y, Schaller GE, Hewezi T, Kieber JJ (2015) The role of cytokinin during infection of *Arabidopsis thaliana* by the cyst nematode *Heterodera schachtii*. Mol Plant Microbe Interact **29:** 57-68

Sijmons PC, Grundler FMW, Vonmende N, Burrows PR, Wyss U (1991) *Arabidopsis thaliana* as a new model host for plant-parasitic nematodes. Plant J **1:** 245-254

Song S, Qi T, Wasternack C, Xie D (2014) Jasmonate signaling and crosstalk with gibberellin and ethylene. Curr Opin Plant Biol **21:** 112-119

Sun T, Zhang Y, Li Y, Zhang Q, Ding Y, Zhang Y (2015) ChIP-seq reveals broad roles of SARD1 and CBP60g in regulating plant immunity. Nat Commun **6:** 10159

Sunkar R, Kapoor A, Zhu JK (2006) Posttranscriptional induction of two Cu/Zn superoxide dismutase genes in Arabidopsis is mediated by downregulation of miR398 and important for oxidative stress tolerance. Plant Cell **18:** 2051-2065

Szakasits D, Heinen P, Wieczorek K, Hofmann J, Wagner F, Kreil DP, Sykacek P, Grundler FM, Bohlmann H (2009) The transcriptome of syncytia induced by the cyst nematode *Heterodera schachtii* in Arabidopsis roots. Plant J **57:** 771-784

Tanaka H, Dhonukshe P, Brewer PB, Friml J (2006) Spatiotemporal asymmetric auxin distribution: a means to coordinate plant development. Cell Mol Life Sci **63:** 2738-2754

van der Knaap E, Kim JH, Kende H (2000) A novel gibberellin-induced gene from rice and its potential regulatory role in stem growth. Plant Physiol **122:** 695-704

Voinnet O (2009) Origin, biogenesis, and activity of plant microRNAs. Cell **136:** 669-687

Wang D, Pajerowska-Mukhtar K, Culler AH, Dong X (2007) Salicylic acid inhibits pathogen growth in plants through repression of the auxin signaling pathway. Curr Biol **17:** 1784-1790

Wang XH, Replogle A, Davis EL, Mitchum MG (2007) The tobacco Cel7 gene promoter is auxin-responsive and locally induced in nematode feeding sites of heterologous plants. Mol Plant Pathol **8:** 423-436

Weiberg A, Wang M, Bellinger M, Jin H (2014) Small RNAs: a new paradigm in plant-microbe interactions. Annu Rev Phytopathol **52:** 495-516

Wieczorek K, Hofmann J, Blochl A, Szakasits D, Bohlmann H, Grundler FM (2008) Arabidopsis endo-1,4-beta-glucanases are involved in the formation of root syncytia induced by *Heterodera schachtii*. Plant J **53:** 336-351

Wubben MJ, Rodermel SR, Baum TJ (2004) Mutation of a UDP-glucose-4-epimerase alters nematode susceptibility and ethylene responses in Arabidopsis roots. Plant J **40:** 712-724

Wubben MJE, Su H, Rodermel SR, Baum TJ (2001) Susceptibility to the sugar beet cyst nematode is modulated by ethylene signal transduction in *Arabidopsis thaliana*. Mol Plant Microbe Interact **14:** 1206-1212

Yu B, Yang ZY, Li JJ, Minakhina S, Yang MC, Padgett RW, Steward R, Chen XM (2005) Methylation as a crucial step in plant microRNA biogenesis. Science **307:** 932-935

Zhang W, Gao S, Zhou X, Chellappan P, Chen Z, Zhou X, Zhang X, Fromuth N, Coutino G, Coffey M, Jin H (2011) Bacteria-responsive microRNAs regulate plant innate immunity by modulating plant hormone networks. Plant Mol Biol **75:** 93-105

Zhang YQ, Wang YS, Xie FL, Li C, Zhang BH, Nichols RL, Pan XP (2016) Identification and characterization of microRNAs in the plant parasitic root-knot nematode *Meloidogyne incognita* using deep sequencing. Funct Integr Genomic **16:** 127-142

Zhao W, Li Z, Fan J, Hu C, Yang R, Qi X, Chen H, Zhao F, Wang S (2015) Identification of jasmonic acid-associated microRNAs and characterization of the regulatory roles of the miR319/TCP4 module under root-knot nematode stress in tomato. J Exp Bot **66:** 4653-4667

Zhu ZQ, An FY, Feng Y, Li PP, Xue L, Mu A, Jiang ZQ, Kim JM, To TK, Li W, Zhang XY, Yu Q, Dong Z, Chen WQ, Seki M, Zhou JM, Guo HW (2011) Derepression of ethylene-stabilized transcription factors (EIN3/EIL1) mediates jasmonate and ethylene signaling synergy in Arabidopsis. Proc Natl Acad Sci USA **108:** 12539-12544

Appendix

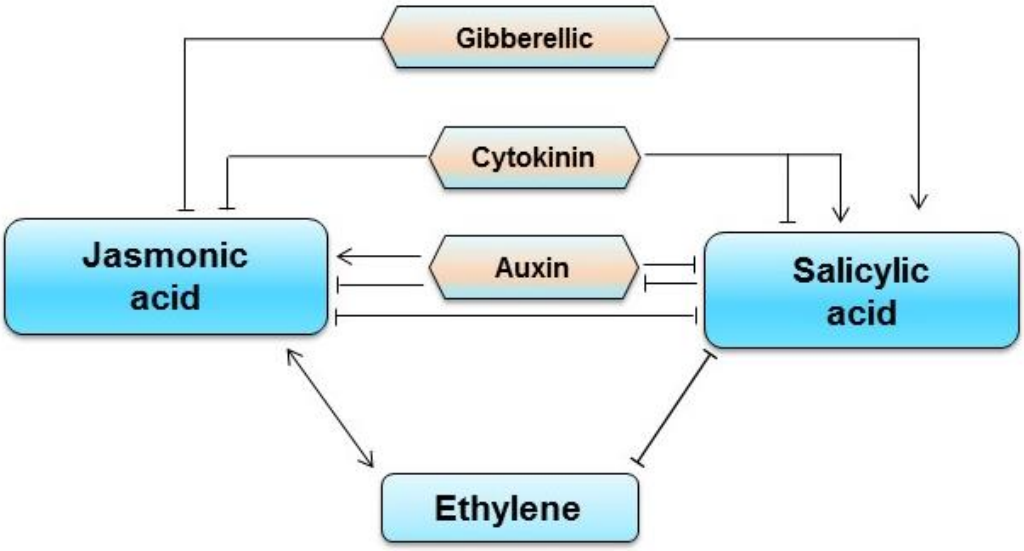

Figure 1-1. Crosstalk between phytohormones during plant pathogen interactions.

Hormonal signaling associated with both defense and growth are often activated during pathogen attack resulting in the hormonal crosstalk to fine-tune the balance between plant

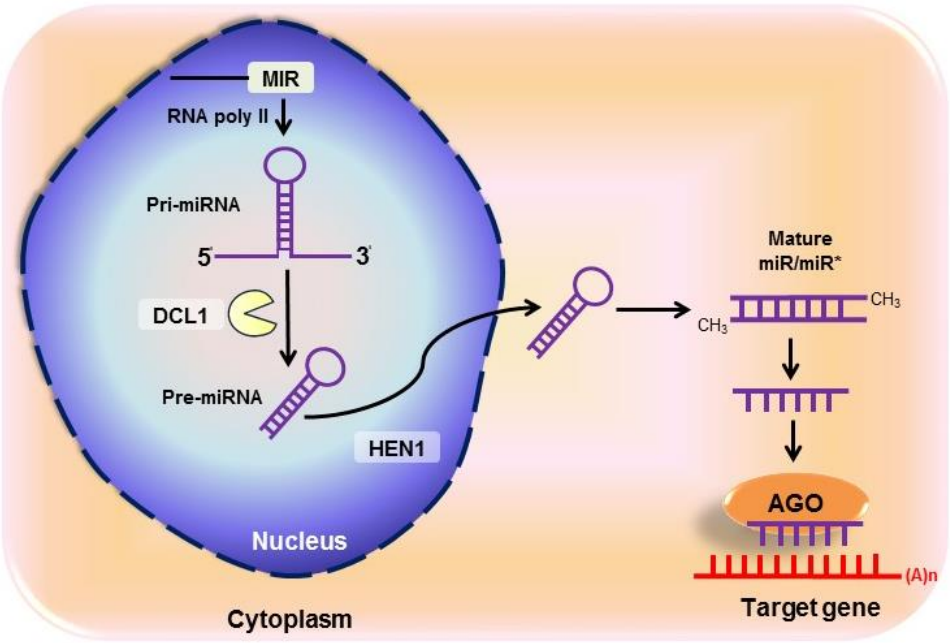

Figure 1-2. Biogenesis of microRNA.

RNA polymerase II transcribes the single stranded miRNA primary transcript from endogenous gene that fold into hairpin-like structure. The hairpin-loop precursor molecules are cleaved by Dicer-like 1 (DCL1) to produce pre-miRNA. This pre-miRNA is transported to the cytoplasm where it is further processed into 21-22 nucleotide mature miRNA. One of the strand of mature miRNA is loaded into ARGONAUTE1 (AGO1) containing RNA-induced silencing complex (RISC). Mature miRNA in RISC serves as guide to bind the target mRNAs that has complementary sequence while the AGO1 protein functions as effector that recruits factors for post-transcriptional gene silencing (PTGS) by endonucleolytic cleavage or translation repression.

Chapter 2

Protein-protein interaction and gene co-expression maps of ARFs and Aux/IAAs in Arabidopsis

This chapter was published in Frontiers in Plant Sciences by Sarbottam Piya, Sandesh Shrestha, Brad Binder, Neal Stewart and Tarek Hewezi.

My contributions to this manuscript include performing experiments, data analysis, results interpretation, and writing.

Abstract

The phytohormone auxin regulates nearly all aspects of plant growth and development. Based on the current model in Arabidopsis thaliana, Auxin/indole-3-acetic acid (Aux/IAA) proteins repress auxin-inducible genes by inhibiting auxin response transcription factors (ARFs). Experimental evidence suggests that heterodimerization between Aux/IAA and ARF proteins are related to their unique biological functions. The objective of this study was to generate the Aux/IAA-ARF protein-protein interaction map using full length sequences and locate the interacting protein pairs to specific gene co-expression networks in order to define tissue-specific responses of the Aux/IAA-ARF interactome. Pairwise interactions between 19 ARFs and 29 Aux/IAAs resulted in the identification of 213 specific interactions of which 79 interactions were previously unknown. The incorporation of co-expression profiles with protein-protein interaction data revealed a strong correlation of gene co-expression for 70% of the ARF-Aux/IAA interacting pairs in at least one tissue/organ, indicative of the biological significance of these interactions. Importantly, ARF4-8 and 19, which were found to interact with almost all Aux-Aux/IAA showed broad co-expression relationships with Aux/IAA genes, thus, formed the central hubs of the co-expression network. Our analyses provide new insights into the biological significance of ARF-Aux/IAA associations in the morphogenesis and development of various plant tissues and organs.

Keywords: Auxin, yeast-two hybrid, co-expression network, BiFC

1. Introduction

The plant hormone auxin (indole-3-acetic acid; IAA), regulates a wide range of developmental and physiological processes in plants including for example, apical dominance, root development, vascular differentiation, shoot elongation, and embryo patterning (Benjamins and Scheres, 2008; Zhao, 2010). Also, auxin regulates various cellular processes that are associated with plant responses to biotic and abiotic stresses (Kazan and Manners, 2009).

Characterization of plant responses to IAA treatments led to the identification of various classes of early auxin-responsive genes. Members of the Aux/IAA gene family were among the first auxin-regulated genes to be identified. In Arabidopsis, the Aux/IAA gene family comprises 29 members and encodes short-lived nuclear proteins. The hallmark characteristic of Aux/IAA proteins is the presence of four highly conserved domains (domains I–IV), which underlie the functional properties of these proteins. Domain I mediates the transcriptional repression of the proteins, whereas domain II mediates protein degradation (Chapman and Estelle, 2009). Domains III and IV are responsible for homo- and hetero-dimerization with other Aux/IAA proteins as well as heterodimerization with the auxin response factors (ARFs) (Chapman and Estelle, 2009). In Arabidopsis, ARFs are encoded by a large gene family containing 22 members. These transcription factors bind specifically to auxin-responsive cis-acting elements that are frequently found in the promoters of early auxin-responsive genes. Aux/IAA proteins negatively regulate the abundance of ARFs, and subsequently the expression of auxin-responsive genes. Extensive molecular and biochemical analyses revealed the mechanism of this regulation (Chapman and Estelle, 2009). More specifically, in the presence of auxin, the degradation of the Aux/IAA proteins is enhanced, thus alleviating the repression of ARF activity and allowing them to drive the transcription of auxin-responsive genes. By contrast, in the absence of auxin, Aux/IAA protein levels increase and they bind to AFRs to inhibit their function. Based on this model, auxin signaling involves TRANSPORT INHIBITOR RESPONSE1/AUXIN-BINDING F-BOX PROTEIN (TIR1/AFB) auxin receptors, Aux/IAA inhibitors, and ARF cis-acting transcription factors regulating the expression of auxin-responsive genes. Because these proteins are encoded by multigene families in Arabidopsis (5 TIR/AFB, 29 Aux/s and 22 ARFs) there are opportunities for numerous combinatorial interactions among these proteins to mediate specific responses.

Experimental evidence suggests that heterodimerization between Aux/IAA and ARF proteins are important to define their unique biological functions (Weijers et al., 2005). For example, ARF7 was found to be regulated by Aux/IAA3 in roots and by Aux/IAA19 in hypocotyls (Tatematsu et al., 2004), suggesting that the activities of ARFs could be regulated by different Aux/IAA proteins in a tissue-dependent fashion. Thus, it is possible that the formation of a wide range of dimer combinations among and between these two gene family proteins represents the mechanisms by which ARF transcription factors regulate diverse cellular processes. Several studies have reported on combinatorial protein-protein interactions between ARFs and Aux/IAAs (Fukaki et al., 2005; Weijers et al., 2005; Uehara et al., 2008; Li et al., 2011; Vernoux et al., 2011; Arase et al., 2012). However, most of these studies used partial ARF sequences containing the C-terminal protein-protein interaction domain (CTD) and discrepancies in protein-protein interactions between Aux/IAA proteins and that of the full-length or truncated ARFs are frequently found. For example, Aux/IAA17 was found to interact strongly with the full-length of ARF1 (Ouellet et al., 2001) but no interaction was detected when a truncated version of ARF1 containing the CTD was used (Tiwari et al., 2003; Vernoux et al., 2011). Similarly, differences in interaction intensity between rice Aux/IAAs and intact or truncated versions of ARFs were observed (Shen et al., 2010).

The global protein-protein interaction network of a specific gene family provides information of all physical associations that can occur among family members. However, weighing the biological significance of such an interactome is a real challenge because of tissue specificities and the dynamic nature of protein-protein interactions. Global gene co-expression analysis has recently emerged as a powerful approach to identify the tissues and the conditions in which important interactions occur. This is based on the idea that proteins can physically interact in particular cell types or tissues only if their genes are co-expressed in these cell types or tissues. The integration of global gene expression data with a protein interaction network has been used to determine the cellular conditions and tissues specificity of protein interaction network of human proteins (Bossi and Lehner, 2009), and Arabidopsis MADS Box transcription factors (de Folter et al., 2005), cell cycle proteins (Boruc et al., 2010), and G-proteins (Klopffleisch et al., 2011).

In this study, we generated the protein–protein interaction map of Arabidopsis ARF and Aux/IAA proteins using full-length sequences in yeast two-hybrid assays. We identified 213 specific interactions between ARFs and Aux/IAAs in which 79 interactions have not been reported previously. In addition, we integrated the global gene co-expression profile with the protein interaction map and identified tissue-specificity for the majority of the ARF-Aux/IAAs interactions.

2. Results

2.1 Construction of Comprehensive Interaction Map of ARFs and Aux/IAA

To generate a comprehensive protein-protein interaction map between ARF and Aux/IAA proteins, yeast co-transformation assays were performed between 19 ARFs and 29 Aux/IAAs. The full-length coding sequences of 19 ARFs (ARF1-13 and ARF16-20 and ARF22) were cloned in a bait vector and full-length coding sequences of 29 Aux/IAAs (Aux/IAA1-20 and Aux/IAA26-34) were cloned in a prey vector. Yeast cells were co-transformed with 551 pairs of bait and prey vectors and potential interactions were visualized by differential growth on the non-selective synthetic dropout (SD) medium (SD/-Leu/-Trp) and on the selective medium (SD/-Leu/-Trp/-His/-Ade). An example of the interaction between ARF10 and Aux/IAAs is provided in Figure 2.1. Of the 551 interactions tested, 213 interactions between ARFs and Aux/IAAs were detected. To confirm the protein-protein interactions in planta, bimolecular fluorescence complementation (BiFC) assays (Citovsky et al., 2006) were performed with ARFs and Aux/IAAs that displayed weak-to-strong interactions in yeast. Coding sequences of ARF5, 6, and 19 were fused to the N-terminal half of a yellow fluorescent protein gene (nEYFP), while Aux/IAA5, 6, 17, 32, and 34 were fused to the C-terminal half of a yellow fluorescent protein gene (cEYFP). Ten different combinations between nEYFP and cEYFP fusions were co-expressed in onion epidermal cells. All ARF-Aux/IAA interaction combinations, including those showing weak interaction in yeast (ARF6-Aux/IAA32 and ARF19-Aux/IAA34), reconstituted the fluorescent YFP in the nucleus of transformed cells (Figure 2.2), validating our yeast co-transformation data. Onion epidermal cells co-transformed with 4 non-interacting pairs yielded no YFP fluorescence.

It is interesting to note that all ARFs that function as activators (ARF5, ARF6, ARF7, ARF8, and ARF19) were found to interact with all Aux/IAA proteins except ARF7 with Aux/IAA7 (Figure

2.3). In contrast, ARFs that function as repressors showed interactions with certain Aux/IAAs. One exception is ARF4, which interacted strongly with all Aux/IAA proteins. One remarkable finding is that ARFs that functioned as repressors dimerized preferentially with Aux/IAA32 and Aux/IAA34 (Figure 2.3). For example, out of the 14 ARFs we included in our analysis that functioned as repressors 9 and 8 ARFs were found to interact with Aux/IAA32 and Aux/IAA34, respectively (Figure 2.3). Of these ARFs, ARF1, 10, 16, and 18 showed strong interactions with both Aux/IAA32 and 34. No interactions were detected for ARF3, ARF11, ARF12 and ARF13. ARF3 and ARF13 do not contain the C-terminal protein-protein interaction domain (CTD), which mediates the interaction with Aux/IAAs through binding to motif III and IV found in Aux/IAAs. ARF17 does not contain the CTD but was found to interact with 9 Aux/IAA proteins including Aux/IAA5, 8, 9, 13–16, 33, and 34 (Figure 2.3).

2.2 Phylogenetically-Related ARFs Exhibited Various Interactions with Aux/IAA Proteins

We tested whether phylogenetically-related ARF and Aux/IAA proteins would have similar protein-protein interaction patterns. In general, we found that phylogenetically-related ARF and Aux/IAA proteins formed similar protein-protein interactomes. For example, ARF5-8 and ARF19, which are phylogenetically-related, interacted with almost all Aux/IAA proteins. Similarly, ARF10 and 16, which clustered together, were found to interact with the same Aux/IAA proteins including Aux/IAA5, and Aux/IAA32-34 (Figure 2.3). In contrast, the closely-rated ARF3 and 4 showed distinct interaction patterns. While ARF4 interacted strongly with all Aux/IAA protein, none of the Aux/IAA proteins was detected as ARF3 interactor, perhaps owing to the absence of the CTD in ARF3. Likewise, ARF11 and 18 showed different interaction patterns despite the fact that they are phylogenetically-related.

2.3 Co-Expression Analysis of Interacting ARF-Aux/IAA Proteins

Auxin-specific response in plant tissues is defined by specific ARF-Aux/IAA pairs that co-express in these tissues (Weijers et al., 2005). Therefore, interacting ARF-Aux/IAA pairs that co-express in particular tissues are the potential combinations that facilitate the conversion of auxin signal into specific responses during morphogenesis. To test the biological significance of the physical ARF-Aux/IAA associations, we integrated the protein interaction map with the co-expression map. We analyzed gene co-expression profiles of ARF and Aux/IAA genes in different Arabidopsis tissues/organs using 65 different RNAseq datasets from the SRA

(Leinonen et al., 2011). Pair-wise gene co-expression values of genes encoding ARFs and Aux/IAAs in various tissues and organs were used to generate the co-expression network of the ARF-Aux/IAA interacting proteins shown in Figure 2.4. The network included 44 nodes (15 ARFs and 29 Aux/IAA) and 213 edges (interacting combinations). Out of the 213 interacting combinations, 149 combinations (70%) had co-expression patterns in at least one tissue and were represented by continuous edges (Figure 2.4). The remaining 64 interacting combinations did not show significant co-expression relationships, represented by dotted edges (Figure 2.4). ARF4-8 and 19, which were found to interact with almost all Aux/IAAs, showed broad co-expression relationships with Aux/IAA genes, and thus constituted the central hubs of the map. Notably, all the interacting combinations of ARF1, 2, and 16 showed significant co-expression correlations. In contrast, ARF20, ARF22 and Aux/IAA33 did not show any co-expression association in the tissues included in our analysis.

In order to map the co-expression events of the interacting ARF-Aux/IAA proteins to specific tissues or organs, the co-expression between pairs was determined using Z score as described in the Material and Methods. We set the "fragments per kilobase of transcript per million mapped reads" (FPKM) value of 2.0 as the threshold for expressed genes. As a result, ARF12-14, ARF20, ARF22 and Aux/IAA15, which have FPKM value less than 2 were considered as non-expressed in the samples included and hence, were not included in the co-expression analysis. Also, IAA33 and IAA34 showed very low expression levels across all tissues except in the roots and seedlings, respectively. The co-expression profiles of ARFs and Aux/IAAs in embryos, floral buds, flowers, hypocotyls, leaves, roots, shoot apical meristems, seedlings, and whole plant are presented as a heatmap in Figure 2.5. It is very interesting to note that we observed general trends of co-expression specificity in which the majority of the ARF/Aux/IAA pairs are expressed in only one tissue/organ. In few cases, the co-expression associations of the pairs were found in two and to a much lower extent in three tissues, these occurred in tissues with related functions such as flowers, floral buds and embryos. For example, ARF5-Aux/IAA12, ARF5-Aux/IAA27, and ARF17-Aux/IAA8 were co-expressed in floral buds and embryos. Similarly, ARF6-Aux/IAA9, ARF6-Aux/IAA11, ARF8-Aux/IAA9, and ARF8/Aux/IAA11 were co-expressed in flowers and floral buds. It is also interesting to note that in each tissue, several co-expression events occurred in which only a few ARFs were observed. For example, the 16 co-expression events detected in roots were contributed by ARF7 and ARF19. In other tissues, the

number of co-expression events was very limited. For example, in SAM only 5 co-expression events between ARFs and Aux/IAAs were detected (ARF5-Aux/IAA8, ARF5-Aux/IAA32, ARF8-Aux/IAA8, ARF8-Aux/IAA32, and ARF10-Aux/IAA32).

3. Discussion

Models for auxin signal transduction pathway have positioned ARF and Aux/IAA proteins centrally in the network in which auxin signals are converted into specific physiological responses (Muday et al., 2012). ARFs contain N-terminal DNA binding domain that binds to the TGTCTC cis regulatory element in the promoters of auxin-response genes, a middle region that functions as activator or repressor, and frequently a CTD involved in protein-protein interactions (Guilfoyle and Hagen, 2007). Likewise, Aux/IAAs contain an N-terminal repression domain (domain I), a degradation domain (domain II) that facilitates degradation of Aux/IAAs through ubiquitin–proteasome pathway in response to auxin, and protein-protein interaction domains (domain III and IV), which resemble CTD of the ARFs (Guilfoyle and Hagen, 2012). The CTD of ARFs and domains III and IV of Aux/IAAs mediate ARF-Aux/IAA heterodimerization (Weijers et al., 2005). Because ARF and Aux/IAA proteins are encoded by multigene families, there are opportunities for many combinatorial interactions between these proteins, which apparently are necessary to mediate auxin-specific responses in various developmental and physiological contexts. Studies of protein-protein interactions between Arabidopsis ARFs and Aux/IAAs have been conducted using truncated ARFs with only CTDs (Tiwari et al., 2003; Tatematsu et al., 2004; Szemenyei et al., 2008; Vernoux et al., 2011) with the assumption that the ARF protein domains other than CTD have no role in facilitating ARF-Aux/IAA interactions. Although the interaction between these two gene families are mediated through the CTD, using truncated proteins might not be physiologically relevant in that the result could be instable or misfolded protein domains or fragments that could impact the interaction outcomes.

In this study, we identified 213 specific interactions between 19 ARFs and 29 Aux/IAAs using yeast two-hybrid assays. A subset of 10 interacting combinations in yeast was also validated in planta using BiFC, indicating that these interactions were functional and of biological relevance in plants. When we compared our protein-protein interaction data with those reported by Vernoux et al. (2011), we found that 134 interaction combinations were common between studies. In contrast, we detected 79 new interactions, but failed to confirm 39 previously-reported

interactions. The identification of 79 new interactions in the current study suggests that protein structure or regions other than CTD of ARFs likely influence ARF-Aux/IAA interactions, which was supported by ARF17, which does not contain a CTD, interacted with 9 Aux/IAA proteins including Aux/IAA5, 8, 9, 13–16, 33, and 34. Thus, using truncated ARFs might constrict the ability of ARFs to interact with Aux/IAA proteins. Consistent with this suggestion, an interaction between intact ARF1 and Aux/IAA17 was observed in our study and also previously (Ouellet et al., 2001), whereas the truncated version of ARF1 containing only CTD failed to produce positive interaction (Tiwari et al., 2003; Vernoux et al., 2011). In addition, a recent study of protein-protein interactions between ARFs and Aux/IAAs in rice indicated that full-length and truncated ARFs could differ in their capacity to interact with Aux/IAA proteins (Shen et al., 2010).

We found that all ARFs that are known to be transcriptional activators (ARF5-8, and 19), interacted with almost all Aux/IAA proteins, a result that was also found in rice (Shen et al., 2010). It is unknown whether this is the case across the plant kingdom. Consistent with previous studies, we found that ARFs that function as repressors have none-to-limited interactions with Aux/IAA proteins (Shen et al., 2010; Vernoux et al., 2011). This limited ability is not primarily due to the absence of the CTD from certain ARFs (ARF3 and 13), because other CTD-containing ARFs (ARF11 and 12) showed no interaction with Aux/IAA proteins. A recent study indicated that truncated ARFs lacking CTD can regulate gene expression in an auxin-dependent manner Wang et al. (2013), suggesting that these ARFs might function through mechanisms other than the ARF-Aux/IAA module. One such hypothesis is that ARF repressors compete with ARFs that function as activators by binding to the promoters of auxin inducible genes without forming heterodimer with Aux/IAAs (Vernoux et al., 2011). If this scenario is accurate, targeting these ARFs by Aux/IAA proteins in absence of auxin is not required. However, it seems most likely that the physical association between ARF repressors and Aux/IAA proteins is of biological significance under specific physiological or developmental circumstances, since 69 interaction combinations between 10 ARF repressors and Aux/IAA proteins were detected in yeast and some were confirmed in planta. In this perspective, the generation and functional characterization of double mutants of various ARF and Aux/IAA genes will deepen our knowledge about the roles of ARFs-Aux/IAA association in mediating auxin-specific responses under specific developmental and physiological settings.

While global protein-protein interaction networks provide an indication for all possible physical interaction combinations that can occur between proteins, the biological significance of such interaction requires the genes coding for these proteins to be co-expressed in particular cells. One approach to investigate the biological importance of such interactomes is to combine expression data with protein interaction data. This is because interacting proteins whose corresponding genes are co-expressed generally co-function in particular processes or pathways (Boruc et al., 2010; Klopffleisch et al., 2011). The incorporation of gene co-expression profiles with protein-protein interaction data revealed a strong correlation of gene expression for 70% of the ARF-Aux/IAA interacting pairs, providing evidence for the biological significance of these interactions. For these interacting pairs one tissue/organ was generally deduced as the site of the co-function, indicative of the specificity of the co-expression patterns. Our data point to previously unknown tissues for the majority of ARF-Aux/IAA associations and confirmed the tissue specificity of previously identified and functionally validated ARF-Aux/IAA pairs. For example, ARF7-Aux/IAA19 were found to co-function in hypocotyls (Tatematsu et al., 2004), whereas ARF7-Aux/IAA14, ARF19-Aux/IAA14, ARF7-Aux/IAA28, and ARF19-Aux/IAA28 were found to co-function in roots (Fukaki et al., 2005; De Rybel et al., 2010; Goh et al., 2012), consistent with our gene co-expression analysis. In addition, the co-expression analysis has assigned particular ARFs for specific tissue/organ. ARF6 and 8 were found to co-express with various Aux/IAA genes only in flowers and floral buds. This finding is in agreement with the redundant function of ARF6 and 8 in regulating floral structures (Nagpal et al., 2005; Tabata et al., 2010).

ARF4-8 and 19, which tend to interact with all Aux/IAAs were also found to be broadly expressed and hence constitute the main hubs in the interaction and co-expression networks (Figure 2.5). Our data show that these ARFs have protein interactions with Aux/IAAs that can occur only in specific tissues/organs. Thus, broadly expressed ARFs can mediate tissue-specific functions through their association with restrictedly expressed Aux/IAAs such as IAA33 and IAA34. It should be noted that several significant gene co-expression associations for the interacting proteins were identified in various tissues. This can be explained by the possibility that co-expression correlations may occur in various subsets of tissues or in specific cell types. In this context, analyzing the temporal and spatial gene expression patterns of the interacting protein pairs in the target tissues will precisely define their specific transcriptional signatures. On

the other hand, we were unable to identify significant co-expression associations for about 30% of the interacting proteins in the tissues included in our analysis. The co-expression associations of these pairs may take place in specific tissues at particular developmental stages that are not included in our analysis. Alternatively, the co-functions of these pairs may be limited to particular physiological circumstances, including biotic and abiotic stresses.

In conclusion, our analysis confirmed most of the published protein-protein interactions between ARFs and Aux/IAAs and provided a new set of previously unknown interactions. In addition, the combination of co-expression data with protein-protein interaction data provided new leads to the site of the co-functions of ARF and Aux/IAA proteins. Taken together, these analyses set the stage for detailed functional analysis to reveal the biological significance of ARF-Aux/IAA interactions in the morphogenesis and development of various plant tissues and organs.

4. Materials and Methods

4.1 Plasmid Construction

Full-length coding sequences for 19 ARFs and 29 Aux/IAAs were obtained from Arabidopsis Biological Resource Center or isolated from cDNA. The coding sequences of these ARF and Aux/IAA genes were PCR amplified using forward and reverse primers containing specific restriction enzyme sites. PCR amplification was performed using PrimeSTAR GXL DNA polymerase (Takara Bio) following manufacturers' instructions. PCR products of ARFs were digested, purified and fused to the GAL4 DNA binding domain of the pGBKT7 vector (Clontech) to generate pGBKT7-ARFs. Similarly, PCR products of Aux/IAAs were digested, purified and fused to the GAL4 DNA activation domain of pGADT7 vector (Clontech) to generate pGADT7-Aux/IAAs. All constructs were verified by sequencing.

4.2 Yeast Two-Hybrid Assays

Saccharomyces cerevisiae strain AH109 was co-transformed with 551 pairs of pGBKT7-ARF and pGADT7-Aux/IAA vectors and yeast cells containing both vectors were selected using SD/-Leu/-Trp medium. The interactions between ARFs and Aux/IAA were assayed by plating the transformed cells onto the stringent SD/-Ade-His-Leu-Trp selective medium using at least 10 independent colonies. Serial dilutions of yeast co-transformed cells were used to measure the strength of the interaction.

4.3 Bimolecular Fluorescence Complementation (BiFC) Assays

The coding sequence of ARF5, 6, and 19 were PCR amplified using forward and reverse primers containing restriction enzyme sites. After digestion, Purified PCR products were cloned into pSAT4-cEYFP-C1-B to generate cEYFP-ARF5, 6, and 19 fusions. Likewise, Aux/IAA5, 6, 17, 32, and 34 were cloned into pSAT4-nEYFP-C1 to generate nEYFP-Aux/IAA5, 6, 17, 32, and 34 fusions. All constructs were verified by sequencing. Ten combinations of cEYFP and nEYFP fusions, in addition to controls, were co-expressed in onion (*Allium cepa*) epidermal cells using particle bombardment as previously described by Hewezi et al. (2008). Co-transformed tissues were incubated at 25°C in dark for 16–24 h before being assayed for YFP activity. Bright field and fluorescent images were observed using EVOS® FL Auto Cell Imaging System (Life Technologies).

4.4 Gene Co-Expression Network Analysis

Raw RNA seq data for 65 samples including root, shoot apical meristem, seedlings, hypocotyls, leaves, floral buds, flowers, embryos, and whole plants were downloaded from NCBI Sequence Read Archive (SRA) (Leinonen et al., 2011). The SRA files were converted to FASTQ file using fastq-dump of SRA Toolkit (http://www.ncbi.nlm.nih.gov/Traces/sra/sra.cgi?view=toolkit_doc&f=fastq-dump). Quality assessment of sequence reads was performed using FastQC (http://www.bioinformatics.babraham.ac.uk/projects/fastqc/). Quality filtering and trimming were conducted using FASTX-Toolkit (http://hannonlab.cshl.edu/fastx_toolkit/). After quality filtering and trimming, each sequence read was aligned to the TAIR10 *Arabidopsis thaliana* reference genome (Swarbreck et al., 2008) using TopHat v2.0.11 (Trapnell et al., 2009). The output from TopHat (bam file) was used to quantify gene expression level as FPKM (fragments per kilobase of transcript per million mapped reads) using Cufflink v2.2.1 (Trapnell et al., 2010). Output from cufflink was filtered to extract the expression value for ARF and Aux/IAA genes using AWK command. FPKM value of 2 was used as a threshold for expressed genes, and hence, only those genes having FPKM values more than two in at least one tissue were included in the gene co-expression analysis. To determine the tissues in which ARF-Aux/IAA pairs are co-expressed, we computed the Z-score for each of the FPKM values. The Z-score values were averaged across different samples of a given tissue and positive values of Z-score indicate high

expression. ARF-Aux/IAA combinations are considered co-expressed in a tissue only if Z-score for both genes in this tissue is positive with a P value less than 0.05. A heatmap of all co-expressed ARF-Aux/IAA pairs in various tissues was constructed using sample contribution score in Multi Experiment Viewer (http://www.tm4.org/mev.html). Sample contribution scores were calculated by multiplying Z-score of ARFs and Aux/IAAs for each tissue as described in CoexViewer available at ATTED-II database (Obayashi et al., 2014). Positive values of sample contribution score resulting from negative Z-scores of both ARFs and Aux/IAAs was made negative. Cytoscape (Shannon et al., 2003) was used to integrate gene co-expression data with protein-protein interaction data.

4.5 Phylogenetic Analysis

Protein sequences of all ARFs and Aux/IAAs were downloaded from the The Arabidopsis Information Resource (TAIR) website. Sequences were aligned using ClustalX (Jeanmougin et al., 1998) and neighbor-joining tree was constructed using MEGA6 (Tamura et al., 2013) with default settings.

Acknowledgments

We thank Sujata Agarwal and the UTIA Genomics Hub for providing access to the imaging system. This work was partially supported by a grant from National Science Foundation (Award #: 1145053) to Tarek Hewezi, Hewezi Laboratory startup funds from the University of Tennessee and a University of Tennessee AgResearch Innovation Grant (2013).

References

Arase F, Nishitani H, Egusa M, Nishimoto N, Sakurai S, Sakamoto N, Kaminaka H (2012) IAA8 involved in lateral root formation interacts with the TIR1 auxin receptor and ARF transcription factors in Arabidopsis. PLoS One **7:** e43414

Benjamins R, Scheres B (2008) Auxin: the looping star in plant development. Annu Rev Plant Biol **59:** 443-465

Boruc J, Van den Daele H, Hollunder J, Rombauts S, Mylle E, Hilson P, Inze D, De Veylder L, Russinova E (2010) Functional modules in the Arabidopsis core cell cycle binary protein-protein interaction network. Plant Cell **22:** 1264-1280

Bossi A, Lehner B (2009) Tissue specificity and the human protein interaction network. Mol Syst Biol **5**

Chapman EJ, Estelle M (2009) Mechanism of auxin-regulated gene expression in plants. Annu Rev Genet **43:** 265-285

de Folter S, Immink RG, Kieffer M, Parenicova L, Henz SR, Weigel D, Busscher M, Kooiker M, Colombo L, Kater MM, Davies B, Angenent GC (2005) Comprehensive interaction map of the Arabidopsis MADS Box transcription factors. Plant Cell **17:** 1424-1433

De Rybel B, Vassileva V, Parizot B, Demeulenaere M, Grunewald W, Audenaert D, Van Campenhout J, Overvoorde P, Jansen L, Vanneste S, Moller B, Wilson M, Holman T, Van Isterdael G, Brunoud G, Vuylsteke M, Vernoux T, De Veylder L, Inze D, Weijers D, Bennett MJ, Beeckman T (2010) A novel aux/IAA28 signaling cascade activates GATA23-dependent specification of lateral root founder cell identity. Curr Biol **20:** 1697-1706

Fukaki H, Nakao Y, Okushima Y, Theologis A, Tasaka M (2005) Tissue-specific expression of stabilized SOLITARY-ROOT/IAA14 alters lateral root development in Arabidopsis. Plant J **44:** 382-395

Goh T, Kasahara H, Mimura T, Kamiya Y, Fukaki H (2012) Multiple AUX/IAA-ARF modules regulate lateral root formation: the role of Arabidopsis SHY2/IAA3-mediated auxin signalling. Philos Trans R Soc Lond B Biol Sci **367:** 1461-1468

Guilfoyle TJ, Hagen G (2007) Auxin response factors. Curr Opin Plant Biol **10:** 453-460

Guilfoyle TJ, Hagen G (2012) Getting a grasp on domain III/IV responsible for Auxin Response Factor-IAA protein interactions. Plant Sci **190:** 82-88

Jeanmougin F, Thompson JD, Gouy M, Higgins DG, Gibson TJ (1998) Multiple sequence alignment with Clustal X. Trends Biochem Sci **23:** 403-405

Kazan K, Manners JM (2009) Linking development to defense: auxin in plant-pathogen interactions. Trends Plant Sci **14:** 373-382

Klopffleisch K, Phan N, Augustin K, Bayne RS, Booker KS, Botella JR, Carpita NC, Carr T, Chen JG, Cooke TR, Frick-Cheng A, Friedman EJ, Fulk B, Hahn MG, Jiang K, Jorda L, Kruppe L, Liu C, Lorek J, McCann MC, Molina A, Moriyama EN, Mukhtar MS, Mudgil Y, Pattathil S, Schwarz J, Seta S, Tan M, Temp U, Trusov Y, Urano D, Welter B, Yang J, Panstruga R, Uhrig JF, Jones AM (2011) Arabidopsis G-protein interactome reveals connections to cell wall carbohydrates and morphogenesis. Mol Syst Biol **7:** 532

Leinonen R, Sugawara H, Shumway M, C INSD (2011) The Sequence Read Archive. Nucleic Acids Research **39:** D19-D21

Li JF, Bush J, Xiong Y, Li L, McCormack M (2011) Large-scale protein-protein interaction analysis in Arabidopsis mesophyll protoplasts by split firefly luciferase complementation. PLoS One **6:** e27364

Muday GK, Rahman A, Binder BM (2012) Auxin and ethylene: collaborators or competitors? Trends Plant Sci **17:** 181-195

Nagpal P, Ellis CM, Weber H, Ploense SE, Barkawi LS, Guilfoyle TJ, Hagen G, Alonso JM, Cohen JD, Farmer EE, Ecker JR, Reed JW (2005) Auxin response factors ARF6 and ARF8 promote jasmonic acid production and flower maturation. Development **132:** 4107-4118

Obayashi T, Okamura Y, Ito S, Tadaka S, Aoki Y, Shirota M, Kinoshita K (2014) ATTED-II in 2014: evaluation of gene coexpression in agriculturally important plants. Plant Cell Physiol **55:** e6

Ouellet F, Overvoorde PJ, Theologis A (2001) IAA17/AXR3: biochemical insight into an auxin mutant phenotype. Plant Cell **13:** 829-841

Shannon P, Markiel A, Ozier O, Baliga NS, Wang JT, Ramage D, Amin N, Schwikowski B, Ideker T (2003) Cytoscape: a software environment for integrated models of biomolecular interaction networks. Genome Res **13:** 2498-2504

Shen C, Wang S, Bai Y, Wu Y, Zhang S, Chen M, Guilfoyle TJ, Wu P, Qi Y (2010) Functional analysis of the structural domain of ARF proteins in rice (*Oryza sativa* L.). J Exp Bot **61:** 3971-3981

Swarbreck D, Wilks C, Lamesch P, Berardini TZ, Garcia-Hernandez M, Foerster H, Li D, Meyer T, Muller R, Ploetz L, Radenbaugh A, Singh S, Swing V, Tissier C, Zhang P, Huala E (2008) The Arabidopsis Information Resource (TAIR): gene structure and function annotation. Nucleic Acids Res **36:** D1009-D1014

Szemenyei H, Hannon M, Long JA (2008) TOPLESS mediates auxin-dependent transcriptional repression during Arabidopsis embryogenesis. Science **319:** 1384-1386

Tabata R, Ikezaki M, Fujibe T, Aida M, Tian C, Ueno Y, Yamamoto KT, Machida Y, Nakamura K, Ishiguro S (2010) Arabidopsis AUXIN RESPONSE FACTOR6 and 8 regulate jasmonic acid biosynthesis and floral organ development via repression of class 1 KNOX genes. Plant Cell Physiol **51:** 164-175

Tamura K, Stecher G, Peterson D, Filipski A, Kumar S (2013) MEGA6: Molecular Evolutionary Genetics Analysis version 6.0. Mol Biol Evol **30:** 2725-2729

Tatematsu K, Kumagai S, Muto H, Sato A, Watahiki MK, Harper RM, Liscum E, Yamamoto KT (2004) MASSUGU2 encodes Aux/IAA19, an auxin-regulated protein that functions together with the transcriptional activator NPH4/ARF7 to regulate differential growth responses of hypocotyl and formation of lateral roots in *Arabidopsis thaliana*. Plant Cell **16:** 379-393

Tiwari SB, Hagen G, Guilfoyle T (2003) The roles of auxin response factor domains in auxin-responsive transcription. Plant Cell **15:** 533-543

Trapnell C, Pachter L, Salzberg SL (2009) TopHat: discovering splice junctions with RNA-Seq. Bioinformatics **25:** 1105-1111

Trapnell C, Williams BA, Pertea G, Mortazavi A, Kwan G, van Baren MJ, Salzberg SL, Wold BJ, Pachter L (2010) Transcript assembly and quantification by RNA-Seq reveals unannotated transcripts and isoform switching during cell differentiation. Nat Biotechnol **28:** 511-515

Uehara T, Okushima Y, Mimura T, Tasaka M, Fukaki H (2008) Domain II mutations in CRANE/IAA18 suppress lateral root formation and affect shoot development in *Arabidopsis thaliana*. Plant Cell Physiol **49:** 1025-1038

Vernoux T, Brunoud G, Farcot E, Morin V, Van den Daele H, Legrand J, Oliva M, Das P, Larrieu A, Wells D, Guedon Y, Armitage L, Picard F, Guyomarc'h S, Cellier C, Parry G, Koumproglou R, Doonan JH, Estelle M, Godin C, Kepinski S, Bennett M, De Veylder L, Traas J (2011) The auxin signalling network translates dynamic input into robust patterning at the shoot apex. Mol Syst Biol **7:** 508

Wang S, Hagen G, Guilfoyle TJ (2013) ARF-Aux/IAA interactions through domain III/IV are not strictly required for auxin-responsive gene expression. Plant Signal Behav **8:** e24526

Weijers D, Benkova E, Jager KE, Schlereth A, Hamann T, Kientz M, Wilmoth JC, Reed JW, Jurgens G (2005) Developmental specificity of auxin response by pairs of ARF and Aux/IAA transcriptional regulators. Embo Journal **24:** 1874-1885

Zhao Y (2010) Auxin biosynthesis and its role in plant development. Annu Rev Plant Biol **61:** 49-64

Appendix

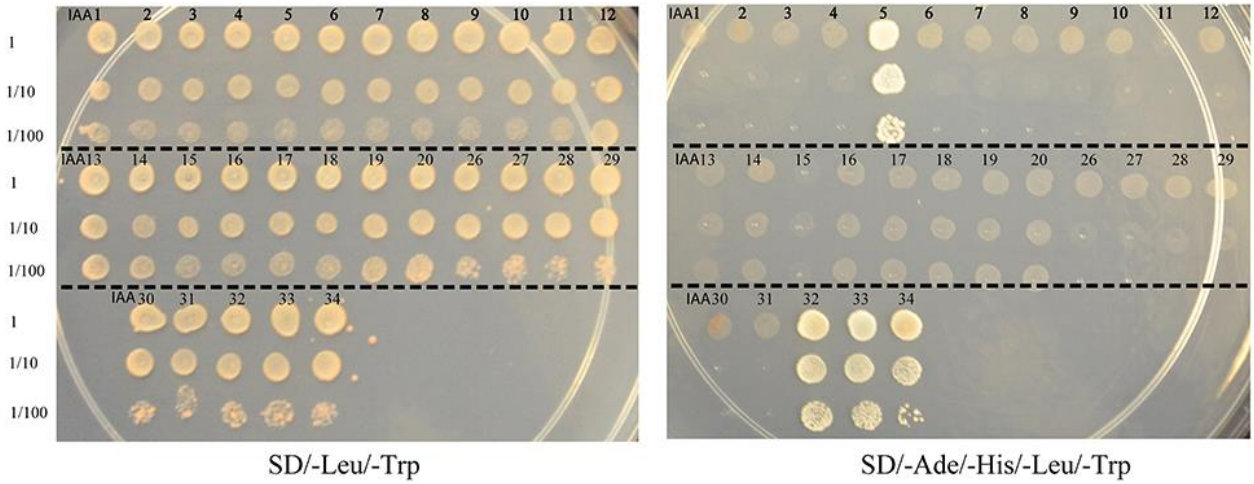

Figure 2-1. Yeast two-hybrid interaction between ARF10 and various Aux/IAAs.

Yeast strain AH109 was co-transformed with ARF10 bait vector in combination with 29 Aux/IAA prey vectors. Protein-protein interactions between ARF10 and each of Aux/IAA5, Aux/IAA32, Aux/IAA33 and Aux/IAA34 were visualized by differential growth on the SD/-Leu/-Trp non-selective medium (left) and on the SD/-Ade/-His/-Leu/-Trp selective medium (right).

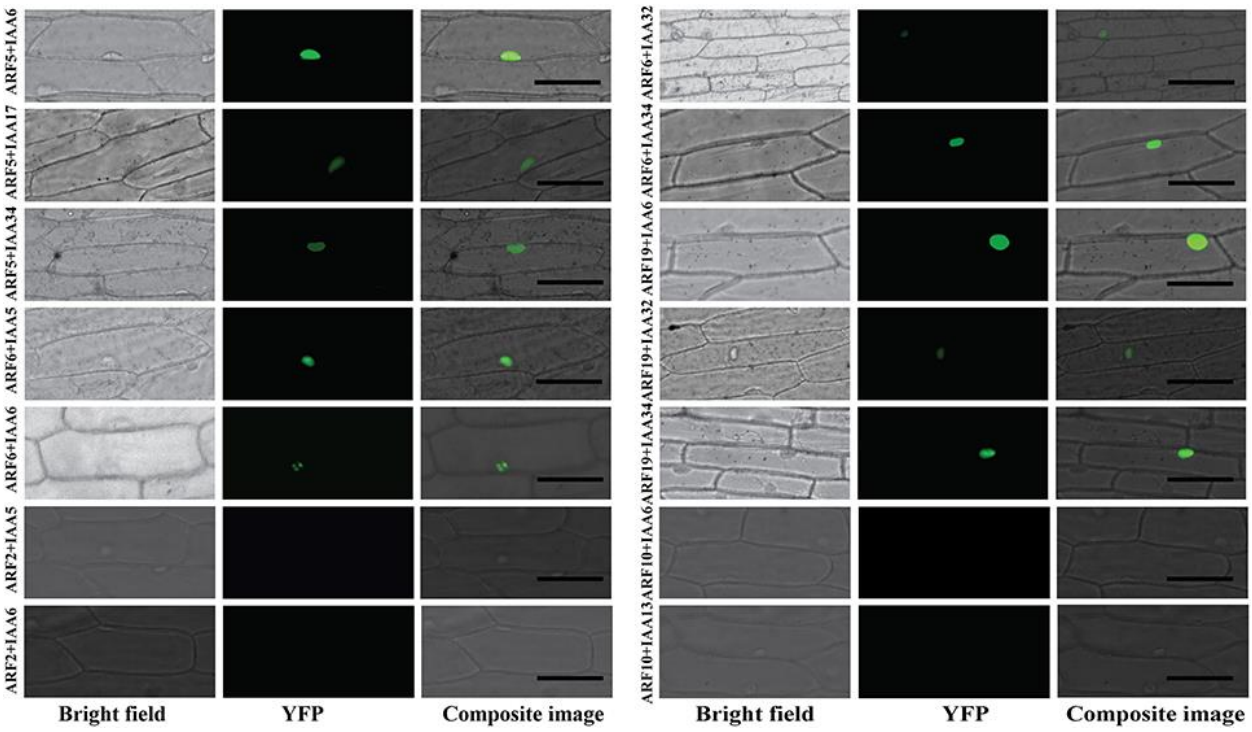

Figure 2-2. BiFC visualization of the ARF-Aux/IAA interactions.

Onion epidermal cells were co-transformed with ten different combinations of constructs expressing cEYFP-ARF5, 6, and 19 fusions and nEYFP-Aux/IAA5, 6, 17, 32, and 34 fusions. Bright field, YFP and composite images were taken 16–24 h after bombardment. Four combinations of non-interacting ARF-Aux/IAA pairs in yeast (ARF2-Aux/IAA5, ARF2-Aux/IAA6, ARF10-Aux/IAA6 and ARF10-Aux/IAA13) were used as negative control and showed no YFP signal. Bar = 100 μM.

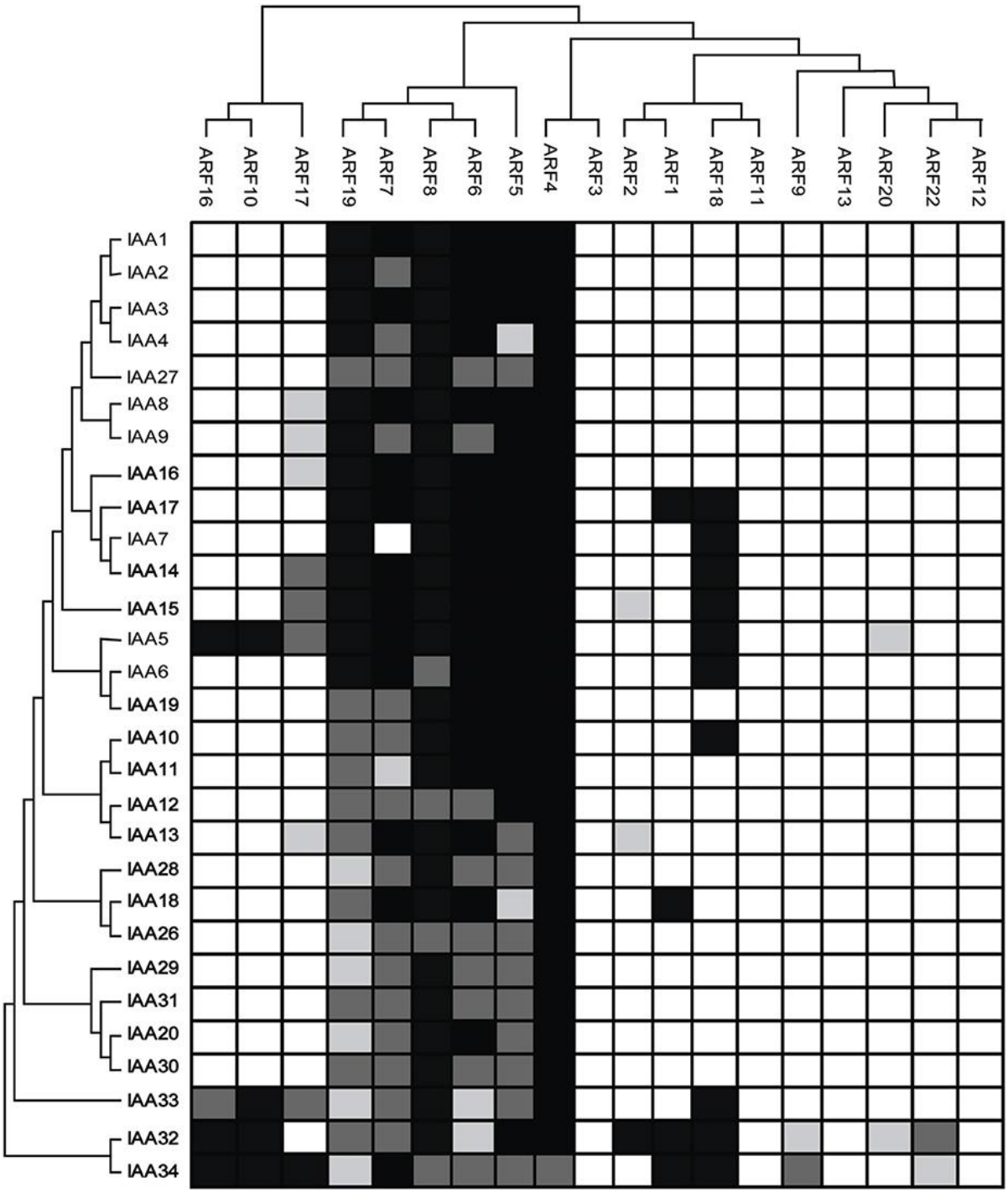

Figure 2-3. Protein-protein interaction map of Arabidopsis ARF and Aux/IAA proteins.

ARFs (top) and Aux/IAAs (left) are arranged according to their sequence similarity. Empty boxes indicate no interaction while gray and black boxes indicate weak and strong interaction, respectively.

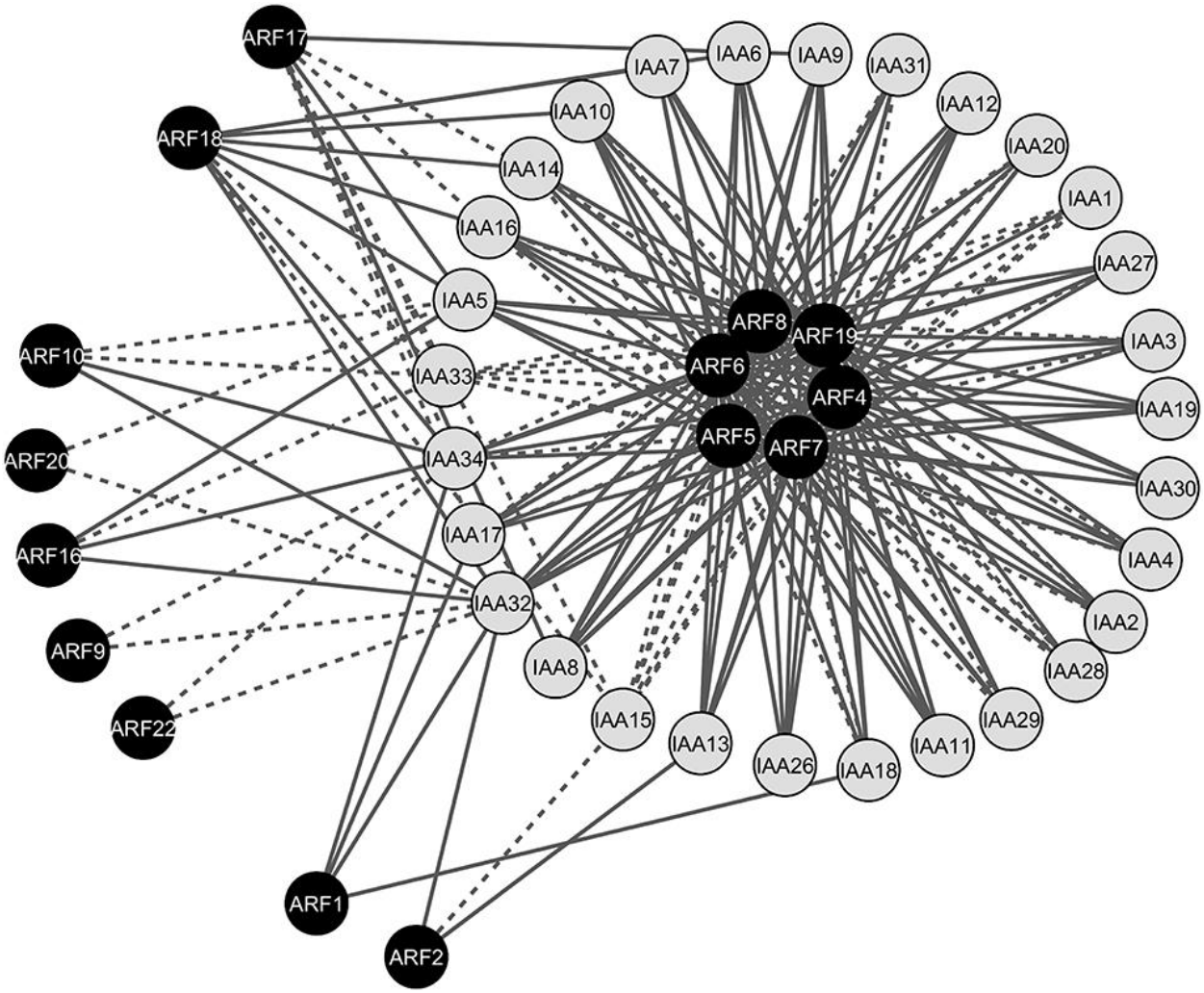

Figure 2-4. Gene co-expression network of the interacting ARF-Aux/IAA proteins.

The network contained 44 nodes (15 ARFs and 29 Aux/IAAs) and 213 edges (interacting combinations). Continuous edges indicate protein pairs with significantly correlated expression profiles in at least one tissue, whereas dotted edges indicate protein pairs without significantly correlated expression profiles.

Figure 2-5. Heatmap demonstrating gene co-expression patterns of the interacting ARF-Aux/IAA proteins in various Arabidopsis tissues and organs.

Sample contribution scores were calculated for each ARF-Aux/IAA interacting combinations and used to construct the heatmap using the Multi Experiment Viewer (http://www.tm4.org/mev.html). Red color represents pairs with highly correlated gene co-expression profiles and green represents highly anti-correlated pairs.

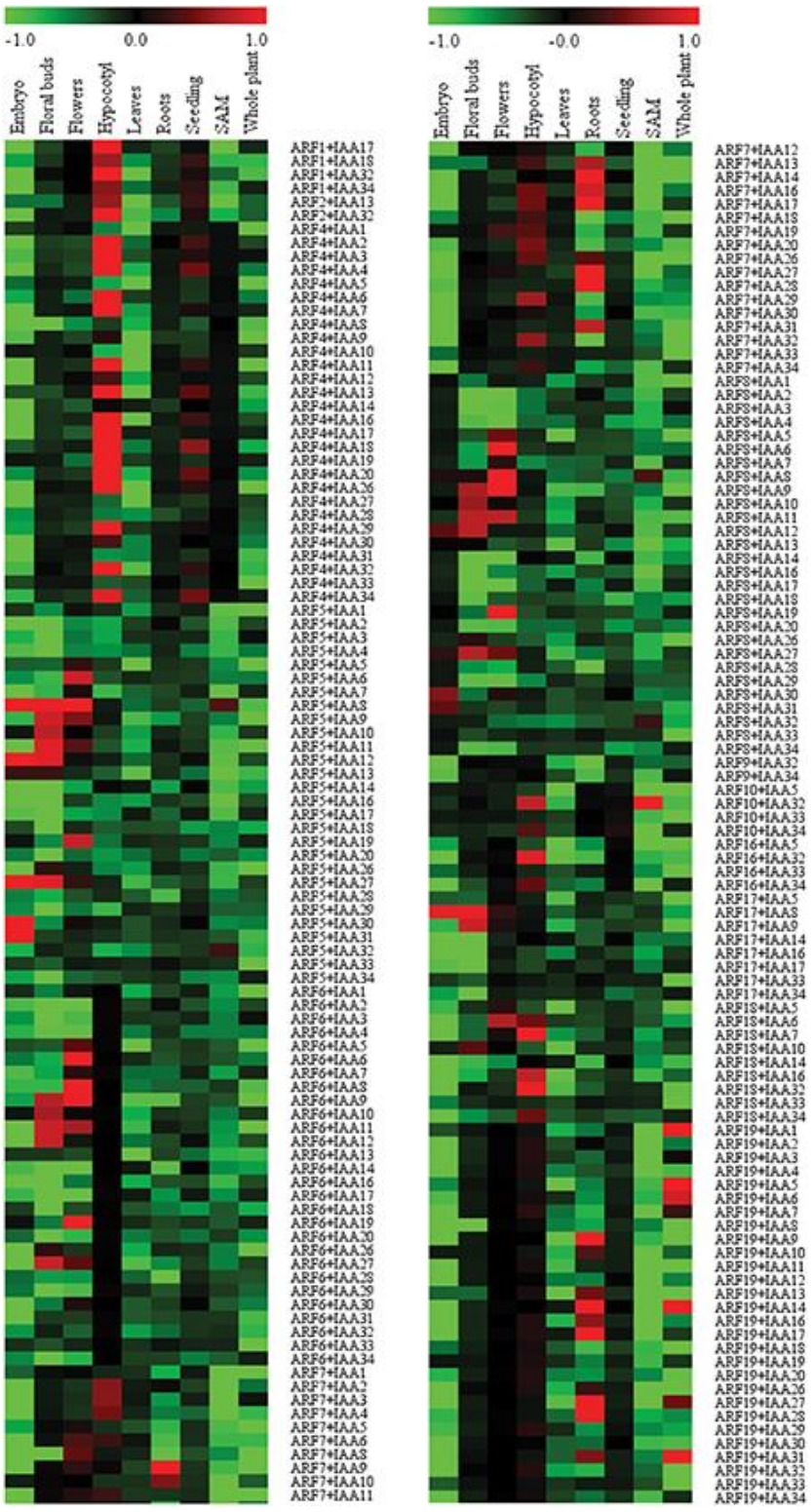

Figure 2-5. contd.

Chapter 3

Elucidating the key roles of Arabidopsis ETHYLENE RESPONSE 1 and ETHYLENE INSENSITIVE factors in mediating plant susceptibility to *Heterodera schachtii*

Abstract

Ethylene regulates various physiological and developmental processes including plant defense responses. Various studies have indicated role of ethylene in plant-nematode interactions. However, role of ethylene in plant-nematode interaction is not well understood. In the current study, we assessed susceptibility of various ethylene signaling mutants of Arabidopsis against *Heterodera schachtii* and identified that ETHYLENE RESPONSE 1 (ETR1), ETHYLENE INSENSITIVE 2 (EIN2) and EIN3/ ETHYLENE INSENSITIVE LIKE 1 (EIL1) positively regulate Arabidopsis susceptibility to *H. schachtii*. Our analysis showed that the receiver domain of ETR1 contributes in ETR1 mediated susceptibility to *H. schachtii*. We observed that a mutation in the ETR1 phosphorylation site and various positions thereafter in the ETR1 receiver domain that are not conserved in ETR1 compared to ETR2 and EIN4 have significant impacts on ETR1 mediated Arabidopsis susceptibility to *H. schachtii*. Our result also suggests that enhanced resistance of the *ein3/eil1* double mutant is due to increased expression of the salicylic acid biosynthesis gene *SALICYLIC ACID INDUCED DEFICIENT 2* (*SID2*) that induce salicylic acid responsive pathogenesis related (PR) protein 1, suggesting crosstalk between ethylene and salicylic acid during Arabidopsis-*H. schachtii* interaction. Taken together our results indicate that ETR1 and EIN3/EIL1 mediate Arabidopsis susceptibility to *H. schachtii* through different pathways where ETR1 alter Arabidopsis susceptibility to *H. schachtii* independent of ethylene signaling via unknown mechanism and EIN3/EIL1 alter Arabidopsis susceptibility to *H. schachtii* by interfering salicylic acid biosynthesis.

1. Introduction

Ethylene is a gaseous plant hormone that regulates a wide range of plant metabolic, physiological, and developmental processes including defense against various pathogens (Broekaert et al., 2006; Schaller, 2012). There are five ethylene receptors in Arabidopsis, ETR1, ETR2, ETHYLENE RESPONSE SENSOR 1 (ERS1), ERS2 and EIN4. These receptors act as negative regulators of ethylene signaling (Hua and Meyerowitz, 1998). In the absence of ethylene, the ethylene receptors activate a Ser/Thr kinase, CTR1 (Kieber et al., 1993; Clark et al., 1998) resulting in inhibition of the downstream ethylene signaling. In the presence of ethylene, the activity of receptors decreases because of ethylene binding to the receptors that, in turn, reduces the activity of CTR1. Reduced activity of CTR1 leads to reduced phosphorylation of EIN2, which in turn results in the proteolytic processing of EIN2, and thus the release of its C-terminal domain that migrates to the nucleus (Ju et al., 2012). The C-terminal domain of EIN2 activates the EIN3 and EIN3 Like1 (EIL1) transcription factors in the nucleus to initiate the transcriptional response to ethylene (Chao et al., 1997; Solano et al., 1998; Alonso et al., 2003).

A role for ethylene signaling in plant-pathogen interactions is well established. In response to pathogen, plants usually show increased ethylene biosynthesis leading to induction of defense related genes (Broekaert et al., 2006). The role of the ethylene receptors in plant-pathogen interactions has not been extensively explored. Arabidopsis and tomato plants with mutations in the ethylene receptor ETR1 were found to be more resistant to *F. oxysporum* (Pantelides et al., 2013). Using Fumonisin B1 (FB1) to induce cell death in various ethylene receptor mutants, Plett et al. (2009) reported that ethylene signaling via ETR1 inhibits cell death while ethylene signaling via EIN4 induces cell death.

There is also strong evidence that the positive regulators of ethylene signaling EIN2, EIN3 and EIL1 play key roles in plant basal defense (Boutrot et al., 2010; Mersmann et al., 2010; Tintor et al., 2013). In addition, previous studies have shown cross-talk of ethylene with other phytohormones, particularly salicylic acid and jasmonic acid. Studies have shown synergistic interactions of ethylene with jasmonic acid and antagonistic interactions with salicylic acid (Chen et al., 2009; Zhu et al., 2011). Zhu et al. (2011) reported that plants with reduced expression of EIN3 and EIL1 showed reduced resistance to *Botrytis cinerea*. With reduced expression of EIN3 and EIL1, expression of JA and ethylene induced genes, PDF1.2, ERF1 and

ORA59, was also reduced when treated with JA that might explain the susceptibility of *ein3/eil1* mutant against *Botrytis cinerea*. Plants with reduced expression of *EIN3* and *EIL1* also showed enhanced pathogen-associated molecular patterns (PAMP) response and reduced susceptibility to *Pseudomonas syringae* (Chen et al., 2009). However, further analysis showed that these two ethylene signaling transcription factors directly regulate the expression of SID2, which encodes isochorismate synthase a key enzyme required for salicylic acid biosynthesis suggesting that EIN3/EIL1 directly target SID2 to repress PAMP response (Wildermuth et al., 2001; Chen et al., 2009).

Cyst nematodes are obligate, biotrophic, sedentary endoparasitic nematodes that belong to the family Heteroderidae. The members of this family induce a feeding site termed a syncytium from where they retrieve all essential nutrient once they become sedentary. Second stage juveniles (J2), which is the only mobile stage of the nematode, penetrate epidermal root cells and migrate intracellularly via the cortex into vascular cylinder. In the vascular cylinder, J2 select a cambial or procambial cell that will become initial feeding cell (IFC). Transition from the IFC to the syncytium involves massive changes in the transcriptome of the host cell (Szakasits et al., 2009; Cabrera et al., 2014). Various transcriptomic studies have shown that large number of genes associated with different phytohormones, particularly auxin and ethylene, are among the genes that are differentially expressed in the syncytium (Gheysen and Mitchum, 2009; Quentin et al., 2012; Cabrera et al., 2014).

The role of ethylene in syncytium development emerged from the finding that Arabidopsis ethylene-overproducing mutants (*eto1, eto2* and *eto3*) are more susceptible to *H. schachtii* (Goverse et al., 2000; Wubben et al., 2001). *H. schachtii* are attracted more toward the ethylene overproducing mutants and ethylene treated plants (Wubben et al., 2001; Kammerhofer et al., 2015; Hu et al., 2017). These findings suggest that ethylene plays positive role in attracting cyst nematodes towards the host root. In contrast, suppression of ethylene responsive genes in the syncytium suggests a negative role of ethylene in cyst nematodes development. The expression of ethylene family genes- *RAP2*.3 and *RAP2*.6 that enhance plant basal defense response, were downregulated in *H. schachtii* induced syncytium (Hermsmeier et al., 2000; Ali et al., 2013). Likewise, expression of soybean ethylene responsive element- binding protein gene (*EREBP1*) was also downregulated in soybean cyst nematode infected susceptible plants and upregulated in

resistant plants (Mazarei et al., 2002; Mazarei et al., 2007). Collectively, these results suggest that ethylene plays a dual role in plant-cyst nematode interaction that is dependent in the stage of parasitism. During early stage, it plays negative regulator of plant defense by attracting nematodes towards the host, and later it plays positive regulator of plant defense against nematode development (Kammerhofer et al., 2015).

Previous studies have shown that ethylene plays important role in plant-nematode interaction. But the underlying mechanism that mediates plant susceptibility to cyst nematode is not well-understood. In this chapter, we present *H. schachtii* susceptibility of various single and higher order Arabidopsis ethylene signaling mutants and explore the underlying mechanisms by which ethylene signaling mediate Arabidopsis susceptibility to *H. schachtii*.

2. Results

2.1 Reduced expression of ETR1 diminishes Arabidopsis susceptibility to H. schachtii

In order to elucidate the role of ethylene receptors on plant susceptibility to *H. schachtii*, various single loss-of-function mutant lines of Arabidopsis ethylene receptors ETR1 (*etr1-6*, *etr1-7*), ETR2 (*etr2-3*), ERS1 (*ers1-2*, *ers1-3*), ERS2 (*ers2-3*), EIN4 (*ein4-4*), and double mutants (*etr1-6/etr2-3*, *etr1-6/ein4-4*, and *etr2-3/ein4-4*) were evaluated for their susceptibility to *H. schachtii* (Figure 3-1A). We observed that ETR1 single mutants were less susceptible to *H. schachtii* compared to wild-type (Col-0). Arabidopsis mutants of ETR2 and EIN4, and their double mutant have no altered susceptibility to *H. schachtii*. Although, *etr2-3* and *ein4-4* single mutants had no altered susceptibility to *H. schachtii* compared to the wild type, their double mutants with ETR1, *etr1-6/etr2-3* and *etr1-6/ein4-4* double mutants, were less susceptible to *H. schachtii*. In addition, mutant for CTR1 that has very short root was also less susceptible to *H. schachtii* compared to wild type (Figure 3-1A). Increased resistance of *ctr1-2* mutant could be attributed to the very short root of *ctr1-2*. Therefore, further analysis of this mutant was not conducted. We also observed inconsistent result for the mutants of ERS1. We observed that knockdown mutant *ers1-2* was less susceptible to *H. schachtii* compared to the wild-type Wassilewskija (WS) but the knockout mutant *ers1-3* showed no difference in Arabidopsis susceptibility to *H. schachtii* compared to the wild type (Figure 3-1B). Likewise, *H. schachtii* susceptibility of *ers2-3* was also comparable to the wild-type (WS). These results provide strong evidence that reduced expression of ETR1 makes Arabidopsis less susceptible to *H. schachtii.*

2.2 ETR1 receiver domain contributes in Arabidopsis susceptibility to H. schachtii

To confirm the role of ETR1 in *H. schachtii*-Arabidopsis interaction, we evaluated nematode susceptibility of *etr1-6/etr2-3/ein4-4* triple mutant transformed with genomic ETR1 (gETR1) transgene and full-length ETR1 cDNA (cETR1). We observed that *H. schachtii* susceptibility of gETR1 was restored at the level of wild type but in cETR1 *H. schachtii* susceptibility was partially restored compared to the wild type (Figure 3-2). This difference could be due to lower ETR1 expression in cETR1 compared to gETR1. We also performed nematode susceptibility of *etr1-6/etr2-3/ein4-4* transformed with truncated ETR1 cDNA lacking receiver domain (cETR1-ΔR). Intriguingly, we observed that there was no change in the nematode susceptibility of cETR1-ΔR compared to the *etr1-6/etr2/3ein4-4* triple mutant. These results suggest that the ETR1 receiver domain has role in ETR1-mediated plant susceptibility to *H. schachtii*.

2.3. Effect of ETR1 receiver domain point mutation on Arabidopsis-H. schachtii interaction

Recently, Bakshi et al. (2015) has identified twelve amino acid sites in the ETR1 receiver domain that are not conserved in the receiver domains of ETR2 and EIN4 and created point mutation in the full length genomic ETR1. To test if specific site in ETR1 receiver domain has role in ETR1-mediated Arabidopsis susceptibility to *H. schachtii*, we evaluated nematode susceptibility of the *etr1-6/etr2-3/ein4-4* triple mutant containing point mutation in the ETR1 receiver domain that include E617A, N618A, C661A, V665A, E666A, N667A, Q681A, R682A, Q682A, Q684A, E730A and L734A (Figure 3-3A and B). We observed that out of these twelve point mutants, E617A and N618A restored nematode susceptibility at the level of wild type or the gETR1, while E666A and Q681A failed to restore nematode susceptibility and showed phenotype similar to the *etr1-6/etr2-3/ein4-4* triple mutant. Nematode susceptibility of the remaining eight mutants (D659A, D661A, V665A, E667A, R682A, Q684A, E730A and L734A) were intermediate between gETR1 and *etr1-6/etr2-3/ein4-4* triple mutant. This suggests that amino acids at position 666 and 681 of ETR1 receiver domain have significant impact on ETR1 mediated Arabidopsis susceptibility to *H. schachtii*.

2.4 Reduced expression of EIN3 and EIL1 makes Arabidopsis more resistant to H. schachtii

To understand the effect of positive regulators of ethylene signaling on Arabidopsis susceptibility to *H. schachtii*, we assessed the nematode susceptibility of the mutants of EIN2,

EIN3 and EIL1. Arabidopsis mutants for the EIN2, *ein2-5*, was less susceptible to *H. schachtii* that showed 28 percent reduction in J4 females compared to the wild type (Figure 3-4A). Unlike the previous study, that showed enhanced nematode resistance to *ein3* mutant (Wubben et al., 2001), we did not observe any difference in the nematode susceptibility of *ein3*-1 compared to the wild type (Figure 3-4A). Also, the nematode susceptibility of *eil1-1* mutant was comparable to the wild type (Figure 3-4A). However, we observed that *ein3-1/eil1-1* double mutant was less susceptible to *H. schachtii* compared to the wild type (Figure 3-4A). We observed 25% reduction in J4 females in *ein3-1/eil1-1* double mutant compared to the wild type. Increased resistance of EIN2 mutant, that fails to accumulate EIN3 and EIL1, and EIN3/EIL1 double mutant suggest redundant function of EIN3 and EIL1 in regulating Arabidopsis susceptibility to *H. schachtii*.

2.5 Increased expression of SID2 in ein/eil1 enhance resistance to H. schachtii

EIN3 and EIL1 negatively regulate the expression of *SID2* that encodes salicylic acid biosynthesis gene ISOCHORISMATE SYNTHASE 1 (ICS1) (Chen et al., 2009). In order to test if the expression of SID2 is induced by EIN3/EIL1 in Arabidopsis root tissue infected by *H. schachtii*, we performed qRT-PCR quantification of *SID2* in *ein3-1/eil1-1* root tissue collected 3 days after *H. schachtii* infection and corresponding non-infected root tissues. The result showed two-fold increase in *SID2* expression under non-infected condition compared to the wild type (Figure 3-4B). Under *H. schachtii* infected condition, we observed that the expression of *SID2* was at least three-fold higher than the non-infected wild type root tissues (Figure 3-4B). Considering the fact that SID2 is involved in salicylic acid biosynthesis, this result implies possible cross-talk between ethylene and salicylic acid during Arabidopsis-*H. schachtii* interaction.

To test if SID2 is responsible for increased resistance to *H. schachtii* in *ein3-1/eil1-1* mutants, we evaluated nematode susceptibility of *sid2-2* and *ein3-1/eil1-1/sid2-2* mutants. We observed that both *sid2-2* and *ein3-1/eil1-1/sid2*-2 mutants were more susceptible to *H. schachtii* compared to the wild type (Figure 3-4C). Number of J4 female nematodes in *sid2-2* and *ein3-1/eil1-1/sid2-2* was 24% and 39% higher than wild type respectively. Loss of increased resistance to *H. schachtii* from *ein3-1/eil1-1* with the reduced expression of SID2 suggests that increased resistance of *ein3-1/eil1-1* to *H. schachtii* is mediated by SID2. This result also confirms cross-

talk between ethylene signaling and salicylic acid biosynthesis during Arabidopsis-*H. schachtii* interaction.

2.6 SID2 induces PR1 expression in response to H. schachtii infection

SA production due to pathogen infection induces various pathogenesis related (PR) genes that include PR-1, PR-2 and PR-5, and these PR genes are used as molecular markers of SA signaling pathway (Durrant and Dong, 2004). We quantified the expression of *PR1*, *PR2* and *PR5* in the root tissues of *ein3-1/eil1-1*, *sid2-2*, *ein3-1/eil1-1/sid2-2*, and wild-type (Col-0) Arabidopsis plants infected with *H. schachtii* at 3 dpi, and the corresponding non-infected root tissues to test if these SA related PR genes are induced in response to *H. schachtii* infection. Under non-infected condition, expression of all three PR genes were lower in all mutants compared to wild type except *PR1* gene that showed more than two-fold higher expression in *ein3-1/eil1-1* compared to the wild type and expression of *PR1* gene in *sid2-2* single mutant was comparable to wild type (Figure 3-5A).

Under *H. schachtii* infected condition, *sid2-2* and *ein3-1/eil1-1/sid2-2* showed reduction in *PR1* expression compared to the wild type while the expression of *PR2* was similar to wild type (Figure 3-5B). Expression of *PR5* in *sid2-2* was similar to wild type while downregulated in *ein3-1/eil1-1/sid2-2*. On the other hand, *ein3-1/eil1-1* showed enhanced expression of all three PR genes, particularly *PR1* that showed six-fold higher expression compared to the wild type (Figure 3-5B). Collectively, our results suggest that reduced susceptibility of *ein3-1/eil1-1* to *H. schachtii* is due to SID2 mediated increased expression of PR1 gene.

3. Discussion

The role of ethylene in plant immunity is complex due to its pleiotropic role in various plant growth and development processes including plant defense responses (Boutrot et al., 2010). In the current study, we evaluated the nematode susceptibility of various single and higher order ethylene receptor loss-of-function mutants and identified that ETR1 contributes to Arabidopsis susceptibility of *H. schachtii*. Similarly, we also assessed nematode susceptibility of the mutant of the downstream components that function as positive regulators of ethylene signaling and identified that EIN2 and EIN3/EIL1 contribute to Arabidopsis susceptibility to *H. schachtii*. The mutants of both the positive and negative regulators of ethylene signaling reduced Arabidopsis

susceptibility to *H. schachtii* suggesting that ethylene signaling regulates plant susceptibility to *H. schachtii* through more than one mechanisms.

Ethylene receptors have overlapping and distinct functions in various plant phenotype (Shakeel et al., 2013). In this study, we observed that the ETR1 ethylene receptor alone can alter Arabidopsis susceptibility to *H. schachtii*. Various plant phenotype regulated by ETR1 has different ETR1 domain requirements (Bakshi et al., 2015). There are various ETR1 regulated traits that require full-length ETR1 while there are other traits that ETR1 can regulate without its receiver domain (Kim et al., 2011; Hall et al., 2012; Wilson et al., 2014; Bakshi et al., 2015). Our analysis showed that the receiver domain of ETR1 contributes to ETR1 mediated susceptibility to *H. schachtii*. Recently, Bakshi et al. (2015) showed that specific regions in the ETR1 receiver domain play vital role in regulating plant phenotype. Assessment of the nematode susceptibility of Arabidopsis triple mutant *etr1-6/etr2-3/ein4-4* transformed with genomic ETR1 containing point mutation in receiver domain that are not conserved in either ETR2 or EIN4 showed that majority of the non-conserved amino acids in ETR1 has role in Arabidopsis-*H. schachtii* interaction. Mutations in gETR1^{E617A} and gETR1^{E618A} that lie upstream of the phosphorylation site (659) did not alter Arabidopsis susceptibility to *H. schachtii* compared to the wild type version (gETR1). Any mutation in and after phosphorylation site, at least partially, altered plant susceptibility to *H. schachtii*. gETR1^{E666A} that comprises mutation in the γ loop and gETR1^{Q681A} containing mutation in the C-terminal tail were among the sites that completely failed to restore Arabidopsis susceptibility to *H. schachtii* to the wild type level. While remaining mutations on other sites (gETR1^{D659A}, gETR1^{D661A}, gETR1^{V665A}, gETR1^{E667A}, gETR1^{R682A}, gETR1^{Q684A}, gETR1^{E730A} and gETR1^{L734A}) partially restored plant susceptibility to *H. schachtii*. Underlying mechanism on how these receiver domain sites affect plant phenotypes are not known. However, γ loop (662-667) that lie adjacent to the phosphorylation site, and the C-terminal tail are predicted to be involved in the interaction with other proteins (Muller-Dieckmann et al., 1999; Mayerhofer et al., 2015). Therefore, it is possible that mutation in these specific sites of the ETR1 receiver domain interfere interaction with other proteins affecting plant susceptibility to *H. schachtii*. These results suggest significant role of ETR1 phosphorylation sites and the region downstream of phosphorylation sites in ETR1-mediated Arabidopsis susceptibility to *H. schachtii.*

The synergistic interaction between ethylene and jasmonic acid to positively regulate plant defense against necrotrophic pathogens is well established (van Loon et al., 2006). However, ethylene also functions antagonistically by interacting with salicylic acid that positively regulates plant defense response, especially against biotrophic pathogens (van Loon et al., 2006; Chen et al., 2009). Roles of both ethylene and salicylic acid in plant defense response against nematode are well established (Wubben et al., 2001; Wubben et al., 2008; Fudali et al., 2013; Kammerhofer et al., 2015). However, the antagonistic interaction between these phytohormones in plant-nematode interaction is not known. Our results showed antagonistic interaction between ethylene signaling and salicylic acid to mediate plant defense response against biotrophic *H. schachtii*. Previously, Wubben et al. (2001) reported that Arabidopsis *ein3* mutant are less susceptible to *H. schachtii* compared to wild type. However, we did not observe significant difference in nematode susceptibility between *ein3-1* mutant and the wild type. Nevertheless, we observed that Arabidopsis double mutant *ein3-1/eil1-1*, and *ein2-5* that failed to accumulate EIN3 and EIL1 were more resistant to *H. schachtii.* This likely indicate redundant function of EIN3 and EIL1 in Arabidopsis susceptibility to *H. schachtii* that has been previously reported for other traits (Chao et al., 1997; Solano et al., 1998). Expression of *SID2* was upregulated in the *ein3/eil1* double mutant. SID2 encodes ICS1 that catalyzes the biosynthesis of salicylic acid (Wildermuth et al., 2001) and positively regulates the plant defense response. Therefore, the enhanced resistance of *ein3/eil1* could be attributed to increased expression of SID2. In agreement with this, the triple mutant *ein3/eil1/sid2* was found to be more susceptible to *H. schachtii* like Arabidopsis *sid2* mutant indicating that EIN3 and EIL1 mediate susceptibility to *H. schachtii* by regulating the expression of SID2. This result is consistent with the finding that EIN3 and EIL1 mediate plant susceptibility to *Pseudomonas syringae* by regulating the salicylic acid biosynthesis (Chen et al., 2009). Our results show that the enhanced resistance of mutant is mainly due to SID2-mediated enhanced expression of salicylic acid responsive *PR1* gene while *PR2* and *PR5* do not have much contribution. This is consistent with the findings that Arabidopsis can induce *PR2* and *PR5* against *H. schachtii* infection in salicylic acid independent manner (Wubben et al., 2008).

Hormonal cross-talk has been considered as one of the mechanisms that mediate trade-off between plant growth and defense responses (Huot et al., 2014). Considering the fact that EIN3/EIL1 are the master regulator of ethylene signaling and regulate various developmental

process and could also regulate defense response by antagonistically interacting with salicylic acid, EIN3/EIL1 may be considered as the node that mediate trade-off between plant growth and defense response (Chen et al., 2009; Chang et al., 2013). Under normal condition increased levels of EIN3/EIL1 inhibit defense response and regulate plant growth and development normally. In response to pathogen infection, expression of EIN3/EIL1 reduces that enhances plant defense response via salicylic acid pathway and divert resources for plant defense instead of growth and development.

In short, our results suggest that the ETR1 receiver domain particularly the putative phosphorylation site and regions downstream of phosphorylation regulate ETR1 mediated plant susceptibility. Our results also indicate cross-talk between ethylene and salicylic acid during *H. schachtii* infection to Arabidopsis where ethylene signaling regulate the expression of salicylic acid biosynthesis gene SID2 to mediate *H. schachtii* infection to Arabidopsis.

4. Methods

Plant material and growth conditions

All mutants are in Coloumbia-0 (Col-0) background except *etr1-9*, *ers1-3*, *ers1-2* and *ers2-3* which are in Wassilewskija (WS) background. Plant materials used in this study include *etr1-6*, *etr1-7*, *etr2-3*, *ers2-3*, *ein4-4*, *etr1-6;etr2-3*, *etr2-3;ein4-4* (Hua and Meyerowitz, 1998), *ers1-2* (Hall and Bleecker, 2003), *ein2-5* (Alonso et al., 2003), *ein3-1* (Chao et al., 1997), *eil1-1*, *ein3-1/eil1-1* (Alonso et al., 2003), *sid2-2* (Dewdney et al., 2000), *ein3-1/eil1-1/sid2-2* (Chen et al., 2009), *etr1-6;etr2-3;ein4-4*, gETR1, cETR1, D659A, cETR1-ΔR (Hall and Bleecker, 2003; Wang et al., 2003; Binder et al., 2006; Kim et al., 2011). Remaining eleven point mutants of ETR1 has been previously described in (Bakshi et al., 2015).

Nematode Susceptibility Assay

Arabidopsis mutant seeds along with wild-type controls (Col-0 and WS) were surface sterilized with 2.8% bleach followed by four washes with sterilized double distilled water. Seeds were then planted in 12-well falcon culture plates (BD Biosciences) containing modified Knop's medium (Sijmons et al., 1994) solidified with 0.8% Daishin agar (Brunschwig Chemie) in a random block design. Plants were grown in growth chamber at 24^0C under long day conditions (16-h-light/8-h-dark). After 10 days, seedlings were inoculated with 200 surface-sterilized J2 *H. schachtii*

nematodes as previously described by (Baum et al., 2000). Inoculated plants were kept under dark at 24^0C for two days and then transferred into growth chamber at 24^0C under long day conditions. After three weeks, number of *H. schachtii* J4 female nematodes were counted. Two independent experiments with at least 20 replications were carried out.

RNA Isolation and Quantitative Real-Time RT-PCR

Total RNA was extracted from 20 mg frozen ground root tissue collected after 3 days of *H. schachtii* infection and corresponding non-infected root tissues following the method described by Verwoerd et al. (1989). The isolated total RNA was treated with DNase I (Invitrogen). Ten nanograms of DNase-treated RNA was used as a template in quantitative RT-PCR reactions to quantify mRNA expression levels using the Verso SYBR green 1-Step qRT-PCR Rox mix (Thermo Scientific) following the manufacturer's protocol. The PCR program was 50°C for 15 min, 95°C for 15 min followed by 40 cycles of 95°C for 15 s, 60°C for 90 s and 72°C for 30 s. Dissociation curve was created by subjecting the PCR amplification products using the following program: 95°C for 15 s and 60°C for 75 s, followed by a slow gradient from 60°C to 95°C. PCR was performed using QuantStudio 6 Flex Real-Time PCR System (Applied Biosystems). Transcript data was normalized using Actin8 (AT1G49240) as internal control. Primers sequences used in this study in presented in Table 3-1.

Acknowledgement

We would like to thank Jian-Min Zhou for providing *sid2-2* and *ein3-1/eil1-1/sid2-2* mutants.

References

Ali MA, Abbas A, Kreil DP, Bohlmann H (2013) Overexpression of the transcription factor RAP2.6 leads to enhanced callose deposition in syncytia and enhanced resistance against the beet cyst nematode *Heterodera schachtii* in Arabidopsis roots. BMC Plant Biol **13**

Alonso JM, Stepanova AN, Leisse TJ, Kim CJ, Chen H, Shinn P, Stevenson DK, Zimmerman J, Barajas P, Cheuk R, Gadrinab C, Heller C, Jeske A, Koesema E, Meyers CC, Parker H, Prednis L, Ansari Y, Choy N, Deen H, Geralt M, Hazari N, Hom E, Karnes M, Mulholland C, Ndubaku R, Schmidt I, Guzman P, Aguilar-Henonin L, Schmid M, Weigel D, Carter DE, Marchand T, Risseeuw E, Brogden D, Zeko A, Crosby WL, Berry CC, Ecker JR (2003) Genome-wide insertional mutagenesis of *Arabidopsis thaliana*. Science **301:** 653-657

Alonso JM, Stepanova AN, Solano R, Wisman E, Ferrari S, Ausubel FM, Ecker JR (2003) Five components of the ethylene-response pathway identified in a screen for weak ethylene-insensitive mutants in Arabidopsis. Proc Natl Acad Sci USA **100:** 2992-2997

Bakshi A, Wilson RL, Lacey RF, Kim H, Wuppalapati SK, Binder BM (2015) Identification of regions in the receiver domain of the ETHYLENE RESPONSE1 ethylene receptor of Arabidopsis important for functional divergence. Plant Physiol **169:** 219-232

Baum TJ, Wubben MJE, Hardy KA, Su H, Rodermel SR (2000) A screen for *Arabidopsis thaliana* mutants with altered susceptibility to *Heterodera schachtii*. J Nematol **32:** 166-173

Binder BM, O'Malley RC, Wang W, Zutz TC, Bleecker AB (2006) Ethylene stimulates nutations that are dependent on the ETR1 receptor. Plant Physiol **142:** 1690-1700

Boutrot F, Segonzac C, Chang KN, Qiao H, Ecker JR, Zipfel C, Rathjen JP (2010) Direct transcriptional control of the Arabidopsis immune receptor FLS2 by the ethylene-dependent transcription factors EIN3 and EIL1. Proc Natl Acad Sci USA **107:** 14502-14507

Broekaert WF, Delaure SL, De Bolle MF, Cammue BP (2006) The role of ethylene in host-pathogen interactions. Annu Rev Phytopathol **44:** 393-416

Cabrera J, Barcala M, Fenoll C, Escobar C (2014) Transcriptomic signatures of transfer cells in early developing nematode feeding cells of Arabidopsis focused on auxin and ethylene signaling. Front Plant Sci **5:** 107

Chang KN, Zhong S, Weirauch MT, Hon G, Pelizzola M, Li H, Huang S-sC, Schmitz RJ, Urich MA, Kuo D (2013) Temporal transcriptional response to ethylene gas drives growth hormone cross-regulation in Arabidopsis. Elife **2:** e00675

Chao Q, Rothenberg M, Solano R, Roman G, Terzaghi W, Ecker JR (1997) Activation of the ethylene gas response pathway in Arabidopsis by the nuclear protein ETHYLENE-INSENSITIVE3 and related proteins. Cell **89:** 1133-1144

Chen HM, Xue L, Chintamanani S, Germain H, Lin HQ, Cui HT, Cai R, Zuo JR, Tang XY, Li X, Guo HW, Zhou JM (2009) ETHYLENE INSENSITIVE3 and ETHYLENE INSENSITIVE3-LIKE1 repress SALICYLIC ACID INDUCTION DEFICIENT2 expression to negatively regulate plant innate immunity in Arabidopsis. Plant Cell **21:** 2527-2540

Clark KL, Larsen PB, Wang X, Chang C (1998) Association of the Arabidopsis CTR1 Raf-like kinase with the ETR1 and ERS ethylene receptors. Proc Natl Acad Sci USA **95:** 5401-5406

Dewdney J, Reuber TL, Wildermuth MC, Devoto A, Cui J, Stutius LM, Drummond EP, Ausubel FM (2000) Three unique mutants of Arabidopsis identify eds loci required for limiting growth of a biotrophic fungal pathogen. Plant J **24:** 205-218

Durrant WE, Dong X (2004) Systemic acquired resistance. Annu Rev Phytopathol **42:** 185-209

Fudali SL, Wang C, Williamson VM (2013) Ethylene signaling pathway modulates attractiveness of host roots to the root-knot nematode *Meloidogyne hapla*. Mol Plant Microbe Interact **26:** 75-86

Gheysen G, Mitchum MG (2009) Molecular insights in the susceptible plant response to nematode infection. *In* RH Berg, CG Taylor, eds, Cell Biology of Plant Nematode Parasitism. Springer, Verlag Berlin Heidelberg

Goverse A, Overmars H, Engelbertink J, Schots A, Bakker J, Helder J (2000) Both induction and morphogenesis of cyst nematode feeding cells are mediated by auxin. Mol Plant Microbe Interact **13:** 1121-1129

Hall AE, Bleecker AB (2003) Analysis of combinatorial loss-of-function mutants in the Arabidopsis ethylene receptors reveals that the *ers1etr1* double mutant has severe developmental defects that are EIN2 dependent. Plant Cell **15:** 2032-2041

Hall BP, Shakeel SN, Amir M, Haq NU, Qu X, Schaller GE (2012) Histidine kinase activity of the ethylene receptor ETR1 facilitates the ethylene response in Arabidopsis. Plant Physiol **159:** 682-695

Hermsmeier D, Hart JK, Byzova M, Rodermel SR, Baum TJ (2000) Changes in mRNA abundance within *Heterodera schachtii*-infected roots of *Arabidopsis thaliana*. Mol Plant Microbe Interact **13:** 309-315

Hu Y, You J, Li C, Williamson VM, Wang C (2017) Ethylene response pathway modulates attractiveness of plant roots to soybean cyst nematode *Heterodera glycines*. Sci Rep **7**

Hua J, Meyerowitz EM (1998) Ethylene responses are negatively regulated by a receptor gene family in *Arabidopsis thaliana*. Cell **94:** 261-271

Huot B, Yao J, Montgomery BL, He SY (2014) Growth–defense tradeoffs in plants: a balancing act to optimize fitness. Mol Plant **7:** 1267-1287

Ju C, Yoon GM, Shemansky JM, Lin DY, Ying ZI, Chang J, Garrett WM, Kessenbrock M, Groth G, Tucker ML, Cooper B, Kieber JJ, Chang C (2012) CTR1 phosphorylates the central regulator EIN2 to control ethylene hormone signaling from the ER membrane to the nucleus in Arabidopsis. Proc Natl Acad Sci USA **109:** 19486-19491

Kammerhofer N, Radakovic Z, Regis JM, Dobrev P, Vankova R, Grundler FM, Siddique S, Hofmann J, Wieczorek K (2015) Role of stress-related hormones in plant defence during early infection of the cyst nematode *Heterodera schachtii* in Arabidopsis. New Phytol **207:** 778-789

Kieber JJ, Rothenberg M, Roman G, Feldmann KA, Ecker JR (1993) CTR1, a negative regulator of the ethylene response pathway in Arabidopsis, encodes a member of the raf family of protein kinases. Cell **72:** 427-441

Kim H, Helmbrecht EE, Stalans MB, Schmitt C, Patel N, Wen C-K, Wang W, Binder BM (2011) Ethylene receptor ETHYLENE RECEPTOR1 domain requirements for ethylene responses in Arabidopsis seedlings. Plant Physiol **156:** 417-429

Mayerhofer H, Panneerselvam S, Kaljunen H, Tuukkanen A, Mertens HD, Mueller-Dieckmann J (2015) Structural model of the cytosolic domain of the plant ethylene receptor 1 (ETR1). J Biol Chem **290:** 2644-2658

Mazarei M, Elling AA, Maier TR, Puthoff DP, Baum TJ (2007) GmEREBP1 is a transcription factor activating defense genes in soybean and Arabidopsis. Mol Plant Microbe Interact **20:** 107-119

Mazarei M, Puthoff DP, Hart JK, Rodermel SR, Baum TJ (2002) Identification and characterization of a soybean ethylene-responsive element-binding protein gene whose mRNA expression changes during soybean cyst nematode infection. Mol Plant Microbe Interact **15:** 577-586

Mersmann S, Bourdais G, Rietz S, Robatzek S (2010) Ethylene signaling regulates accumulation of the FLS2 receptor and is required for the oxidative burst contributing to plant immunity. Plant Physiol **154:** 391-400

Muller-Dieckmann HJ, Grantz AA, Kim SH (1999) The structure of the signal receiver domain of the *Arabidopsis thaliana* ethylene receptor ETR1. Structure **7:** 1547-1556

Pantelides IS, Tjamos SE, Pappa S, Kargakis M, Paplomatas EJ (2013) The ethylene receptor ETR1 is required for *Fusarium oxysporum* pathogenicity. Plant Pathol **62:** 1302-1309

Plett JM, Cvetkovska M, Makenson P, Xing T, Regan S (2009) Arabidopsis ethylene receptors have different roles in Fumonisin B 1-induced cell death. Physiol Mol Plant Pathol **74:** 18-26

Quentin M, Hewezi T, Damiani I, Abad P, Baum T, Favery B (2012) How pathogens affect root structure. Root Genomics and Soil Interactions**:** 189-210

Shakeel SN, Wang X, Binder BM, Schaller GE (2013) Mechanisms of signal transduction by ethylene: overlapping and non-overlapping signalling roles in a receptor family. AoB Plants **5:** plt010

Sijmons PC, Atkinson HJ, Wyss U (1994) Parasitic Strategies of Root Nematodes and Associated Host-Cell Responses. Annu Rev Phytopathol **32:** 235-259

Solano R, Stepanova A, Chao Q, Ecker JR (1998) Nuclear events in ethylene signaling: a transcriptional cascade mediated by ETHYLENE-INSENSITIVE3 and ETHYLENE-RESPONSE-FACTOR1. Genes Dev **12:** 3703-3714

Szakasits D, Heinen P, Wieczorek K, Hofmann J, Wagner F, Kreil DP, Sykacek P, Grundler FM, Bohlmann H (2009) The transcriptome of syncytia induced by the cyst nematode *Heterodera schachtii* in Arabidopsis roots. Plant J **57:** 771-784

Tintor N, Ross A, Kanehara K, Yamada K, Fan L, Kemmerling B, Nurnberger T, Tsuda K, Saijo Y (2013) Layered pattern receptor signaling via ethylene and endogenous elicitor peptides during Arabidopsis immunity to bacterial infection. Proc Natl Acad Sci USA **110:** 6211-6216

van Loon LC, Geraats BPJ, Linthorst HJM (2006) Ethylene as a modulator of disease resistance in plants. Trends Plant Sci **11:** 184-191

Verwoerd TC, Dekker BMM, Hoekema A (1989) A small-scale procedure for the rapid isolation of plant RNAs. Nucleic acids Res **17:** 2362-2362

Wang W, Hall AE, O'Malley R, Bleecker AB (2003) Canonical histidine kinase activity of the transmitter domain of the ETR1 ethylene receptor from Arabidopsis is not required for signal transmission. Proc Natl Acad Sci USA **100:** 352-357

Wildermuth MC, Dewdney J, Wu G, Ausubel FM (2001) Isochorismate synthase is required to synthesize salicylic acid for plant defence. Nature **414:** 562-565

Wilson RL, Kim H, Bakshi A, Binder BM (2014) The ethylene receptors ETHYLENE RESPONSE1 and ETHYLENE RESPONSE2 have contrasting roles in seed germination of Arabidopsis during salt stress. Plant Physiol **165:** 1353-1366

Wubben MJE, Jin J, Baum TJ (2008) Cyst nematode parasitism of *Arabidopsis thaliana* is inhibited by salicylic acid (SA) and elicits uncoupled SA-independent pathogenesis-related gene expression in roots. Mol Plant Microbe Interact **21:** 424-432

Wubben MJE, Su H, Rodermel SR, Baum TJ (2001) Susceptibility to the sugar beet cyst nematode is modulated by ethylene signal transduction in *Arabidopsis thaliana*. Mol Plant Microbe Interact **14:** 1206-1212

Zhu ZQ, An FY, Feng Y, Li PP, Xue L, Mu A, Jiang ZQ, Kim JM, To TK, Li W, Zhang XY, Yu Q, Dong Z, Chen WQ, Seki M, Zhou JM, Guo HW (2011) Derepression of ethylene-stabilized transcription factors (EIN3/EIL1) mediates jasmonate and ethylene signaling synergy in Arabidopsis. Proc Natl Acad Sci USA **108:** 12539-12544.

Appendix

Table 3-1. Primers sequences used in this study

Gene	Direction	Sequence (5'-3')
PR1	Forward	TTCACAACCAGGCACGAGGAG
	Reverse	GCCAGACAAGTCACCGCTACC
PR2	Forward	CTTGAACGTCTCGCCTCCAGTC
	Reverse	TCCAGAAACCGCGTTCTCGATG
PR5	Forward	CAATTGCCCTACCACCGTCTGG
	Reverse	CTTAGACCGCCACAGTCTCCG
SID2	Forward	ATGAAGTTGAGAAACAGATCT
	Reverse	GGTGAACTTTTCTGGTTAATC

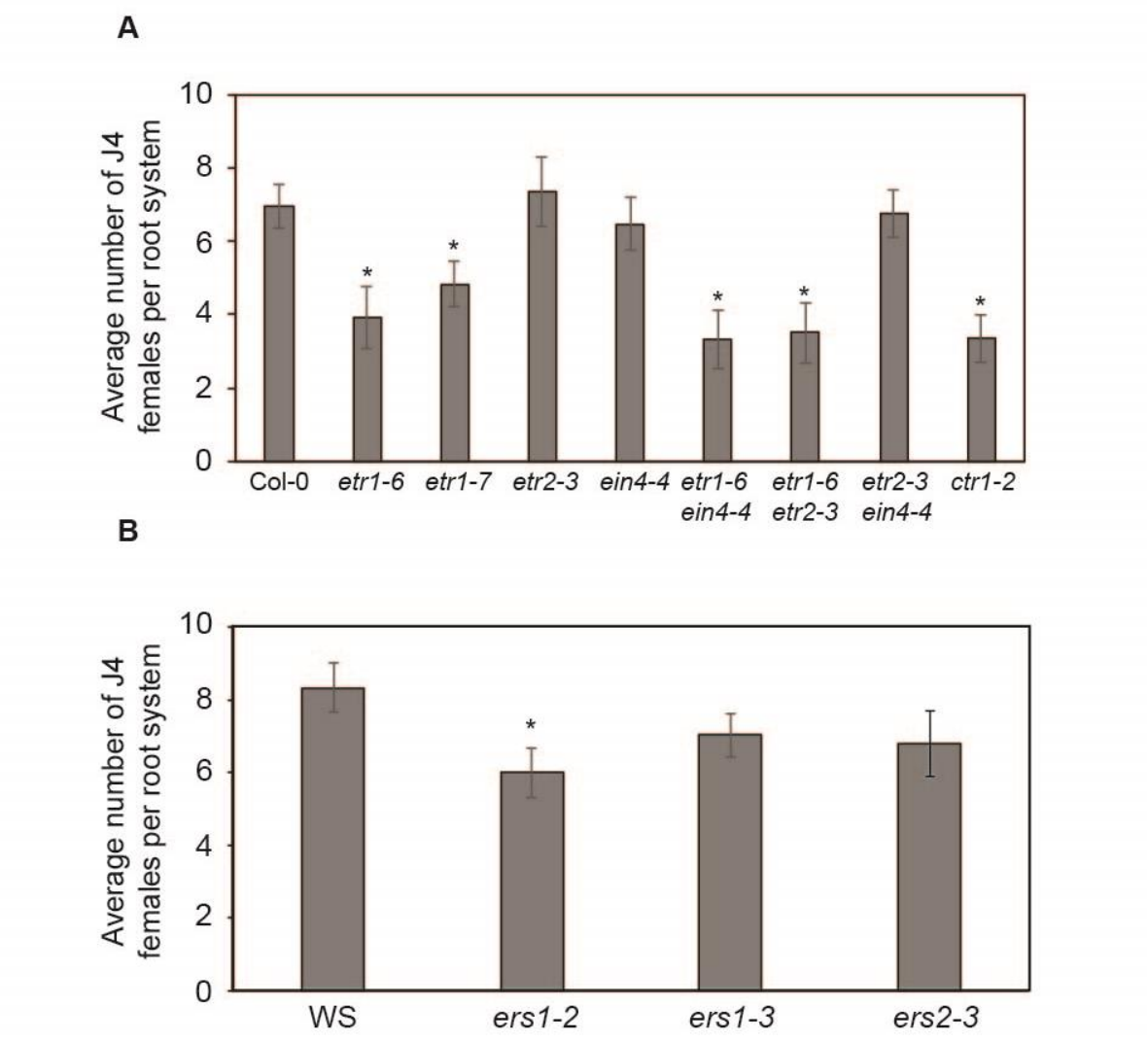

Figure 3-1. ETR1 positively regulates plant susceptibility to *H. schachtii*.

Single and higher order mutants of *ETR1* is less susceptible to *H. schachtii* compared to the wild-type Col-0 plants. (B) The *ers1-2* mutant is less susceptible to *H. schachtii* compared with the wild-type WS. Bar represents average numbers of J4 females per root system ± SE (n =20) counted three weeks post nematode inoculation. Asterisks indicate statistically significant difference at *P* value 0.05.

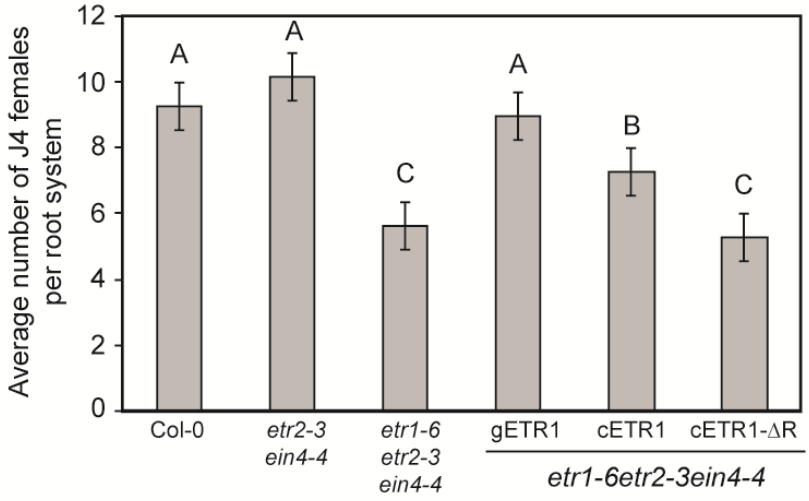

Figure 3-2. ETR1 receiver domain contributes to ETR1-mediated susceptibility to *H. schachtii*.

Nematode infection assays of *etr2-3/ein4-4*, *etr1-6/etr2-3/ein4-4* and *etr1-6/etr2-3/ein4-4* transformed with genomic ETR1, ETR1 cDNA or truncated ETR1 cDNA without receiver domain. Bars represent average numbers of J4 females per root system ± SE (n =20) counted three weeks post nematode inoculation. Different alphabets in the bar indicate statistically significant difference at *P* value 0.05.

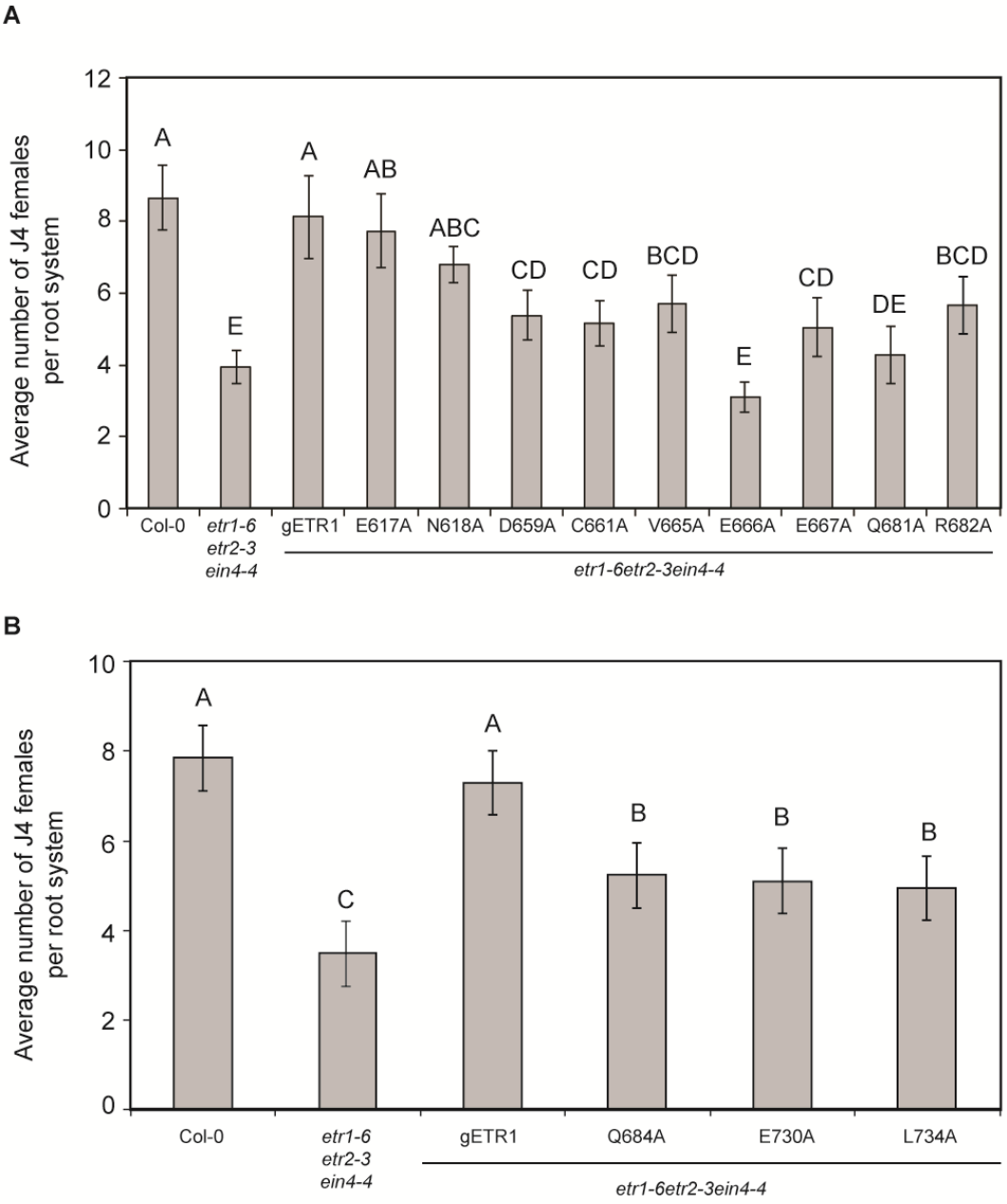

Figure 3-3. Effect of ETR1 receiver domain point mutation on Arabidopsis susceptibility to *H. schachtii*.

Bars represent average numbers of J4 females per root system ± SE (n =20) determined three weeks after nematode inoculation. Different alphabets in the bar indicate statistically significant difference at *P* value 0.05.

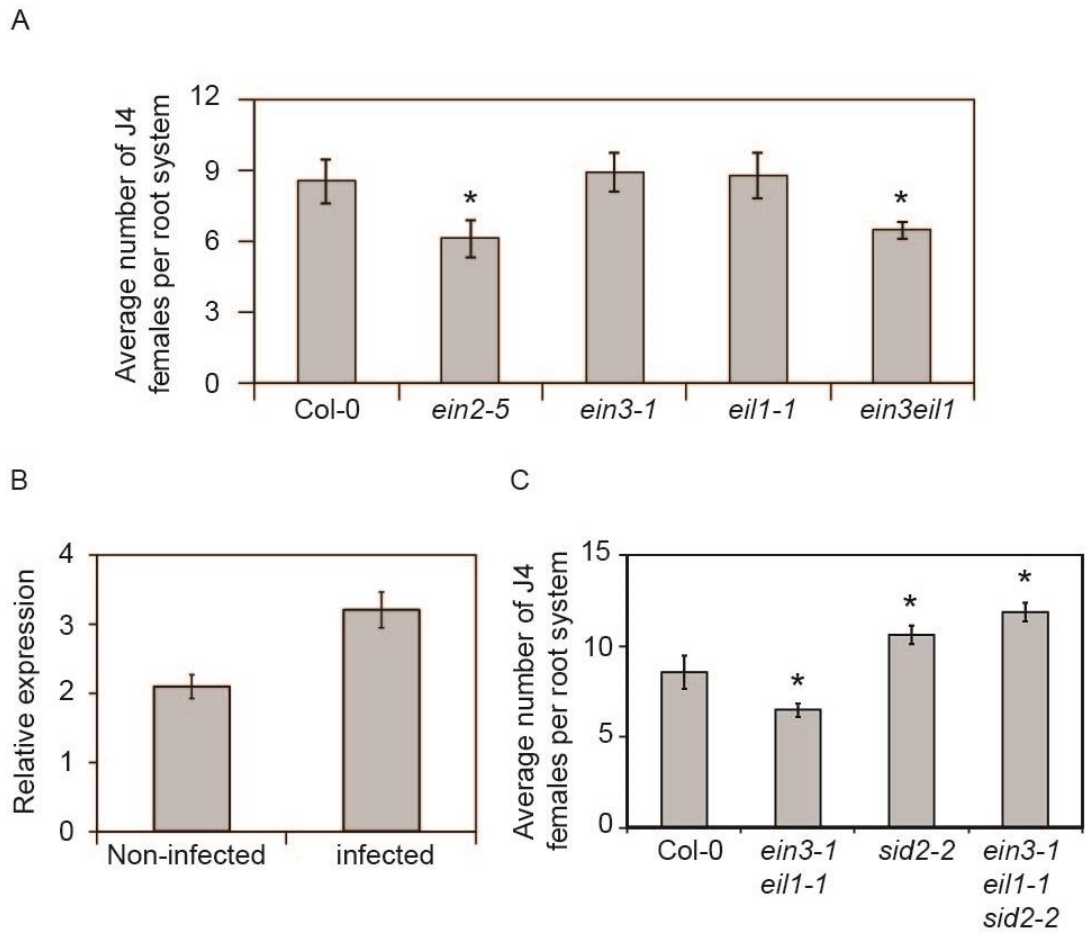

Figure 3-4. Increased expression of *SID2* is responsible for increased resistance of the *ein3/eil1* mutant.

Nematode infection assays showing increased resistance of *ein2* and *ein3/eil1* mutants compared to the wild-type Col-0 plants. (B) Expression of *SID2* is increased in the *ein3/eil1* mutant compared to the wild-type plants under both *H. schachtii*-infected and non-infected conditions. (C) *SID2* functions downstream of EIN3 and EIL1. While the *ein3-1/eil1-1* double mutant was more resistant to *H. schachtii*, *sid2* and *ein3/eil1/sid2* mutants showed the opposite phenotype of increased susceptibility compared with the wildtype Col-0 plants. Bar represents average numbers of J4 females per root system ± SE (n =20) determined three weeks post nematode inoculation. Asterisks indicate statistically significant differences at *P* value 0.05.

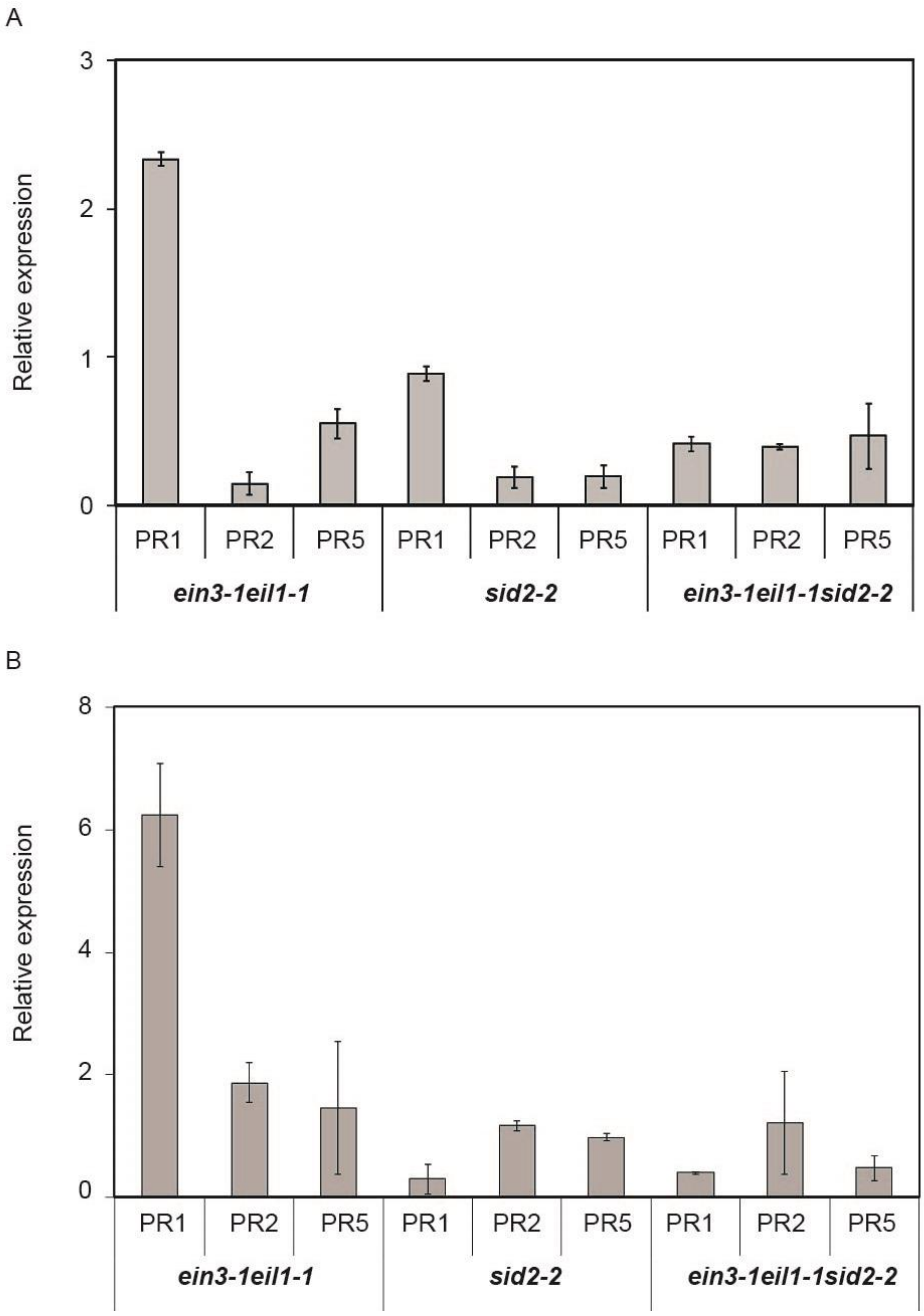

Figure 3-5. The *ein3-1/eil1-1* mutant abolishes the repression of SID2–mediated activation of *PR* genes.

Expression levels of salicylic acid responsive pathogenesis-responsive genes *PR1*, *PR2* and *PR5* under non-infected (A), and *H. schachtii*-infected conditions (B) were quantified using qPCR with three biological samples.

Chapter 4

Cooperative regulatory functions of miR858 and MYB83 in transcriptome reprogramming during cyst nematode parasitism of Arabidopsis

This chapter has been accepted for publication in Plant Physiology by Sarbottam Piya, Christina Kihm, John Hollis Rice, Thomas J. Baum and Tarek Hewezi.

My contributions to this manuscript include performing experiments, data analysis, results interpretation, and writing.

Abstract

microRNAs (miRNAs) recently have been established as key regulators of transcriptome reprogramming that defines cell function and identity. Nevertheless, the molecular functions of the greatest number of miRNA genes remain to be determined. Here, we report cooperative regulatory functions of miR858 and its MYB83 transcription factor target gene in transcriptome reprogramming during *Heterodera* cyst nematode parasitism of Arabidopsis. Gene expression analyses and promoter–GUS fusion assays documented a role of miR858 in post-transcriptional regulation of *MYB83* in the *Heterodera schachtii*–induced feeding sites, the syncytia. Constitutive overexpression of miR858 interfered with *H. schachtii* parasitism of Arabidopsis, leading to reduced susceptibility, while reduced miR858 abundance enhanced plant susceptibility. Similarly, *MYB83* expression increases were conducive to nematode infection because overexpression of a non-cleavable coding sequence of *MYB83* significantly increased plant susceptibility, whereas a *myb83* mutation rendered the plants less susceptible. In addition, RNA-seq analysis revealed that genes involved in hormone signaling pathways, defense response and glucosinolate biosynthesis, cell wall modification, sugar transport, and transcriptional control are the key etiological factors by which MYB83-facilitates nematode parasitism of Arabidopsis. Furthermore, we discovered that miR858-mediated silencing of *MYB83* is tightly regulated through a feedback loop that might contribute to fine-tuning the expression of more than a thousand of MYB83-regulated genes in the *H. schachtii*–induced syncytium. Together, our results suggest a role of the miR858–MYB83 regulatory system in finely balancing gene expression patterns during *H. schachtii* parasitism of Arabidopsis to ensure optimal cellular function.

1. Introduction

Mature microRNAs (miRNAs) are small 21-22 nucleotides-long non-coding RNAs that are processed from transcripts forming a stem-loop secondary structure. miRNAs operate through base pairing with their target genes (Bartel, 2004; Voinnet, 2009). Once they bind to their target sequences, miRNAs can trigger mRNA degradation or translational repression, causing downregulation of the target genes. With the fast expansion of high throughput sequencing platforms, genome-wide identification and differential expression analysis of miRNAs have been accomplished in an increasing number of plant species (Zhang et al., 2011; Li et al., 2014). Despite the large number of miRNA genes showing differential expression under various developmental and stress conditions, only few of these miRNAs have been functionally characterized.

Initial functional studies of miRNA genes revealed their involvement in regulating a number of developmental processes (Kidner and Martienssen, 2005; Chen, 2009; Chuck et al., 2009; Weiberg et al., 2014). Nonetheless, the key regulatory roles of miRNAs in mediating plant responses to pathogen infection are now being increasingly recognized (Seo et al., 2013; Staiger et al., 2013; Weiberg et al., 2014; Fei et al., 2016). Recent studies have generated compelling proof for the implication of miRNAs in regulating defense signaling and immune responses during plant interaction with various phytopathogens, including bacteria, fungi, oomycetes, viruses, and nematodes (Seo et al., 2013; Gupta et al., 2014; Yang and Huang, 2014; Hewezi and Baum, 2015). miRNAs can function as negative regulators of plant defenses, leading to increasing plant susceptibility to pathogen infection. For instance, miR844 and miR400 were found to enhance plant susceptibility to *Pseudomonas syringae* and *Botrytis cinerea*, respectively, when overexpressed in Arabidopsis (Park et al., 2014; Lee et al., 2015). In barley, various miR9863 family members have been demonstrated to target distinct alleles of the *Mla* immune receptors to inhibit immune response signaling in response to infection by the powdery mildew fungus, *Blumeria graminis* (Liu et al., 2014). A limited number of miRNA genes have also been shown to modulate plant innate immunity. For instance, overexpression of Arabidopsis miR160a, which targets *ARF10, ARF16* and *ARF17,* activated callose deposition, resulting in enhanced plant resistance to *Pseudomonas syringae* (Li et al., 2010). More recently, miR444 has been found to activate plant innate immunity against rice stripe virus in rice. The expression of miR444 was activated upon virus infection and this activation was accompanied by downregulation of its target genes OsMADS23, OsMADS27a, and OsMADS57, the repressors of RNA-DEPENDENT RNA

POLYMERASE1 (RdRP1), leading to activation of the RdRP1–dependent antiviral silencing pathway (Wang et al., 2016).

Detailed functional studies also revealed that the same miRNA gene can execute diverse functions against different pathogens. For example, overexpression of rice miR398b resulted in increasing plant susceptibility to *P. syringae* via inhibiting callose deposition (Li et al., 2010). In contrast, miR398b overexpression can also enhance plant resistance against the blast fungus *Magnaporthe oryzae* via increasing the production of hydrogen peroxide (Li et al., 2014). Similarly, it has been shown that miR863-3p can mutually regulate negative and positive mediators of defense signaling in a pathogen infection stage-specific fashion to fine-tune the timing of defense response (Niu et al., 2016).

Plant-parasitic cyst nematodes are the most destructive root parasites, causing substantial yield losses in many crop plants. These obligate parasites form, in the root vascular tissues, a specialized multi-nucleate feeding site, termed syncytium. The syncytium is a metabolically hyperactive sink-like structure from which the nematodes feed throughout the parasitic stages. Formation of functional syncytia is a sophisticated cellular process that involves an intricate interplay of numerous signaling and developmental pathways, whose regulation remains poorly understood. However, recent studies point at vital regulatory functions of miRNAs in syncytium formation and function. For example, miR396–targeting of growth regulating factor 1 (*GRF1*) and *GRF3* was found to control syncytium initiation and development via regulating numerous hormonal signaling and developmental pathways (Hewezi et al., 2012; Hewezi and Baum, 2012; Liu et al., 2014). More recently, it has been shown that *Heterodera schachtii*–induced upregulation of miR827 post-transcriptionally silences the Nitrogen Limitation Adaptation (*NLA*) gene specifically in the syncytium to permanently attenuate immune responses and enable successful parasitism (Hewezi et al., 2016). Also, miRNAs seem to have functional roles in regulating phytohormone signaling during plant interactions with root-knot nematodes. It has been recently demonstrated that tomato miR319 regulates jasmonic acid level during *Meloidogyne incognita* infection (Zhao et al., 2015). Another recent study has suggested a role of Arabidopsis miR319 in modulating auxin signaling during *M. javanica* parasitism (Cabrera et al., 2016).

miRNA-mediated post transcriptional control of gene activity is a highly dynamic process that determines not only transcript stability and protein level but also allows plant cells to establish metabolic and physiological re-adjustment to cope with new functions or fluctuating conditions.

In plants, a significant number of miRNA genes target transcription factors (Bonnet et al., 2004; Jones-Rhoades and Bartel, 2004). In turn, miRNAs-regulated transcription factors have tremendous potential to achieve such re-adjustment in cellular metabolism and physiology because of their ability to control numerous downstream targets. In addition, miRNA genes and their targeted transcription factors may correspondingly adjust the expression of each other through feedback regulatory loops, in which the transcription factors directly regulate the expression of their negative regulators, resulting in tight control over gene expression patterns (Meng et al., 2011). Furthermore, a transcription factor and its miRNA regulators may antagonistically regulate common targets, although such mechanisms have not yet been described in plants.

In Arabidopsis, miR858 post-transcriptionally silences the expression of several MYB transcription factors including *MYB6, MYB11, MYB12, MYB13, MYB20, MYB42, MYB63, MYB83* and *MYB111* (Fahlgren et al., 2007; Addo-Quaye et al., 2008; Sharma et al., 2016). These miR858-targeted MYBs are involved in a variety of cellular processes, including plant responses to drought (MYB20 and 60), the phenylpropanoid pathway (MYB11, 12, and 111), and secondary wall biosynthesis (MYB46 and 83) (Cominelli et al., 2005; McCarthy et al., 2009; Oh et al., 2011; Gao et al., 2014; Sharma et al., 2016). Here, we report a novel function of the *miR858*-MYB83 regulatory system in plant-cyst nematode interaction. Both miR858 and *MYB83* were transcriptionally activated in the syncytia of *H. schachtii*, and modulation of their expression through gain- and loss-of-function approaches altered Arabidopsis response to nematode infection. In line with the function of MYB83 in facilitating nematode infection of Arabidopsis, our transcriptome analysis revealed that MYB83 regulates a substantial number of syncytial genes encoding components essential for syncytium formation and function. Also, our results establish that MYB83 through a feedback loop activates the expression of miR858 thereby stabilizing its own transcript abundance and its downstream regulated genes during the initiation and progression of nematode parasitism.

2. Results

2.1 miR858 is expressed in the syncytium during the initiation and progression of nematode parasitism

In Arabidopsis, miR858 is encoded by one functional genomic locus (miR858a, AT1G71002) that produces 21-nucleotide mature molecules and targets ten *MYB* transcription factor genes that

contain the miR858 complementary sequences (Sharma et al., 2016). To elucidate the functional role of miR858 during the compatible interactions between Arabidopsis and the beet cyst nematode *Heterodera schachtii*, we first generated several transgenic Arabidopsis lines expressing the β-glucuronidase (GUS) reporter gene under the control of miR858 promoter (pmiR858:GUS). GUS activity of four independent transgenic lines (T2 generation) were assayed both under non-infected and *H. schachtii*–infected conditions. In non-infected 2-week-old-plants, GUS activity was observed in the vascular tissues of both leaves and roots (Figure 4-1, A-C). Under *H. schachtii*–infected conditions, GUS activity was observed in the developing syncytium of the second stage nematode juvenile (J2) at 3 days post infection (dpi) as well as in the syncytium of the early J3 stage at 7 dpi (Figure 4-1, D and E). However, at 10 and 14 dpi (late J3 and J4 stages), GUS activity in the syncytium was dramatically reduced (Figure 4-1, F and G). The expression patterns of miR858 in the syncytium point to a functional role of miR858 of suppressing its target genes during the initiation and progression of nematode parasitism. Reduced miR858 promoter activity at later stages, therefore, suggests an uninhibited expression of these target genes at these time points.

2.2 miR858 post-transcriptionally regulates MYB83 transcription factor during H. schachtii parasitism of Arabidopsis

It has been shown recently that miR858 post-transcriptionally silences the ten MYB transcription factors *MYB6, MYB11, MYB12, MYB13, MYB20, MYB42, MYB48, MYB63, MYB83* and *MYB111* that contain the miR858 binding site (Sharma et al., 2016). Among these transcription factors, MYB83 was reported to be differentially expressed in the *H. schachtii*-induced syncytium (Szakasits et al., 2009). In addition, recent functional analyses have implicated MYB83 (AT3G08500) in the regulation of secondary wall biosynthesis and cell wall modifications in Arabidopsis (McCarthy et al., 2009; Zhong and Ye, 2012), both of which are functions of fundamental cellular processes impacting syncytium formation and development (Bohlmann and Sobczak, 2014; Hewezi, 2015), Therefore, we directed our focus to elucidating the potential regulatory role of the miR858-MYB83 system in modulating the interactions between Arabidopsis and *H. schachtii*. We generated pMYB83:GUS transgenic lines to determine if *MYB83* shares the temporal expression patterns with miR858 in the syncytium, which would suggest that *MYB83* is post-transcriptionally regulated by miR858 also in the syncytium. GUS activities were assayed in

four independent transgenic lines (T2 generation) both under non-infected and *H. schachtii*–infected conditions. In non-infected 2-week-old plants, GUS activity was observed in leaf and root vascular tissues (Figure 4-1, H-J). Under *H. schachtii* infection, strong GUS activity was observed in the syncytium during the J2, early J3, late J3 and J4 developmental stage at 3, 7, 10, and 14 dpi, respectively (Figure 4-1, K-N). The coincident upregulation of miR858 and *MYB83* promoters in the syncytium at 3 and 7 dpi suggests that *MYB83* is targeted by miR858 for post-transcriptional regulation during the early syncytium development stage. At later stages, *MYB83* expression appears to be uninhibited by miR858.

In order to provide additional evidence that miR858 mediates post-transcriptional regulation of *MYB83* during *H. schachtii* infection of Arabidopsis, we used quantitative real-time RT-PCR (qPCR) to quantify the abundance of miR858 primary transcripts (pri-miR858), mature miR858 as well as total and uncleaved transcript levels of *MYB83* in the roots of wild-type (Col-0) Arabidopsis plants inoculated with *H. schachtii* at 4, 7, 10 and 14 dpi, relative to the corresponding non-inoculated controls. The relative levels of uncleaved *MYB83* transcripts were determined using a primer pair flanking the miR858 binding site, whereas the relative levels of total (cleaved and uncleaved) *MYB83* transcripts were determined using a primer pair located downstream of the miR858 binding site as previously described by Hewezi et al. (2016). Expression data from three biologically independent replicates revealed upregulation of both primary and mature miR858 in *H. schachtii*–infected roots at 4 and 7 dpi relative to non-infected roots (Figure 4-2), a result which is consistent with the increased activity of the miR858 promoter in the syncytium at the same time points. Meanwhile, the levels of uncleaved *MYB83* transcripts was lower than the level of total transcripts in infected roots relative to non-infected roots at both time points (Figure 4-2). At 10 dpi, the expression levels of both primary and mature miR858 were slightly upregulated and this upregulation was accompanied with small insignificant reduction in the level of uncleaved *MYB83* transcripts compared with the total transcript level (Figure 4-2). At 14 dpi, the expression of primary and mature miR858 was sharply decreased in the infected roots compared to the control, and this downregulation was associated with comparable levels of total and uncleaved *MYB83* transcripts (Figure 4-2). These temporal expression patterns, which show that the abundance of uncleaved *MYB83* transcripts are inversely correlated with the expression level of miR858, indicate that *MYB83* is subjected to

post-transcriptional regulation by miR858 following *H. schachtii* infection. Given our promoter data, this regulation likely is at work in the syncytium.

2.3 Overexpression of miR858 confers enhanced resistance to H. schachtii

Promoter and qPCR analyses of miR858 expression during nematode infection revealed two distinct patterns (i.e. upregulation during J2 and early J3 stages, and downregulation during late J3 and J4 stages). Thus, we investigated whether constitutive overexpression of miR858 would modulate Arabidopsis susceptibility to *H. schachtii*. To this end, we generated transgenic Arabidopsis lines overexpressing the primary miR858 sequence under the control of 35S promoter (35S:miR858). Four independent non-segregating T2 overexpression lines (1-3, 1-4, 19-1, and 21-1) showing between 6 to 18 fold increases in miR858 expression levels relative to the wild-type Col-0 plants were selected (Figure 4-3, A). *MYB83* transcripts accumulated at significantly lower levels in these lines relative to Col-0 plants (Figure 4-3A), which is consistent with post-transcriptional degradation of *MYB83* transcripts by miR858. The root lengths of miR858 overexpression lines were comparable to the wild-type Col-0 plants, with the exception that line 21-1 showed a slight increase of about 5% (Figure 4-4B). No other developmental defects were observed when these lines were grown under standard growth conditions, which is in line with the results recently obtained by Sharma et al. (2016) (Figure 4-4, B and C). The four miR858 overexpression lines along with the wild-type Col-0 were assayed for *H. schachtii* susceptibility. These lines showed statistically significant decreases in susceptibility levels with 30 to 42% reduction in J4 female nematode counts compared to Col-0 plants (Figure 4-4D). These results indicate that constitutive overexpression of miR858 interferes with *H. schachtii* parasitism of Arabidopsis.

2.4 Overexpression of a mimic sequence for miR858 augments plant susceptibility to H. schachtii

The involvement of miR858 in the modulation of Arabidopsis response to *H. schachtii* infection was further examined by generating transgenic Arabidopsis plants with reduced miR858 expression. This was accomplished by expressing a mimic sequence for miR858 in its mature form (MIM858) (Figure 4-5A). The artificial non-cleavable binding site for the mature miR858 contained a three-nucleotide bulge (TGA) that does not interfere with miR858 binding but would prevent transcript cleavage and hence sequester miR858 activity. Three independent transgenic

lines showing between 2.7 and 6.8 fold reduction in the mature miR858 expression levels were selected (Figure 4-3B). qPCR quantification revealed that miR858 downregulation in the MIM858 lines was correlated with significant increases in *MYB83* expression levels (Figure 4-5B), a finding that confirms the efficiency of our target mimicry construct in sequestering the activity of miR858. Other than minor reductions in root lengths of MIM858 plants, no noticeable morphological differences between MIM858 lines and Col-0 plants were detected (Figure 4-5, C and D). Interestingly, when the susceptibility of the MIM858 lines to *H. schachtii* was determined, these lines were significantly more susceptible than the wild-type plants, showing up to 56% increase in the number of J4 nematodes (Figure 4-5E). Together, these data confirm that increased expression of miR858 is responsible for the reduced susceptibility phenotype observed in miR858 overexpression plants.

2.5 Ectopic overexpression of a non-cleavable variant of MYB83 enhances plant susceptibility to H. schachtii

The gene expression analyses and nematode susceptibility assays of miR858 and *MIM858* overexpression lines mentioned above indicate that inhibition of miR858 activity facilitates *H. schachtii* infection, most likely through the upregulation of its MYB target genes. If miR858 modulates plant susceptibility mainly through post-transcriptional regulation of *MYB83*, manipulation of *MYB83* expression should also impact plant susceptibility to *H. schachtii* but in the opposite direction. To test this hypothesis, we generated transgenic Arabidopsis lines overexpressing a miR858-resistant variant of *MYB83* under the control of 35S promoter (*35S:rMYB83*). The non-cleavable variant *rMYB83* was generated by introducing six nucleotide mismatches in the miR858 binding sites without changing the encoding protein sequences (Figure 4-6A). Four non-segregating T2 lines showing between 16 and 31 fold *MYB83* mRNA upregulation were selected and phenotypically analyzed (Figure 4-3, C). These lines were indistinguishable from the wild-type plants in term of root and shoot growth and development. Interestingly, when these lines were used in *H. schachtii* infection assays, all lines exhibited statistically significant increases in susceptibility with up to 65% increase in the number of J4 nematodes compared with the wild-type Col-0 plants (Figure 4-6B). In contrast to the *rMYB83* overexpression lines, a *MYB83* T-DNA mutant line (CS1004395) (Figure 4-7) showed reduced susceptibility to *H. schachtii* relative to the wild-type Col-4 plants (Figure 4-6C). Taken together,

these results link the activity of the MYB83 transcription factor to the function of miR858 in modulating plant responses to *H. schachtii* infection.

2.6 RNA-seq analysis of miR858 and rMYB83 overexpression plants-regulated genes

The robust effects of *MYB83* overexpression and knockout mutant lines on nematode susceptibility suggest that this transcription factor may control downstream target genes encoding proteins necessary for syncytium formation/function. Therefore, we performed RNA-seq analysis on root tissues isolated from the 35S:miR858 (Line 1-4), *35S:rMYB83* (line 8-1), and wild-type (Col-0) plants in order to identify the downstream targets that may be directly or indirectly controlled by MYB83. Three biological samples of root tissues were collected from each plant line (2-week-old) for mRNA isolation and library preparation. After sequencing, high quality reads were mapped to the Arabidopsis reference genome (TAIR10), and differentially expressed genes (DEGs) were determined using a false discovery rate of 0.05. We identified 4,386 and 2,908 DEGs in P35S:miR858 and *35S:rMYB83*, respectively, compared with the wild-type Col-0 plants. Out of the 4,386 DEGs identified in the 35S:miR858 plants 2,082 genes were upregulated and 2,304 genes were downregulated. In the *35S:rMYB83* plants 1,249 genes were upregulated and 1,659 genes were downregulated. Comparison of the DEGs in these two transgenic lines revealed that 2,193 genes were common to both sets (Figure 4-8A). The fact that this overlapping gene list represents more than 50% of the DEGs identified in the 35S:miR858 plants, indicates that *MYB83* is the main target of miR858 in roots.

Gene Ontology (GO) classification and enrichment analyses of the DEGs in the 35S:miR858 and *35S:rMYB83* plants were performed. Thirty five GO biological process terms, which are mainly associated with metabolic processes and response to biotic and abiotic stimuli were identified (Figure 4-8B). While several GO terms were enriched among the upregulated or downregulated genes in both lines, enriched GO terms specific to each line were also seen. For example, GO terms corresponding to defense response, response to bacterium, and response to abscisic acid stimulus were enriched uniquely among the upregulated genes in 35S:miR858 plants (Figure 4-8B). Similarly, GO terms corresponding to carbohydrate metabolic processes as well as secondary metabolic process were significantly overrepresented uniquely among the upregulated genes in *35S:rMYB83* plants, (Figure 4-8B). The same observation is equally evident among the downregulated genes. For example, enrichment of GO terms corresponding to flavonoid

biosynthesis and metabolic processes were identified only among the downregulated genes in 35S:miR858 plants (Figure 4-8B). GO terms corresponding to signal transduction, auxin transport, lignin metabolic process, cell wall organization, and responses to wounding, osmotic stress, oxidative stress, salt stress, chitin, auxin stimulus, and jasmonic acid stimulus were significantly enriched exclusively among the downregulated genes in the *35S:rMYB83* plants (Figure 4-8B).

2.7 Identification of putative direct targets of MYB83

ACC(A/T)A(A/C)(T/C) consensus sequence has been identified as the MYB83-responsive element in Arabidopsis (Zhong and Ye, 2012). Therefore, we scanned the promoters of the DEGs identified in the *35S:rMYB83* plants (2,908 genes) for the presence of this *cis* element within 1.5 kb upstream of the transcription start site (TSS) to identify putative direct targets of MYB83. The number of *cis* elements identified in these DEGs ranged between 0 and 15 elements, with the large majority containing between 0 and 2 elements (Figure 4-9, A). Also, we determined the average number of this *cis* element in the promoters of 2,908 randomly selected genes to be 1.02 elements. Thus, DEGs with at least three MYB83 *cis*-binding elements in the promoters of the MYB83-regulated genes were considered as putative direct targets of MYB83 (*P* value 2.69E-65, Fisher's exact test). As a result, 1,055 of the MYB83-regulated genes were identified as bona fide direct target candidates. The *cis* elements are equally distributed across the gene promoters (Figure 4-9, B). However, 77% (815/1055) of these putative direct targets contain at least one *cis* element within 500 bp of the TSS (Figure 4-9, C). GO analysis showed that genes involved in transport, primary metabolic processes, secondary metabolic processes, particularly glucosinolate, and responses to biotic and abiotic stresses were significantly enriched among the direct targets that were positively regulated in the *35S:rMYB83* plants. GO categories associated with transcription, metabolic process, defense response, and responses to stress, nematode, hormone and biotic stimuli were significantly enriched among the putative direct target genes that were negatively regulated in the *35S:rMYB83* plants (Figure 4-10).

2.8 MYB83 regulates key cellular processes in the syncytium of H. schachtii

Consistent with the role of MYB83 in promoting plant response to *H. schachtii* parasitism we found a significant overlap between the MYB83-regulated genes and the syncytium DEGs previously reported by Szakasits et al. (2009). Of the 2,908 MYB83-regulated genes 1,286

overlapped with the 7,725 syncytium DEGs (Figure 4-8C). This significant overlap (44.2%, χ^2= 224.729, P value = 1.909E-48) indicates that 16.6 % of the syncytium transcriptome is regulated by MYB83. Also, we compared the identified 1,055 direct target genes of MYB83 with the syncytium DEGs to determine the extent to which MYB83 directly regulates gene expression in the syncytium. A common set of 471 genes (44.6%, χ^2= 79.765, P value = 3.452E-17) was identified, implying that 6% of syncytium genes are under direct control of MYB83 (Figure 4-8D). Of these 471 genes, 216 (46%) were upregulated in of MYB83 overexpression plants and 255 (54%) were downregulated, suggesting that MYB83 has a dual transactivation and transrepression function. GO term analysis of the 1,286 MYB83-regulated genes overlapping with the syncytium DEGs revealed an enrichment of genes involved in receptor-mediated signaling pathways, transport, metabolic processes, cell-wall organization, and responses to stress, chitin, and bacterium, as well as responses to biotic, abiotic, hormone, auxin, and ethylene stimuli (Figure 4-8E). When this analysis was conducted to include only the 471 genes predicted as putative direct targets of MYB83 in the syncytium, GO terms associated with transcription, transport, metabolic process, responses to stress, oxidative stress, bacterium, and biotic stimulus were significantly enriched (Figure 4-8E).

In addition to GO analysis, careful examination of the known functions of MYB83-regulated genes overlapping with the syncytium DEGs enabled more detailed insights into the functional role of MYB83 during *H. schachtii* infection. As shown in Figure 4-11, genes involved in hormone signaling pathways (Figure 4-11A), defense response and glucosinolate biosynthesis (Figure 4-11B), cell wall modification and sugar transport (Figure 4-11C) and transcriptional control (Figure 4-11D) seem to be the key etiological factors of MYB83 in facilitating nematode parasitism of Arabidopsis.

2.9 miR858 and MYB83 constitute a feedback regulatory loop that involves MYB12

We next examined the promoter of miR858, 2 kb upstream of the primary transcript, for the presence of MYB83 *cis*-binding element. Interestingly, 7 *cis*-elements were identified, emphasizing the possibility that MYB83 regulates the expression of miR858. To investigate this possibility, we quantified the expression of primary and mature miR858 in the *35S:rMYB83* plants as well as the *myb83* knockout mutant line (CS1004395) using qPCR. Data from three biological samples indicated about 2-fold upregulation of both primary and mature miR858 in the transgenic

plants overexpressing *MYB83* (Figure 4-12A) compared to Col-0 plants. In contrast, both primary and mature miR858 transcripts were downregulated in the *myb83* mutant compared with the wild-type Col-4 (Figure 4-12B). Taken together, these results imply that MYB83 positively regulates the expression of its negative regulator through a feedback regulatory loop to maintain proper level of its transcripts.

We then examined our RNA-seq data set to find out if any of the confirmed targets of miR858 were inversely regulated in the *MYB83* overexpression plants, and hence constitute part of the regulatory loop. Interestingly, we identified *MYB12*, a confirmed target of miR858, among the MYB83-positively regulated genes. This finding guided us to test whether MYB12 is an integral part of the miR858/MYB83 regulatory circuit impacting plant response to nematode infection. To this end, we generated transgenic plants overexpressing a miR858-resistant variant of *MYB12* (*rMYB12*) driven by the 35S promoter (Figure 4-13). A nematode infection assay of 3 independent overexpression lines displayed significant increases in plant susceptibility to nematode infection compared with Col-0 plants (Figure 4-12C). Contrary to *rMYB12* overexpression lines the *myb12* mutant FLAG_150B05 (Figure 4-14) exhibited reduced susceptibility compared with the wild-type Wassilewskija (WS) plants (Figure 4-12D). Together, these results suggest that MYB12 may constitute part of miR858/MYB83 regulatory loop regulating plant response to nematode infection.

3. Discussion

Arabidopsis miR858 has been shown to regulate various growth and plant developmental processes (Guan et al., 2014; Jia et al., 2015; Sharma et al., 2016). However, a regulatory function of miR858 in plant-pathogen interactions has not been reported. Here, we report a crucial regulatory role of miR858 during *H. schachtii* parasitism of Arabidopsis. In response to *H. schachtii* infection miR858 exhibited a biphasic expression pattern, including strong activation in the developing syncytia at 3 and 7 dpi and a subsequent downregulation in the mature syncytia at 10 and 14 dpi. This pattern of miR858 expression suggests different functions during the two distinct stages of syncytium formation and maintenance. As a result, constitutive overexpression of miR858 resulted in significant decreases in nematode infection. In contrast, inactivation of miR858 by overexpressing an artificial target mimic sequence produced the opposite phenotype of enhanced susceptibility. The influence of miR858 expression changes on plant responses to *H.*

schachtii seems to be mediated through post-transcriptional regulation of its *MYB* transcription factor genes, specifically *MYB83*. The *MYB83* promoter was predominantly active in the syncytium during all nematode parasitic stages. Post-transcriptional silencing of *MYB83* by miR858 was evident at 4 and 7 dpi as shown by low levels of uncleaved MYB83 transcripts compared with the total transcript levels. *MYB83* expression increase seems to be conducive to *H. schachtii* infection of Arabidopsis because *rMYB83* overexpression enhanced plant susceptibility, whereas a *myb83* mutation rendered the plants less susceptible.

The regulatory relationship between miR858 and MYB83 seems to be established through a feedback regulatory loop. Our finding that the MYB83 binding motif occurs repeatedly in the miR858 promoter led us to examine a possible role of MYB83 in regulating the expression of miR858. The transcript abundance of pri-miR858 and mature miR858 was considerably increased in the *rMYB83* overexpressing plants but decreased in the *myb83* mutant, indicating that MYB83 participates in a feedback loop with its negative regulator to stabilize its own transcript abundance. A reciprocal feedback loop controlling the expression of miR396 and its target transcription factors *GRF1* and *GRF3* has been demonstrated to coordinate transcriptional events required for proper syncytium formation and function (Hewezi and Baum, 2012; Hewezi et al., 2012; Liu et al., 2014). In addition, a number of miRNAs and their trans-acting targets were found to be intricately connected through feedback circuits in different growth and developmental contexts, where robust and adaptable transcriptional responses were established (Xie et al., 2003; Gutierrez et al., 2009; Wu et al., 2009; Marin et al., 2010; Yant et al., 2010; Merelo et al., 2016). Our data suggest that the miR858/MYB83 regulatory circuit may involve *MYB12*, a confirmed target of miR858, whose transcript abundance was positively regulated by MYB83. Thus, miR858 appears to fine-tune the function of MYB83 at various levels. MYB12 is also of functional importance for nematode parasitism since constitutive changes in its expression levels through overexpression and T-DNA insertional mutant lines altered plant response to nematode infection.

The miR858/MYB83 regulatory loop may enable controlling precise expression levels of genes involved in critical cellular processes required for syncytium differentiation without turning gene expression on and off to prevent syncytium degeneration and collapse. Our finding that 1,286 genes of the 2,193 MYB83-regulated genes were among the previously identified syncytium DEGs (Szakasits et al., 2009), may reflect a key regulatory function of MYB83 in reprogramming syncytium transcriptomes. We therefore focused our discussion on this gene list. Levels and

signaling of phytohormones play fundamental roles in determining syncytium cell fate reprograming and differentiation (Grunewald et al., 2009; Gheysen and Mitchum, 2011; Goverse and Bird, 2011; Cabrera et al., 2015; Kammerhofer et al., 2015). In particular, auxin signaling has been shown to be rapidly activated upon nematode infection leading to syncytium differentiation and development (Goverse et al., 2000; Karczmarek et al., 2004; Grunewald et al., 2009; Absmanner et al., 2013; Hewezi et al., 2014). Several genes encoding numerous functions of the auxin signal transduction cascade including the auxin receptor TIR1, the auxin response factors 2, 4, 6, 9, and 10, the auxin influx carrier LAX1, and the auxin efflux transporter ABCB4 were among MYB83-regulated genes in the syncytium (Figure 4-11A). Additional key genes involved in the auxin response (*SHY2*, *ARGOS*, and *PLDP2*) and auxin homeostasis (*GH3.17*) were also regulated by MYB83 in the syncytium (Figure 4-11A). It has been recently reported that cytokinin signaling is critical for syncytium development and successful *H. schachtii* parasitism of Arabidopsis (Shanks et al., 2015; Siddique et al., 2015). MYB83-regulated genes overlapping with syncytium DEGs included various components of cytokinin signaling pathway, namely, the cytokinin synthase IPT5, the histidine kinase receptors AHK2 and AHK4, and the histidine phosphotransfer proteins AHP (Figure 4-11A). Together, these results indicate that MYB83 regulates auxin and cytokinin responses at various levels of biosynthesis, signal transduction, and downstream responses.

Also, ethylene has been shown to play contrasting dual functions during various nematode parasitic stages (Wubben et al., 2001; Kammerhofer et al., 2015). Notably, numerous ethylene response factors (*ERFs*), which control the downstream signaling of ethylene response, were also identified among the MYB83-indcued genes overlapping with the syncytium DEGs (Figure 4-11A). This included *ERF6*, *ERF9*, and *ERF72*, which play key regulatory functions in biotic stress responses (Ogawa et al., 2005; Camehl and Oelmüller, 2010; Moffat et al., 2012; Maruyama et al., 2013; Meng et al., 2013; Chen et al., 2014; Xu et al., 2016), as well as *ERF109*, which regulates the accumulation of reactive oxygen species following biotic and abiotic stresses stimuli (Matsuo et al., 2015). Remarkably, a substantial number of genes associated with gibberellin, jasmonic acid, and abscisic acid signal transduction networks were directly or indirectly regulated by MYB83 in the syncytium (Figure 4-11A). While the function of jasmonic acid and abscisic acid signaling in directing plant response to cyst nematodes is poorly understood, it has been recently demonstrated that these pathways regulate defense responses and basal immunity against sedentary

and migratory nematodes (Nahar et al., 2011; Nahar et al., 2012; Ozalvo et al., 2014; Kammerhofer et al., 2015).

Interestingly, we noted that genes encoding functions that mediate the interplay between various hormone signaling pathways were also regulated by MYB83 (Figure 4-11A). This included for example ERF109 and ANTHRANILATE SYNTHASE ALPHA SUBUNIT 1, which mediate the interplay between jasmonic acid and auxin biosynthesis and transport in roots (Sun et al., 2009; Cai et al., 2014), and the acyl acid amido synthetase GH3.5, which regulates the homeostasis and responses of salicylic acid and auxin following pathogen infection (Zhang et al., 2007; Westfall et al., 2016). Thus, miR858/MYB83-mediated precise regulation of transcript levels of various phytohormone signaling genes may allow infected root cells to properly differentiate and develop into functional syncytia in a stage-specific fashion, taking into consideration that the levels of these phytohormones are anticipated to vary throughout various stages of syncytium initiation, formation and maintenance. It is plausible also that MYB83 may integrate signals from these hormone pathways to fine-tune the biosynthesis of defense components. In this context, pathogenesis-related (PR) genes, whose expression is linked to the signaling pathways of salicylic acid (thaumatin-like) and jasmonic acid (*PR4* and *PDF2.1*), were among the identified MYB83–regulated genes in the syncytium (Figure 4-11B). *PDF2.1* was recently confirmed to be strongly expressed in the syncytium using reporter lines (Siddique et al., 2011). Interestingly, two genes encoding the cytochrome P450 enzymes CYP79B2 and CYP79B3, which are involved in the conversion of tryptophan to indole-3-acetaldoxime (IAOx) (Hull et al., 2000; Mikkelsen et al., 2000), were oppositely regulated by MYB83 (Figure 4-11B and E). The fact that IAOx is the metabolic branch node bringing about the biosynthesis of auxin and indole glucosinolate (Bak et al., 2001) suggests a role of MYB83 in regulating the balance between auxin homeostasis and glucosinolate biosynthesis. In support with this suggestion, several syncytium DEGs that are involved in the biosynthesis of glucosinolate were among the identified MYB83–regulated genes, from which four were considered as direct target gene candidates (Figure 4-11E).

Several transcription factors of MYB, NAC and WRKY families were among the MYB83–regulated genes in the syncytium (Figure 4-11D), suggesting a role of MYB83 in forming a complex and highly interconnected regulatory network in the syncytium. Of the MYB transcription factors, *MYB108*, which regulates wound-induced cell death in an abscisic acid-dependent manner (Cui et al., 2013), and *MYB51*, a key regulator of indole glucosinolate biosynthesis (Frerigmann

and Gigolashvili, 2014) were found. Additional MYB transcription factors included *MYB12* and *MYB59* that are involved in phenylpropanoid biosynthesis and cell cycle progression, respectively (Mehrtens et al., 2005; Mu et al., 2009). Thus, cross-regulation among certain MYB transcription factors in the syncytium may constitute a sub-regulatory network that contributes to the establishment of a syncytium-specific transcriptional program. Of the WRKY transcription factors regulated by MYB83, WRKY72 was previously reported to contribute to basal resistance against the root-knot nematode *M. incognita* and the oomycete *Hyaloperonospora arabidopsidis* (Bhattarai et al., 2010). Also, *WRKY60* and *WRKY11*, the negative regulators of defense response (Journot-Catalino et al., 2006; Xu et al., 2006), were found to be regulated by MYB83 in opposite direction, implying a role of MYB83 in the control of defense response and inhibition of autoimmunity.

Positive and negative regulators of plant immunity are frequently dysregulated upon cyst nematode infection (Szakasits et al., 2009; Kandoth et al., 2011). Notably, master regulators of plant immunity were identified among the MYB83-regulated genes in the syncytium (Figure 4-11B). This included the *KUNITZ TRYPSIN INHIBITOR 1* (*KTI1*) and the *alpha-dioxygenase1* (*DOX1*), which encode functions that antagonize oxidative stress and cell death during pathogen infection (De León et al., 2002; Li et al., 2008). Other regulators of plant immunity included, for example, PROPEP1, the precursor of Pep1, which stimulates the transcription of the plant defensin gene *PDF1.2* (Huffaker et al., 2006), the SUPPRESSOR OF MKK1 MKK2 2 (SUMM2), an immune receptor which is involved in triggering defense responses against bacteria (Zhang et al., 2012), and the BON ASSOCIATION PROTEIN 1 (BAP1), a general suppressor of defense responses and programmed cell death (Yang et al., 2006; Yang et al., 2007).

Further inspection of the MYB83-regulated genes in the syncytium provided additional insights into the function of MYB83 during nematode parasitism. Interestingly, a number of genes encoding transmembrane sugar transport proteins were positively or negatively regulated by MYB83, including SWEET2, 12, 13, and 14, the sugar transporter protein 7 and 12, and the MONOSACCHARIDE TRANSPORTER 6 (PMT6) (Figure 4-11C). These sugar transporters may function in sugar remobilization to the syncytium during nematode feeding and development (Hofmann et al., 2009). As shown in Figure 8C, MYB83–regulated genes in the syncytium also included several expansins and genes coding for enzymes that participate in cell wall biogenesis and modification, comprising cellulose-synthases, beta-glucosidases, pectate lyases, and

peroxidases; some of them were previously shown to modulate plant-nematode interactions (Wieczorek et al., 2006; Jin et al., 2011; Bohlmann and Sobczak, 2014; Wieczorek et al., 2014). Collectively, these data suggest a functional role of MYB83 in a variety of cellular processes associated with nematode infection.

Finally, we propose a model for miR858-MYB83 interaction during *H. schachtii* parasitism of Arabidopsis (Figure 4-15). *H. schachtii*–induced activation of miR858 during the initiation and progression of nematode parasitism post-transcriptionally silences *MYB83*. MYB83 in turn positively regulates the expression of miR858, which contains several MYB83 *cis*-binding elements in its promoter. This feed-back regulatory circuit may function as a homeostatic control mechanism to ensure proper expression levels of more than a thousand of MYB83-regulated genes in the *H. schachtii*–induced syncytium. The miR858/MYB83 regulatory system may also involve MYB12, which was oppositely regulated by miR858 and MYB83, providing additional layer of tight control over unidentified MYB12-regulated genes in the syncytium.

4. Materials and Methods

4.1 Plant material and growth conditions

All transgenic Arabidopsis lines were generated in Coloumbia-0 (Col-0) background. The *myb83* T-DNA insertional mutant (CS1004395) in the Col-4 background was obtained from the Arabidopsis Biological Resource Center. The *myb12* T-DNA mutant (FLAG_150B05) in the Wassilewskija (WS) background was obtained from the Genomic Resource Center, INRA-Versailles, France. Plants were grown under long day conditions 16 hour light/8 hour dark at 24°C.

4.2 Nematode infection assay

Seeds of the transgenic and mutant lines as well as the wild-type controls (Col-0 or Col-4) were sterilized using a 2.8 % bleach solution for five minutes followed by four washes with sterilized double-distilled water. The sterilized seeds were then distributed in 12-well culture plates (BD Biosciences) containing modified Knop's medium solidified with 0.8% Daishin agar (Brunschwig Chemie) using a randomized complete block design with 20 replicates per line. The plates were placed in a growth chamber at 24^0C with 16 hour light/8 hour dark conditions. Freshly hatched J2 *H. schachtii* nematodes were surface-sterilized using a fresh solution of 0.01% mercuric chloride

for five minutes followed by four washes with sterilized double-distilled water. The sterilized J2 nematodes were then suspended in a 0.1% agarose solution and used to inoculate ten-day-old seedlings with approximately 250 nematodes per seedling. The nematode susceptibility of the lines was determined three weeks after inoculation by counting the number of J4 female nematodes per plant using a dissecting microscope. Statistically significant differences between the lines and the corresponding wild-type control were determined using a modified t test on SAS with a *P* value cut-off of 0.05.

4.3 Histochemical analysis of GUS activity

GUS activity of the pmiR858:GUS and pMYB83:GUS transgenic plants was determined by staining the plants at various time points post *H. schachtii* infection using the method previously described by Jefferson et al. (1987). The images of both infected and non-infected plants were taken using a Zeiss digital camera and then analyzed using Zeiss Axio Vision SE64 software (version 4.8).

4.4 Plasmid construction and generation of transgenic plants

The binary vector of miR858 overexpression was constructed by amplifying the miR858 precursor (a 200-bp) from Col-0 genomic DNA using a primer pair containing BamHI and SacI restriction sites. The amplified fragment was digested, gel-purified and then ligated into the binary vector pBI121 under the control of 35S promoter. The wild-type MYB83 coding sequence was amplified from first-strand cDNA and the non-cleavable MYB83 variant was generated by introducing 10 mismatches in the miR858-binding sites without altering the amino acid sequences. The modified MYB83 sequence was then cloned in the pBI121 binary vector under 35S promoter using XbaI and SacI restriction sites. The MIM858 overexpression was generated as recently described by Hewezi et al. (2016). Briefly, the 22 nucleotide miR399-complementary region in the Arabidopsis IPS1 gene, a non-coding phosphate starvation-induced transcript, was substituted with a mimic sequence for the mature miR858 sequences. The miR858 mimic sequence contained a three-nucleotide bulge (TGA) between the nucleotide number 10 and 11 of the binding region and two additional mismatches at the nucleotides number 1 and 10 of the binding site. The modified IPS1 genes containing the miR858 mimic sequence was cloned in the pBI121 vector under the control of 35S promoter using SacI and BamHI restriction sites.

The miR858 promoter, 2KB upstream of the transcription start site, was amplified from Col-0 genomic DNA using a primer pair containing BamHI and SacI restriction sites. Similarly, the MYB83 promoter (2 kb upstream of the translation start codon) was amplified using a primer pair containing BamHI and SalI restriction sites. The PCR-amplified products were digested, gel-purified, and finally ligated to the binary vector pBI101 in the corresponding restriction sites to drive GUS gene expression. All constructs were verified by sequencing and then introduced into *Agrobacterium tumefaciens* strain C58 by the freeze-thaw method. The bacteria were used to transform Arabidopsis ecotype Col-0 plants by the floral dip method (Clough and Bent, 1998). Transgenic T1 lines were identified by screening the seeds on MS agar medium supplemented with 50 mg/L kanamycin. Transgene expression in various transgenic lines was quantified using qPCR.

4.5 RNA isolation and quantitative real-time RT-PCR analysis

To assess the expression level of miR858 (both mature and primary transcripts), total RNA was isolated from 20 mg root tissues using TRIzol reagent (Invitrogen) following the manufacturer's instructions. Mir-X miRNA First-Strand Synthesis Kit (Clontech) was used for polyadenylation and reverse transcription of the total RNA. Approximately, 50 ng of the synthesized cDNA was used as a template for qPCR reaction. qPCR was performed using SYBR Advantage qPCR Premix (Clontech). The mature miR858 sequence appended with two adenine residues on the 3' end was used as forward primer sequence to ensure correct binding of the primer to the poly(T) region of the mature miR858 cDNA and prevent potential binding to the miR858 precursor. The primary transcript of miR858 was quantified using forward primer specific to miRNA precursor. U6 small nuclear RNA, the most commonly used internal control for miRNA gene expression normalization, was used to normalize the expression levels of both mature and primary miR858 transcripts. The mRQ 3' primer (supplied with Mir-X miRNA First-Strand Synthesis Kit) was used as a universal reverse primer. The PCR reactions were performed in QuantStudio 6 Flex Real-Time PCR System (Applied Biosystems) using the following program: 95°C for 3 min followed by 40 cycles of 95°C for 30 s and 60°C for 30 s. The amplified products were then subjected to a temperature ramp to create the dissociation curves and determine amplification specificity. The dissociation program was 95°C for 15 s and 50°C for 15 s, followed by a slow gradient from 50°C to 95°C. For the quantification of MYB83 expression levels, total RNA was extracted from 20 mg

frozen ground root tissues following the method described by (Verwoerd et al., 1989). The isolated total RNA was treated with DNase I (Invitrogen) and approximately 25 ng of DNase-treated RNA was used as a template in qPCR reactions to quantify gene expression levels using Verso SYBR green One-Step qRT-PCR Rox mix (Thermo Scientific) following the manufacturer's protocol: 50°C for 15 min, 95°C for 15 min, and 40 cycles of 95°C for 15 s, 60°C for 90 s and 72°C for 30S. The PCR amplification products were then subjected to a temperature ramp to create the dissociation curves using the following program: 95°C for 15 s and 60°C for 75 s, followed by a slow gradient from 60°C to 95°C.

4.6 RNA-seq library preparation and data analysis

P35S:miR858 (Line 1-4), P35S:rMYB83 (Line 8-1) and Col-0 were grown in MS plates using a randomized complete-block design with three independent replications per line. Root tissues were collected of two-week-old plants. mRNA was isolated from 20 mg grounded root tissue using magnetic mRNA isolation kit (NEB) following manufacturer's protocol. Approximately, 250 ng of mRNA was used for RNA-seq library preparation using NEBnext mRNA library prep master mix (NEB) following manufacturer's protocol. The nine RNA-seq libraries were multiplexed and sequenced using HiSeq 2500 system with 100 bp single-end reads. Quality of the sequenced data was assessed using FastQC (http://www.bioinformatics.babraham.ac.uk/projects/fastqc/). Low quality reads were trimmed using Trimmomatic (Bolger et al., 2014). After trimming, uniquely mapped read was aligned to the *Arabidopsis* reference genome (TAIR10) using TopHat v2.0.14 (Trapnell et al., 2009). Number of reads assigned to each gene were counted using HTSeq (Anders et al., 2015). Differentially expressed genes (DEGs) were determined using the R package DESeq2 (Love et al., 2014) using an adjusted *P* value less than 0.05. GO terms enrichment analysis of the DEGs was performed using agriGO database (Du et al., 2010) using Fisher's exact test and Bonferroni multi-test adjustment with a significance cut-off *P* value of 0.05.

Accession numbers

Sequence data of Arabidopsis genes described in this study can be found in The Arabidopsis Information Resource database under the following accession numbers: miR858 (AT1G71002), *MYB83* (AT3G08500), *MYB12* (AT2G47460), and *Actin8* (AT1G49240).

The RNA-seq data described in this manuscript were submitted to the National Center for Biotechnology Information, Gene Expression Omnibus under accession number GSE95198.

References

Absmanner B, Stadler R, Hammes UZ (2013) Phloem development in nematode-induced feeding sites: the implications of auxin and cytokinin. Front Plant Sci **4:** 241

Addo-Quaye C, Eshoo TW, Bartel DP, Axtell MJ (2008) Endogenous siRNA and miRNA targets identified by sequencing of the Arabidopsis degradome. Curr Biol **18:** 758-762

Anders S, Pyl PT, Huber W (2015) HTSeq-a Python framework to work with high-throughput sequencing data. Bioinformatics **31:** 166-169

Bak S, Tax FE, Feldmann KA, Galbraith DW, Feyereisen R (2001) CYP83B1, a cytochrome P450 at the metabolic branch point in auxin and indole glucosinolate biosynthesis in Arabidopsis. Plant Cell **13:** 101-111

Bartel DP (2004) MicroRNAs: genomics, biogenesis, mechanism, and function. Cell **116:** 281-297

Bhattarai KK, Atamian HS, Kaloshian I, Eulgem T (2010) WRKY72-type transcription factors contribute to basal immunity in tomato and Arabidopsis as well as gene-for-gene resistance mediated by the tomato R gene Mi-1. Plant J **63:** 229-240

Bohlmann H, Sobczak M (2014) The plant cell wall in the feeding sites of cyst nematodes. Front Plant Sci **5:** 89

Bolger AM, Lohse M, Usadel B (2014) Trimmomatic: a flexible trimmer for Illumina sequence data. Bioinformatics **30:** 2114-2120

Bonnet E, Wuyts J, Rouzé P, Van de Peer Y (2004) Detection of 91 potential conserved plant microRNAs in *Arabidopsis thaliana* and *Oryza sativa* identifies important target genes. Proc Natl Acad Sci USA **101:** 11511-11516

Cabrera J, Barcala M, Garcia A, Rio-Machin A, Medina C, Jaubert-Possamai S, Favery B, Maizel A, Ruiz-Ferrer V, Fenoll C, et al. (2016) Differentially expressed small RNAs in Arabidopsis galls formed by *Meloidogyne javanica*: a functional role for miR390 and its TAS3-derived tasiRNAs. New Phytol **209:** 1625-1640

Cabrera J, Diaz-Manzano FE, Fenoll C, Escobar C (2015) Developmental pathways mediated by hormones in nematode feeding sites. *In* Plant Nematode Interactions: A View on Compatible Interrelationships, Vol 73. Elsevier, Boston, pp 167-188

Cai X-T, Xu P, Zhao P-X, Liu R, Yu L-H, Xiang C-B (2014) Arabidopsis ERF109 mediates cross-talk between jasmonic acid and auxin biosynthesis during lateral root formation. Nat Commun **5:** 5833

Camehl I, Oelmüller R (2010) Do ethylene response factors-9 and -14 repress PR gene expression in the interaction between *Piriformospora indica* and Arabidopsis? Plant Signal Behav **5:** 932-936

Chen XM (2009) Small RNAs and their roles in plant development. Annu Rev Cell Dev Biol **25:** 21-44

Chen YC, Wong CL, Muzzi F, Vlaardingerbroek I, Kidd BN, Schenk PM (2014) Root defense analysis against *Fusarium oxysporum* reveals new regulators to confer resistance. Sci Rep **4:** 5584

Chuck G, Candela H, Hake S (2009) Big impacts by small RNAs in plant development. Curr Opin Plant Biol **12:** 81-86

Clough SJ, Bent AF (1998) Floral dip: a simplified method for Agrobacterium-mediated transformation of *Arabidopsis thaliana*. Plant J **16:** 735-743

Cominelli E, Galbiati M, Vavasseur A, Conti L, Sala T, Vuylsteke M, Leonhardt N, Dellaporta SL, Tonelli C (2005) A guard-cell-specific MYB transcription factor regulates stomatal movements and plant drought tolerance. Curr Biol **15:** 1196-1200

Cui F, Brosché M, Sipari N, Tang S, Overmyer K (2013) Regulation of ABA dependent wound induced spreading cell death by MYB108. New Phytol **200:** 634-640

De León IP, Sanz A, Hamberg M, Castresana C (2002) Involvement of the Arabidopsisα-DOX1 fatty acid dioxygenase in protection against oxidative stress and cell death. Plant J **29:** 61-72

Du Z, Zhou X, Ling Y, Zhang Z, Su Z (2010) agriGO: a GO analysis toolkit for the agricultural community. Nucleic acids Res **38:** W64-70

Fahlgren N, Howell MD, Kasschau KD, Chapman EJ, Sullivan CM, Cumbie JS, Givan SA, Law TF, Grant SR, Dangl JL, et al. (2007) High-throughput sequencing of Arabidopsis microRNAs: evidence for frequent birth and death of MIRNA genes. Plos One **2:** e219

Fei Q, Zhang Y, Xia R, Meyers BC (2016) Small RNAs add zing to the zig-zag-zig model of plant defenses. Mol Plant Microbe Interact **29:** 165-169

Frerigmann H, Gigolashvili T (2014) MYB34, MYB51, and MYB122 distinctly regulate indolic glucosinolate biosynthesis in *Arabidopsis thaliana*. Mol Plant **7:** 814-828

Gao S, Zhang YL, Yang L, Song JB, Yang ZM (2014) AtMYB20 is negatively involved in plant adaptive response to drought stress. Plant and soil **376:** 433-443

Gheysen G, Mitchum MG (2011) How nematodes manipulate plant development pathways for infection. Curr Opin Plant Biol **14:** 415-421

Goverse A, Bird D (2011) The role of plant hormones in nematode feeding cell formation. *In* J Jones, G Gheysen, C Fenoll, eds, Genomics and Molecular Genetics of Plant-Nematode Interactions. Springer, pp 325-347

Goverse A, Overmars H, Engelbertink J, Schots A, Bakker J, Helder J (2000) Both induction and morphogenesis of cyst nematode feeding cells are mediated by auxin. Mol Plant Microbe Interact **13:** 1121-1129

Grunewald W, Cannoot B, Friml J, Gheysen G (2009) Parasitic nematodes modulate PIN-mediated auxin transport to facilitate infection. Plos Pathog **5:** e1000266

Grunewald W, Van Noorden G, Van Isterdael G, Beeckman T, Gheysen G, Mathesius U (2009) Manipulation of auxin transport in plant roots during Rhizobium symbiosis and nematode parasitism. Plant Cell **21:** 2553-2562

Guan X, Pang M, Nah G, Shi X, Ye W, Stelly DM, Chen ZJ (2014) miR828 and miR858 regulate homoeologous MYB2 gene functions in Arabidopsis trichome and cotton fibre development. Nat Commun **5:** 3050

Gupta OP, Sharma P, Gupta RK, Sharma I (2014) Current status on role of miRNAs during plant–fungus interaction. Physiol Mol Plant Pathol **85:** 1-7

Gutierrez L, Bussell JD, Pacurar DI, Schwambach J, Pacurar M, Bellini C (2009) Phenotypic plasticity of adventitious rooting in Arabidopsis is controlled by complex regulation of AUXIN RESPONSE FACTOR transcripts and microRNA abundance. Plant Cell **21:** 3119-3132

Hewezi T (2015) Cellular signaling pathways and posttranslational modifications mediated by nematode effector proteins. Plant Physiol **169:** 1018-1026

Hewezi T, Baum TJ (2012) Complex feedback regulations govern the expression of miRNA396 and its GRF target genes. Plant Signal Behav **7:** 749-751

Hewezi T, Baum TJ (2015) Gene silencing in nematode feeding sites. *In* C Escobar, C Fenoll, eds, Advances in Botanical Research, Vol 73. Elsevier, Boston, pp 221-239

Hewezi T, Maier TR, Nettleton D, Baum TJ (2012) The Arabidopsis microRNA396-GRF1/GRF3 regulatory module acts as a developmental regulator in the reprogramming of root cells during cyst nematode infection. Plant Physiol **159:** 321-335

Hewezi T, Piya S, Qi M, Balasubramaniam M, Rice JH, Baum TJ (2016) Arabidopsis miR827 mediates post-transcriptional gene silencing of its ubiquitin E3 ligase target gene in the syncytium of the cyst nematode *Heterodera schachtii* to enhance susceptibility. Plant J **88:** 179-192

Hewezi T, Piya S, Richard G, Rice JH (2014) Spatial and temporal expression patterns of auxin response transcription factors in the syncytium induced by the beet cyst nematode *Heterodera schachtii* in Arabidopsis. Mol Plant Pathol **15:** 730-736

Hofmann J, Hess PH, Szakasits D, Blöchl A, Wieczorek K, Daxböck-Horvath S, Bohlmann H, van Bel AJ, Grundler FM (2009) Diversity and activity of sugar transporters in nematode-induced root syncytia. J Exp Bot **60:** 3085-3095

Huffaker A, Pearce G, Ryan CA (2006) An endogenous peptide signal in Arabidopsis activates components of the innate immune response. Proc Natl Acad Sci USA **103:** 10098-10103

Jefferson RA, Kavanagh TA, Bevan MW (1987) GUS fusions: beta-glucuronidase as a sensitive and versatile gene fusion marker in higher plants. EMBO J **6:** 3901-3907

Jia X, Shen J, Liu H, Li F, Ding N, Gao C, Pattanaik S, Patra B, Li R, Yuan L (2015) Small tandem target mimic-mediated blockage of microRNA858 induces anthocyanin accumulation in tomato. Planta **242:** 283-293

Jin J, Hewezi T, Baum TJ (2011) Arabidopsis peroxidase AtPRX53 influences cell elongation and susceptibility to *Heterodera schachtii*. Plant Signal Behav **6:** 1778-1786

Jones-Rhoades MW, Bartel DP (2004) Computational identification of plant microRNAs and their targets, including a stress-induced miRNA. Mol Cell **14:** 787-799

Journot-Catalino N, Somssich IE, Roby D, Kroj T (2006) The transcription factors WRKY11 and WRKY17 act as negative regulators of basal resistance in *Arabidopsis thaliana*. Plant Cell **18:** 3289-3302

Kammerhofer N, Radakovic Z, Regis JM, Dobrev P, Vankova R, Grundler FM, Siddique S, Hofmann J, Wieczorek K (2015) Role of stress-related hormones in plant defence during early infection of the cyst nematode *Heterodera schachtii* in Arabidopsis. New Phytol **207:** 778-789

Kandoth PK, Ithal N, Recknor J, Maier T, Nettleton D, Baum TJ, Mitchum MG (2011) The soybean Rhg1 locus for resistance to the soybean cyst nematode *Heterodera glycines* regulates expression of a large number of stress-and defense-related genes in degenerating feeding cells. Plant Physiol **155:** 1960-1975

Karczmarek A, Overmars H, Helder J, Goverse A (2004) Feeding cell development by cyst and root-knot nematodes involves a similar early, local and transient activation of a specific auxin-inducible promoter element. Mol Plant Pathol **5:** 343-346

Kidner CA, Martienssen RA (2005) The developmental role of microRNA in plants. Curr Opin Plant Biol **8:** 38-44

Lee HJ, Park YJ, Kwak KJ, Kim D, Park JH, Lim JY, Shin C, Yang KY, Kang H (2015) MicroRNA844-guided downregulation of Cytidinephosphate Diacylglycerol Synthase3 (CDS3) mRNA affects the response of *Arabidopsis thaliana* to bacteria and fungi. Mol Plant Microbe Interact **28:** 892-900

Li J, Brader G, Palva ET (2008) Kunitz trypsin inhibitor: an antagonist of cell death triggered by phytopathogens and fumonisin b1 in Arabidopsis. Mol Plant **1:** 482-495

Li Y, Lu YG, Shi Y, Wu L, Xu YJ, Huang F, Guo XY, Zhang Y, Fan J, Zhao JQ, et al. (2014) Multiple rice microRNAs are involved in immunity against the blast fungus *Magnaporthe oryzae*. Plant Physiol **164:** 1077-1092

Li Y, Zhang Q, Zhang J, Wu L, Qi Y, Zhou JM (2010) Identification of microRNAs involved in pathogen-associated molecular pattern-triggered plant innate immunity. Plant Physiol **152:** 2222-2231

Liu J, Cheng X, Liu D, Xu W, Wise R, Shen QH (2014) The miR9863 family regulates distinct Mla alleles in barley to attenuate NLR receptor-triggered disease resistance and cell-death signaling. PLoS Genet **10:** e1004755

Liu J, Rice JH, Chen N, Baum TJ, Hewezi T (2014) Synchronization of developmental processes and defense signaling by growth regulating transcription factors. Plos One **9:** e98477

Love MI, Huber W, Anders S (2014) Moderated estimation of fold change and dispersion for RNA-seq data with DESeq2. Genome Biol **15:** 550

Marin E, Jouannet V, Herz A, Lokerse AS, Weijers D, Vaucheret H, Nussaume L, Crespi MD, Maizel A (2010) miR390, Arabidopsis TAS3 tasiRNAs, and their AUXIN RESPONSE FACTOR targets define an autoregulatory network quantitatively regulating lateral root growth. Plant Cell **22:** 1104-1117

Maruyama Y, Yamoto N, Suzuki Y, Chiba Y, Yamazaki K, Sato T, Yamaguchi J (2013) The Arabidopsis transcriptional repressor ERF9 participates in resistance against necrotrophic fungi. Plant Sci **213:** 79-87

Matsuo M, Johnson JM, Hieno A, Tokizawa M, Nomoto M, Tada Y, Godfrey R, Obokata J, Sherameti I, Yamamoto YY, et al. (2015) High REDOX RESPONSIVE TRANSCRIPTION FACTOR1 levels result in accumulation of reactive oxygen species in *Arabidopsis thaliana* shoots and roots. Mol Plant **8:** 1253-1273

McCarthy RL, Zhong RQ, Ye ZH (2009) MYB83 is a direct target of SND1 and acts redundantly with MYB46 in the regulation of secondary cell wall biosynthesis in Arabidopsis. Plant Cell Physiol **50:** 1950-1964

Mehrtens F, Kranz H, Bednarek P, Weisshaar B (2005) The Arabidopsis transcription factor MYB12 is a flavonol-specific regulator of phenylpropanoid biosynthesis. Plant Physiol **138:** 1083-1096

Meng X, Xu J, He Y, Yang KY, Mordorski B, Liu Y, Zhang S (2013) Phosphorylation of an ERF transcription factor by Arabidopsis MPK3/MPK6 regulates plant defense gene induction and fungal resistance. Plant Cell **25:** 1126-1142

Meng Y, Shao C, Chen M (2011) Toward microRNA-mediated gene regulatory networks in plants. Briefings in bioinformatics**:** bbq091

Merelo P, Ram H, Pia Caggiano M, Ohno C, Ott F, Straub D, Graeff M, Cho SK, Yang SW, Wenkel S, et al. (2016) Regulation of MIR165/166 by class II and class III homeodomain leucine zipper proteins establishes leaf polarity. Proc Natl Acad Sci USA **113:** 11973-11978

Moffat CS, Ingle RA, Wathugala DL, Saunders NJ, Knight H, Knight MR (2012) ERF5 and ERF6 play redundant roles as positive regulators of JA/Et-mediated defense against Botrytis cinerea in Arabidopsis. Plos One **7:** e35995

Mu R-L, Cao Y-R, Liu Y-F, Lei G, Zou H-F, Liao Y, Wang H-W, Zhang W-K, Ma B, Du J-Z (2009) An R2R3-type transcription factor gene AtMYB59 regulates root growth and cell cycle progression in Arabidopsis. Cell Res **19:** 1291-1304

Nahar K, Kyndt T, De Vleesschauwer D, Höfte M, Gheysen G (2011) The jasmonate pathway is a key player in systemically induced defense against root knot nematodes in rice. Plant Physiol **157:** 305-316

Nahar K, Kyndt T, Nzogela YB, Gheysen G (2012) Abscisic acid interacts antagonistically with classical defense pathways in rice–migratory nematode interaction. New Phytol **196:** 901-913

Niu D, Lii YE, Chellappan P, Lei L, Peralta K, Jiang C, Guo J, Coaker G, Jin H (2016) miRNA863-3p sequentially targets negative immune regulator ARLPKs and positive regulator SERRATE upon bacterial infection. Nat Commun **7:** 11324

Ogawa T, Pan L, Kawai-Yamada M, Yu LH, Yamamura S, Koyama T, Kitajima S, Ohme-Takagi M, Sato F, Uchimiya H (2005) Functional analysis of Arabidopsis ethylene-responsive element binding protein conferring resistance to Bax and abiotic stress-induced plant cell death. Plant Physiol **138:** 1436-1445

Oh JE, Kwon Y, Kim JH, Noh H, Hong SW, Lee H (2011) A dual role for MYB60 in stomatal regulation and root growth of *Arabidopsis thaliana* under drought stress. Plant Mol Biol **77:** 91-103

Ozalvo R, Cabrera J, Escobar C, Christensen SA, Borrego EJ, Kolomiets MV, Castresana C, Iberkleid I, Brown Horowitz S (2014) Two closely related members of Arabidopsis 13-lipoxygenases (13-LOXs), LOX3 and LOX4, reveal distinct functions in response to plant-parasitic nematode infection. Mol Plant Pathol **15:** 319-332

Park YJ, Lee HJ, Kwak KJ, Lee K, Hong SW, Kang H (2014) MicroRNA400-guided cleavage of Pentatricopeptide repeat protein mRNAs Renders *Arabidopsis thaliana* more susceptible to pathogenic bacteria and fungi. Plant Cell Physiol **55:** 1660-1668

Seo JK, Wu J, Lii Y, Li Y, Jin H (2013) Contribution of small RNA pathway components in plant immunity. Mol Plant Microbe Interact **26:** 617-625

Shanks CM, Rice JH, Zubo Y, Schaller GE, Hewezi T, Kieber JJ (2015) The role of cytokinin during infection of *Arabidopsis thaliana* by the cyst nematode *Heterodera schachtii*. Mol Plant Microbe Interact **29:** 57-68

Sharma D, Tiwari M, Pandey A, Bhatia C, Sharma A, Trivedi PK (2016) MicroRNA858 is a potential regulator of phenylpropanoid pathway and plant development in Arabidopsis. Plant Physiol **171:** 944-959.

Siddique S, Radakovic ZS, Carola M, Chronis D, Novák O, Ramireddy E, Holbein J, Matera C, Hütten M, Gutbrod P (2015) A parasitic nematode releases cytokinin that controls cell division and orchestrates feeding site formation in host plants. Proc Natl Acad Sci USA **112:** 12669-12674

Siddique S, Wieczorek K, Szakasits D, Kreil DP, Bohlmann H (2011) The promoter of a plant defensin gene directs specific expression in nematode-induced syncytia in Arabidopsis roots. Plant Physiol Biochem **49:** 1100-1107

Staiger D, Korneli C, Lummer M, Navarro L (2013) Emerging role for RNA-based regulation in plant immunity. New Phytol **197:** 394-404

Sun J, Xu Y, Ye S, Jiang H, Chen Q, Liu F, Zhou W, Chen R, Li X, Tietz O (2009) Arabidopsis ASA1 is important for jasmonate-mediated regulation of auxin biosynthesis and transport during lateral root formation. Plant Cell **21:** 1495-1511

Szakasits D, Heinen P, Wieczorek K, Hofmann J, Wagner F, Kreil DP, Sykacek P, Grundler FM, Bohlmann H (2009) The transcriptome of syncytia induced by the cyst nematode *Heterodera schachtii* in Arabidopsis roots. Plant J **57:** 771-784

Trapnell C, Pachter L, Salzberg SL (2009) TopHat: discovering splice junctions with RNA-Seq. Bioinformatics **25:** 1105-1111

Verwoerd TC, Dekker BMM, Hoekema A (1989) A small-scale procedure for the rapid isolation of plant RNAs. Nucleic acids Res **17:** 2362-2362

Voinnet O (2009) Origin, biogenesis, and activity of plant microRNAs. Cell **136:** 669-687

Wang H, Jiao X, Kong X, Hamera S, Wu Y, Chen X, Fang R, Yan Y (2016) A signaling cascade from miR444 to RDR1 in rice antiviral RNA silencing pathway. Plant Physiol **170:** 2365-2377

Weiberg A, Wang M, Bellinger M, Jin H (2014) Small RNAs: a new paradigm in plant-microbe interactions. Annu Rev Phytopathol **52:** 495-516

Westfall CS, Sherp AM, Zubieta C, Alvarez S, Schraft E, Marcellin R, Ramirez L, Jez JM (2016) Arabidopsis thaliana GH3.5 acyl acid amido synthetase mediates metabolic crosstalk in auxin and salicylic acid homeostasis. Proc Natl Acad Sci USA **113:** 13917-13922

Wieczorek K, Elashry A, Quentin M, Grundler F, Favery B, Seifert G, Bohlmann H (2014) A distinct role of pectate lyases in the formation of feeding structures induced by cyst and root-knot nematodes. Mol Plant Microbe Interact **27:** 901-912

Wieczorek K, Golecki B, Gerdes L, Heinen P, Szakasits D, Durachko DM, Cosgrove DJ, Kreil DP, Puzio PS, Bohlmann H, et al. (2006) Expansins are involved in the formation of nematode-induced syncytia in roots of *Arabidopsis thaliana*. Plant J **48:** 98-112

Wu G, Park MY, Conway SR, Wang JW, Weigel D, Poethig RS (2009) The sequential action of miR156 and miR172 regulates developmental timing in Arabidopsis. Cell **138:** 750-759

Wubben MJE, Su H, Rodermel SR, Baum TJ (2001) Susceptibility to the sugar beet cyst nematode is modulated by ethylene signal transduction in *Arabidopsis thaliana*. Mol Plant Microbe Interact **14:** 1206-1212

Xie Z, Kasschau KD, Carrington JC (2003) Negative feedback regulation of Dicer-Like1 in Arabidopsis by microRNA-guided mRNA degradation. Curr Biol **13:** 784-789

Xu J, Meng J, Meng X, Zhao Y, Liu J, Sun T, Liu Y, Wang Q, Zhang S (2016) Pathogen-responsive MPK3 and MPK6 reprogram the biosynthesis of indole glucosinolates and their derivatives in Arabidopsis immunity. Plant Cell **28:** 1144-1162

Xu X, Chen C, Fan B, Chen Z (2006) Physical and functional interactions between pathogen-induced Arabidopsis WRKY18, WRKY40, and WRKY60 transcription factors. Plant Cell **18:** 1310-1326

Yang H, Li Y, Hua J (2006) The C2 domain protein BAP1 negatively regulates defense responses in Arabidopsis. Plant J **48:** 238-248

Yang H, Yang S, Li Y, Hua J (2007) The Arabidopsis BAP1 and BAP2 genes are general inhibitors of programmed cell death. Plant Physiol **145:** 135-146

Yang L, Huang H (2014) Roles of small RNAs in plant disease resistance. J Integr Plant Biol **56:** 962-970

Yant L, Mathieu J, Dinh TT, Ott F, Lanz C, Wollmann H, Chen X, Schmid M (2010) Orchestration of the floral transition and floral development in Arabidopsis by the bifunctional transcription factor APETALA2. Plant Cell **22:** 2156-2170

Zhang W, Gao S, Zhou X, Chellappan P, Chen Z, Zhou X, Zhang X, Fromuth N, Coutino G, Coffey M, et al. (2011) Bacteria-responsive microRNAs regulate plant innate immunity by modulating plant hormone networks. Plant Mol Biol **75:** 93-105

Zhang Z, Li Q, Li Z, Staswick PE, Wang M, Zhu Y, He Z (2007) Dual regulation role of GH3.5 in salicylic acid and auxin signaling during Arabidopsis-*Pseudomonas syringae* interaction. Plant Physiol **145:** 450-464

Zhang Z, Wu Y, Gao M, Zhang J, Kong Q, Liu Y, Ba H, Zhou J, Zhang Y (2012) Disruption of PAMP-induced MAP kinase cascade by a *Pseudomonas syringae* effector activates plant immunity mediated by the NB-LRR protein SUMM2. Cell Host Microbe **11:** 253-263

Zhao W, Li Z, Fan J, Hu C, Yang R, Qi X, Chen H, Zhao F, Wang S (2015) Identification of jasmonic acid-associated microRNAs and characterization of the regulatory roles of the miR319/TCP4 module under root-knot nematode stress in tomato. J Exp Bot **66:** 4653-4667

Zhong R, Ye ZH (2012) MYB46 and MYB83 bind to the SMRE sites and directly activate a suite of transcription factors and secondary wall biosynthetic genes. Plant Cell Physiol **53:** 368-380

Appendix

Figure 4-1. Histochemical staining of GUS activity driven by miR858 and MYB83 promoters in transgenic Arabidopsis lines in response to *H. schachtii* infection.
(A) to (C) GUS activity of the pmiR858:GUS plants under non-infected condition in leaves (A), and root tissues (B and C) of two-week-old plants. (D) to (G) GUS activity of the pmiR858:GUS plants in response to *H. schachtii* infection. Strong GUS activity was observed in the *H. schachtii*–induced syncytia at 3 (D) and 7 (E) dpi, whereas at 10 and 14 dpi GUS activity was dramatically reduced in the syncytia (F and G). (H) to (I) GUS activity of the pMYB83:GUS under non-infected conditions. Strong GUS activity was observed in in leaves (H), and vascular root tissues (I and J) of two-week-old plants. (K) to (N) GUS activity of the pMYB83:GUS plants in response to *H. schachtii* infection. Strong GUS activity was observed in the *H. schachtii*–induced syncytia at 3 (K) and 7 (L), 10 (M) and 14 (N) dpi. "N" indicates nematode and "S" indicates syncytium. Bars = 100 μm.

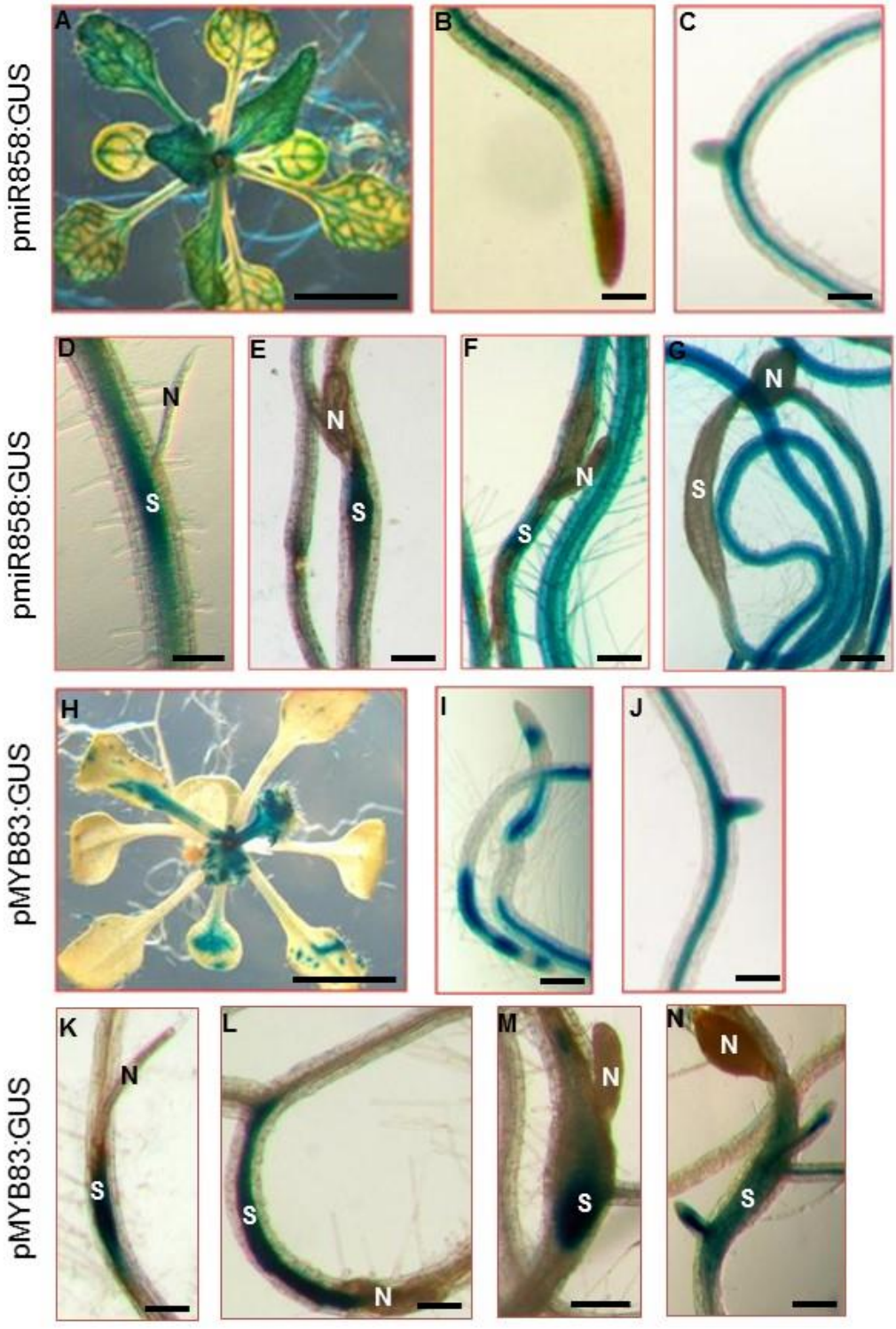

Figure 4-1. contd.

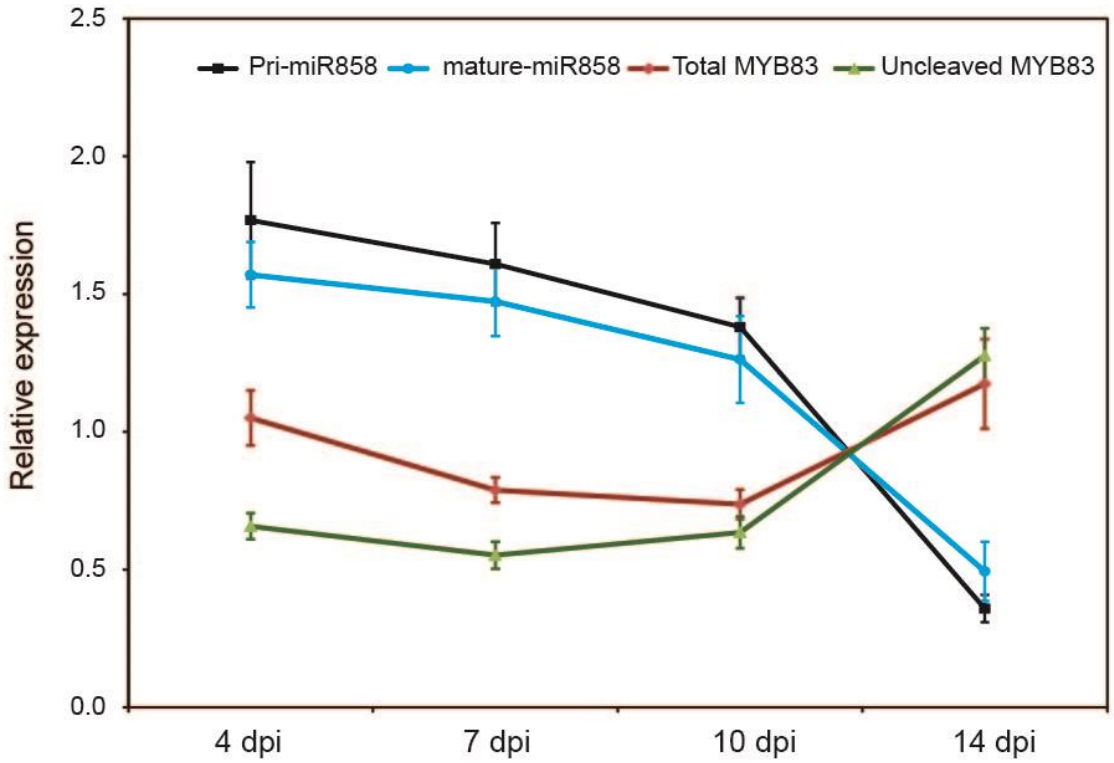

Figure 4-2. miR858 post-transcriptionally downregulates MYB83 during *H. schachtii* parasitism of Arabidopsis.

The abundance of primary and mature miR858 as well as total and uncleaved transcript levels of *MYB83* were measured using qPCR in the roots of wild-type Col-0 plants at 4, 7, 10 and 14 d post *H. schachtii* infection, relative to non-infected control plants. The total transcript levels of *MYB83* were inversely correlated with the expression levels of primary and mature miR858 at the four time points. In addition, the levels of uncleaved *MYB83* transcripts were lower than the level of total transcripts at 4 and 7 dpi, indicative of a post-transcriptional downregulation of *YB83* by miR858 at these two time points. Data were obtained from three biological samples and represented as mean ± SE.

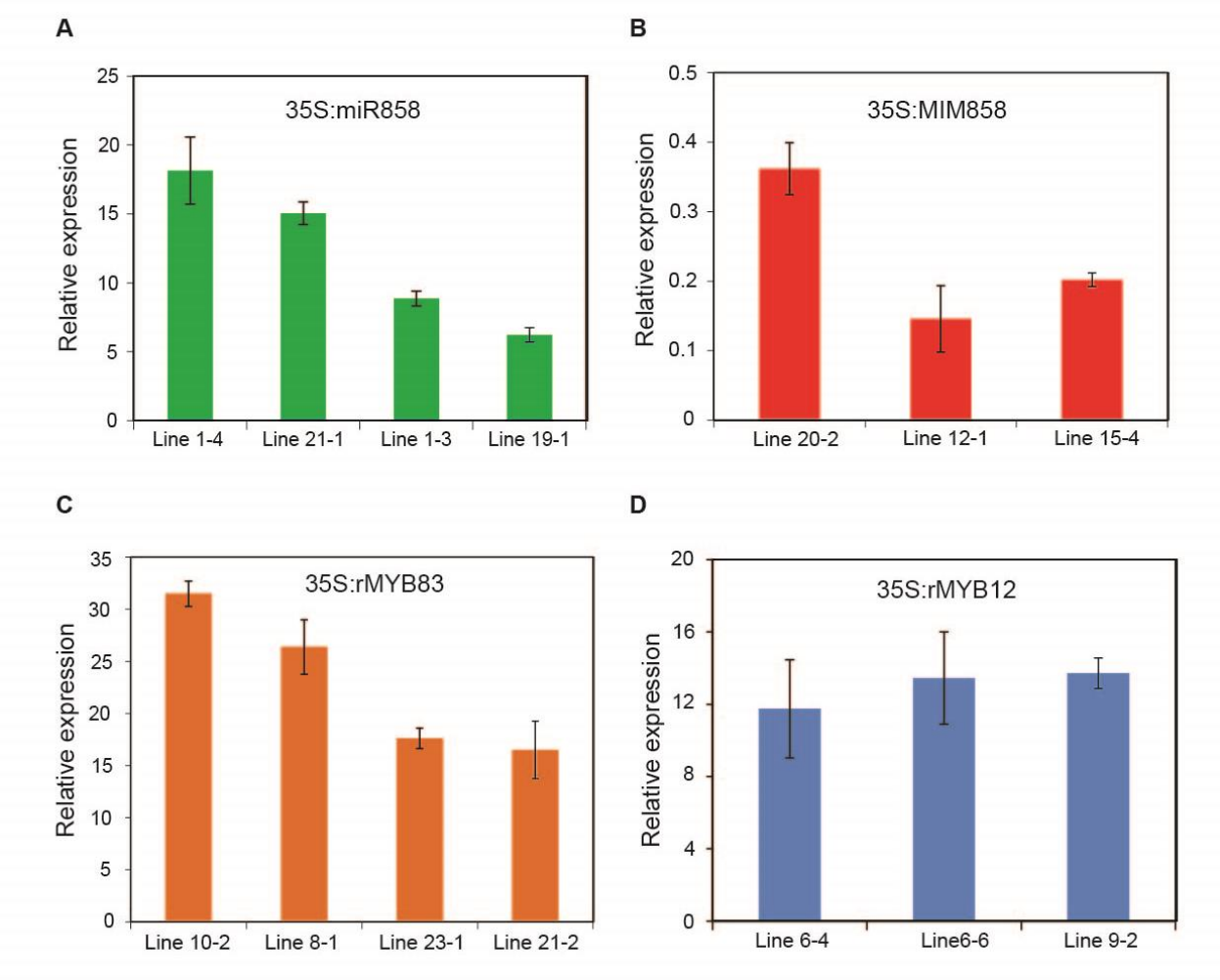

Figure 4-3. Gene expression levels of miR858, *MIM858*, *rMYB83* and *rMYB12* in transgenic lines.

Gene expression levels was quantified using qPCR in two-week-plants overexpressing miR858 (A), *MIM858* (B), *rMYB83* (C) or *rMYB12* (D), relative to wild-type Col-0 plants. Gene expression levels were normalized using *Actin8* as internal reference control. Shown are averages of three biological samples ± SE.

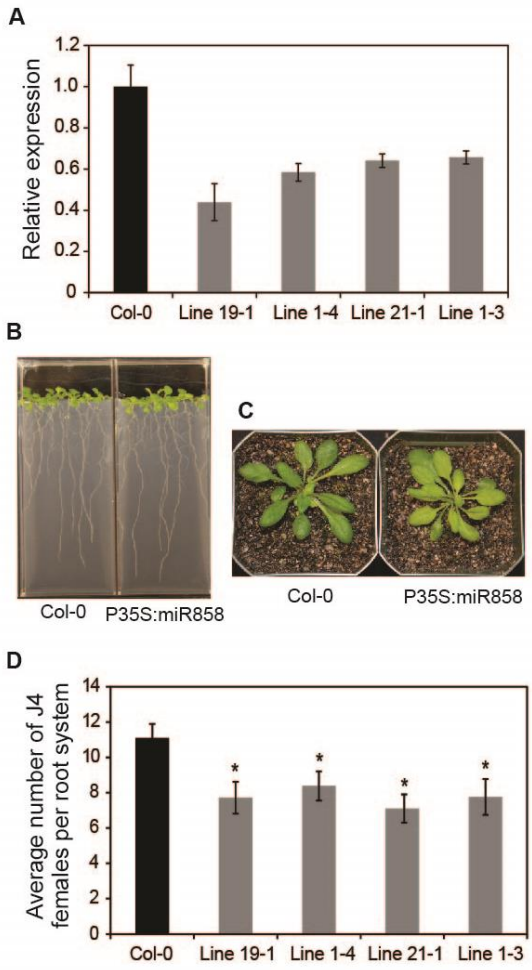

Figure 4-4. Overexpression of miR858 confers enhanced resistance to *H. schachtii.*

(A) Constitutive overexpression of miR858 in four independent transgenic Arabidopsis lines resulted in significant decreases in *MYB83* expression levels. The expression levels of *MYB83* were determined in the roots of two-week-old transgenic lines relative to the wild-type Col-0 plants using qPCR. Shown are average expression levels obtained from three biological samples ± SE. (B) and (C), Root (C) and shoot (B) phenotypes of three-week-old transgenic Arabidopsis plants overexpression miR858. (D) Nematode infection assays of the miR858 overexpression lines showing reduced susceptibility to *H. schachtii* compared with the wild-type Col-0 plants. Shown are average numbers of J4 females per root system ± SE (n =20) at three weeks post inoculation. Asterisks indicate statistically significant differences from wild-type Col-0 plants at P value less than 0.05.

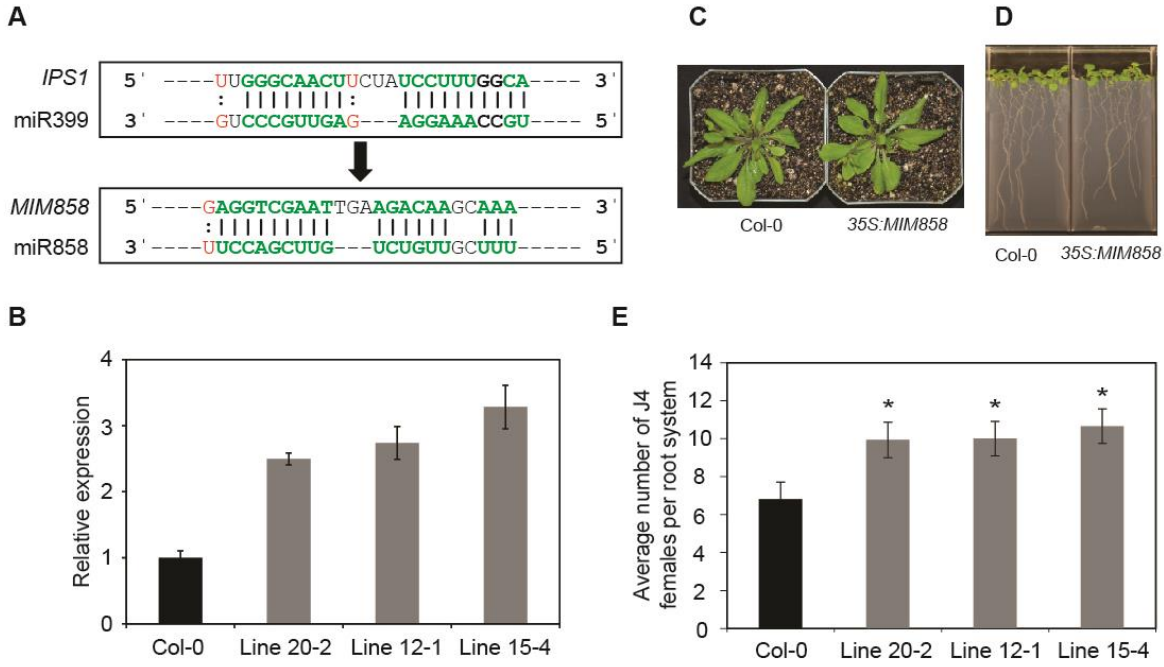

Figure 4-5. Constitutive downregulation of miR858 increased plant susceptibility to *H. schachtii.*

(A) Approach for creating a mimic binding site for miR858 (MIM858). The miR399 mimic sequence in the *IPS1* was replaced by an artificial non-cleavable binding site for the mature miR858. The artificial binding site contained a three-nucleotide bulge (TGA) that would prevent transcript cleavage and hence sequester miR858 activity. (B) and (C), Shoot (B) and root (C) phenotypes of three-week-old transgenic Arabidopsis plants overexpression *MIM858*. (D) Constitutive overexpression of *MIM858* in three independent transgenic Arabidopsis lines resulted in significant upregulation of *MYB83*. The expression levels of *MYB83* were quantified in the roots of two-week-old transgenic lines relative to the wild-type Col-0 plants using qPCR. Shown are average expression levels obtained from three biological samples ± SE. (E) Nematode infection assays of the *MIM858* overexpression lines showing increased susceptibility to *H. schachtii* compared with the wild-type Col-0 plants. Shown are average numbers of J4 females per root system ± SE (*n* =20) at three weeks post inoculation. Asterisks indicate statistically significant differences from wild-type Col-0 plants at P value less than 0.05.

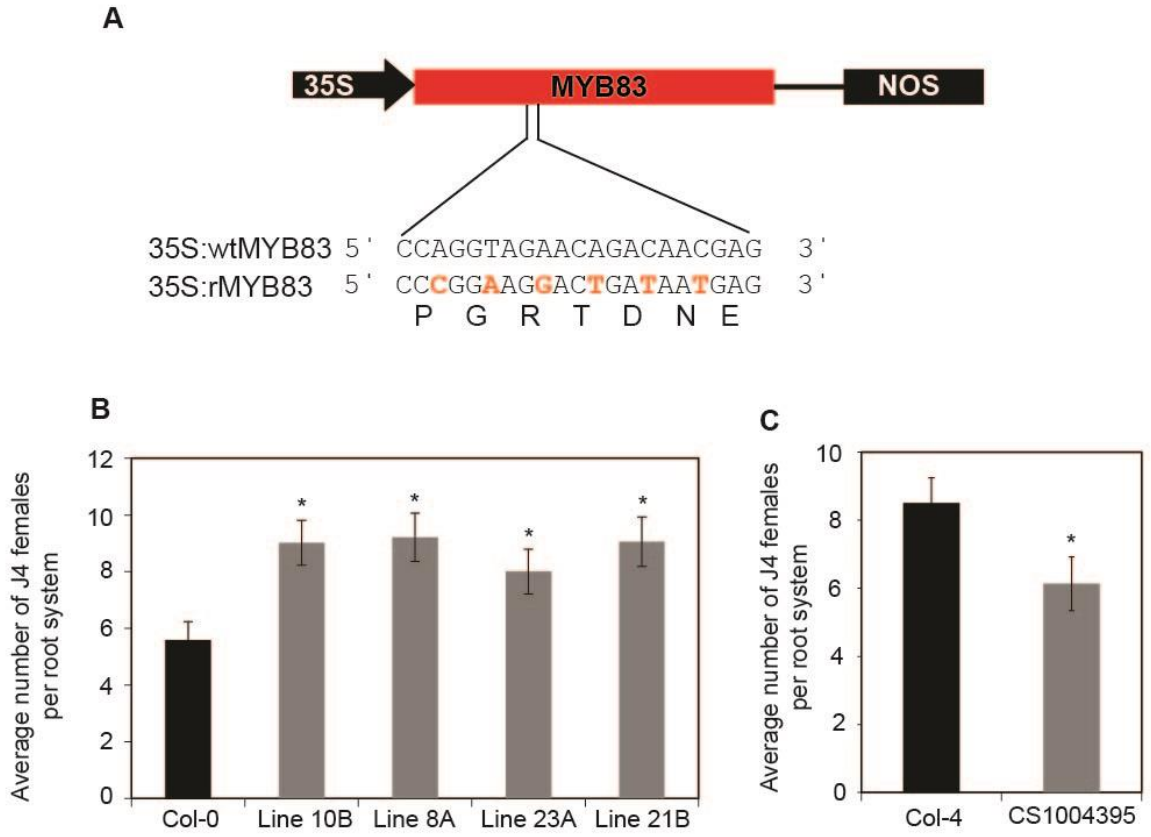

Figure 4-6. Constitutive overexpression of miR858-resistant variant of *MYB83* increased plant susceptibility to *H. schachtii.*

(A) Schematic representation showing the generation of a miR858-resistant variant of *MYB83* (*rMYB83*) by introducing synonymous mutations to the miR858 binding site in the MYB83 coding sequence. (B and C) Nematode infection assays of *rMYB83* overexpression lines and a *MYB83* mutant line. Three independent transgenic lines overexpressing *35S:rMYB83* construct showed increased susceptibility to *H. schachtii* compared with the wild-type Col-0 plants (B). In contrast, the *myb83* knockout mutant line CS1004395 showed reduced susceptibility compared with the wild-type Col-4 plants (C). Shown are average numbers of J4 females per root system ± SE (*n* =20) at three weeks post inoculation. Asterisks indicate statistically significant differences from the corresponding wild-type plants at P value less than 0.05.

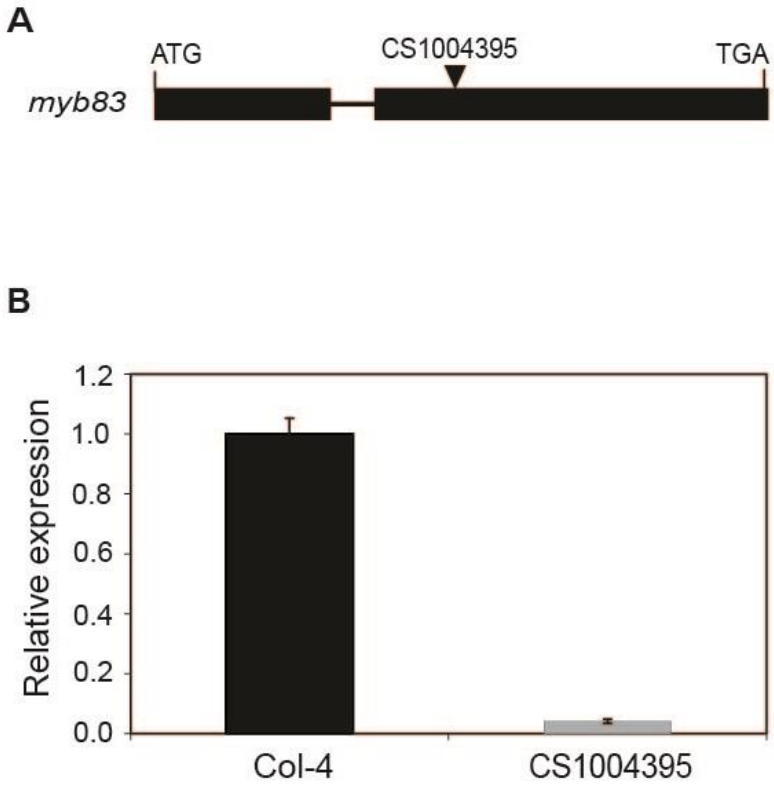

Figure 4-7. Characterization of the *MYB83* T-DNA mutant line (CS1004395).

(A) Schematic representation of T-DNA insertion site in the *myb83* mutant. (B) *MYB83* expression level in the *myb83* mutant relative to the wild-type Col-4 plants. *MYB83* expression level was quantified in two-week- old plants using qPCR and *Actin8* as internal reference control. Shown are averages of three biological samples ± SE.

Figure 4-8. Functional classification and Gene Ontology enrichment analyses of differentially expressed genes identified in 35S:miR858 and 35S:rMYB83 lines.

(A) Venn diagram displaying the number and overlap of the differentially expressed genes (DEGs) identified in miR858 and *rMYB83* overexpression lines. (B) Gene Ontology classification and enrichment analyses of the DEGs identified in 35S:miR858 and *35S:rMYB83* lines. Enrichment analyses of upregulated and downregulated genes were performed separately. (C) Venn diagram shown the overlap between MYB83-regulated genes and syncytium differentially expressed genes. (D) Venn diagram shown the overlap between MYB83 putative targets and syncytium differentially expressed genes. (E) Gene Ontology classification and enrichment analyses of MYB83-regulated genes and its putative direct targets overlapping with syncytium differentially expressed genes. Enrichment analyses of upregulated and downregulated genes were performed separately. Enrichment analysis was performed using Fisher's exact test and Bonferroni multi-test correction with a significance cut-off $P < 0.05$.

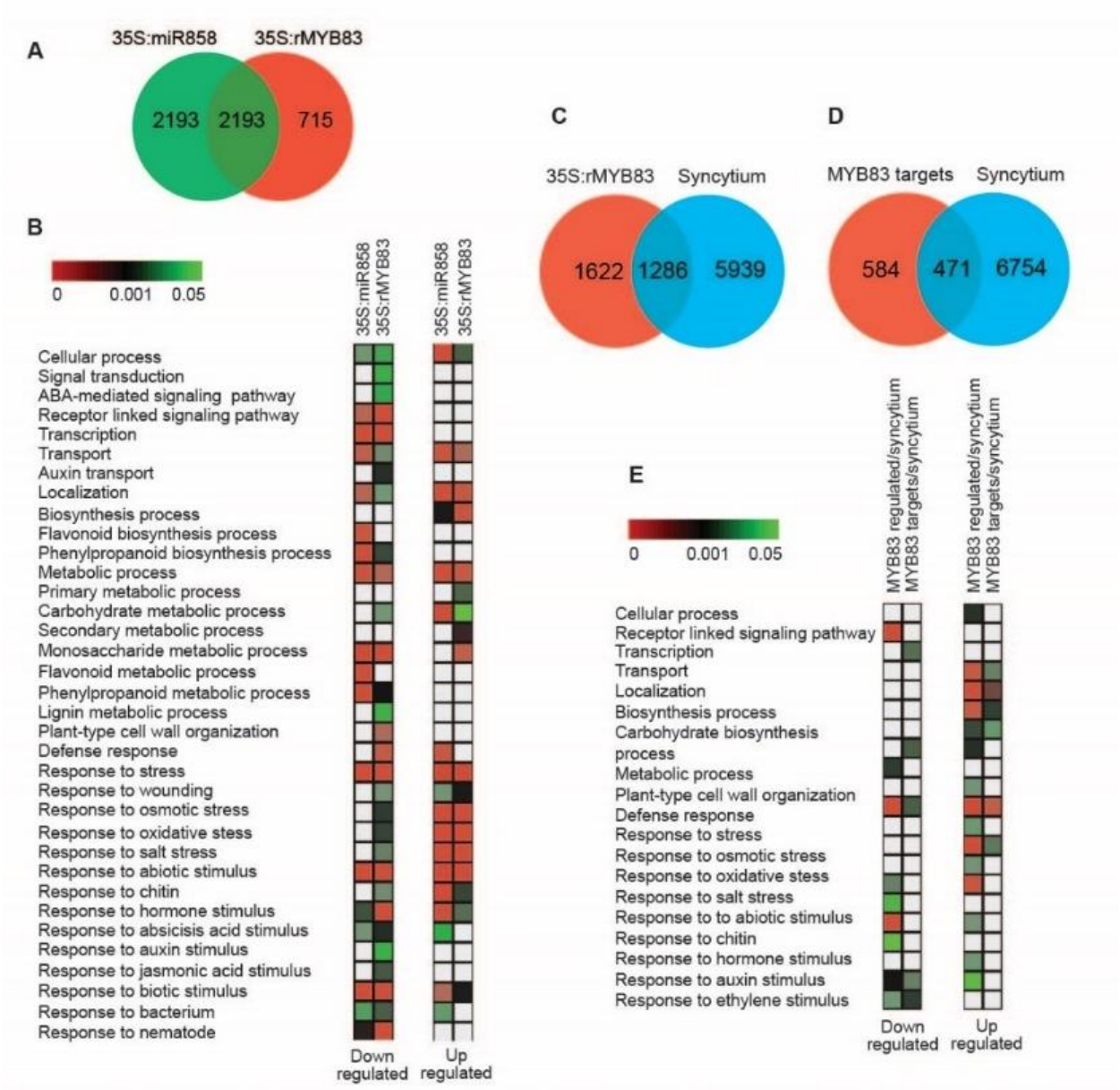

Figure 4-8. contd.

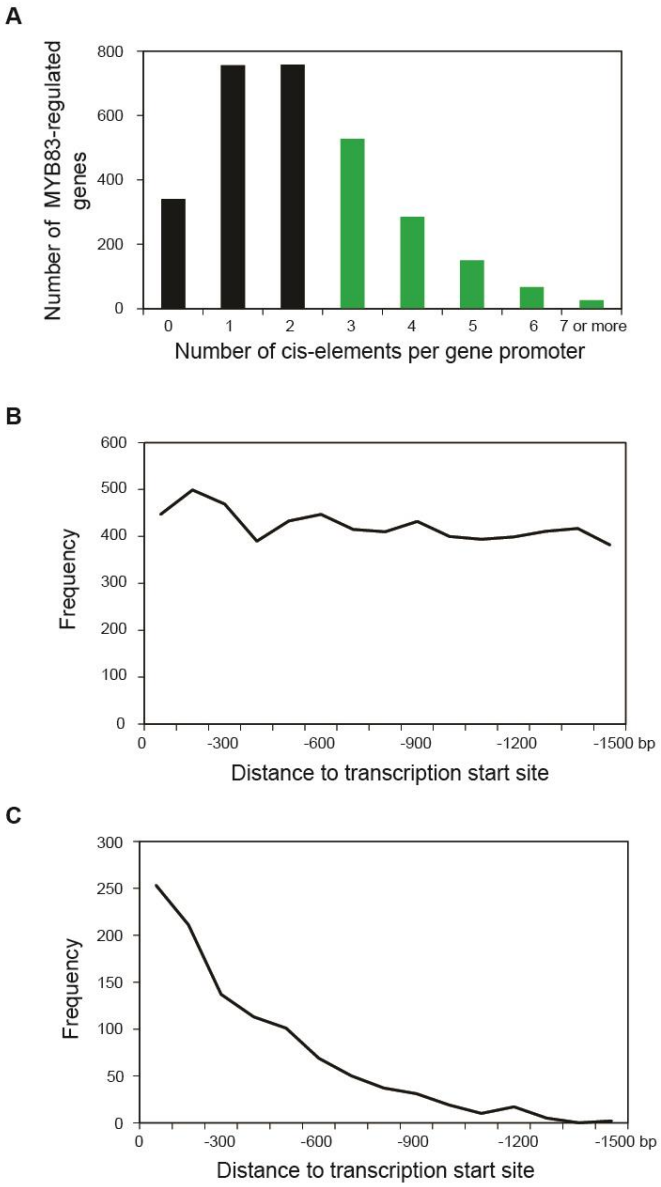

Figure 4-9. Enrichment of MYB83 *cis*-binding element in the MYB83-regulated genes.

(A) Frequency of the MYB83 *cis*-binding elements in the promoters of MYB83-regulated genes. MYB83-regulated genes containing 3 or more *cis* elements were considered as putative direct targets (highlighted in green). (B) Frequency of the MYB83 *cis*-binding elements in the promoters of the putative direct targets with respect to their distance from the transcription start site. (C) Frequency of the first MYB83 *cis*-binding elements in the promoters of the putative direct targets with respect to their distance from the transcription start site.

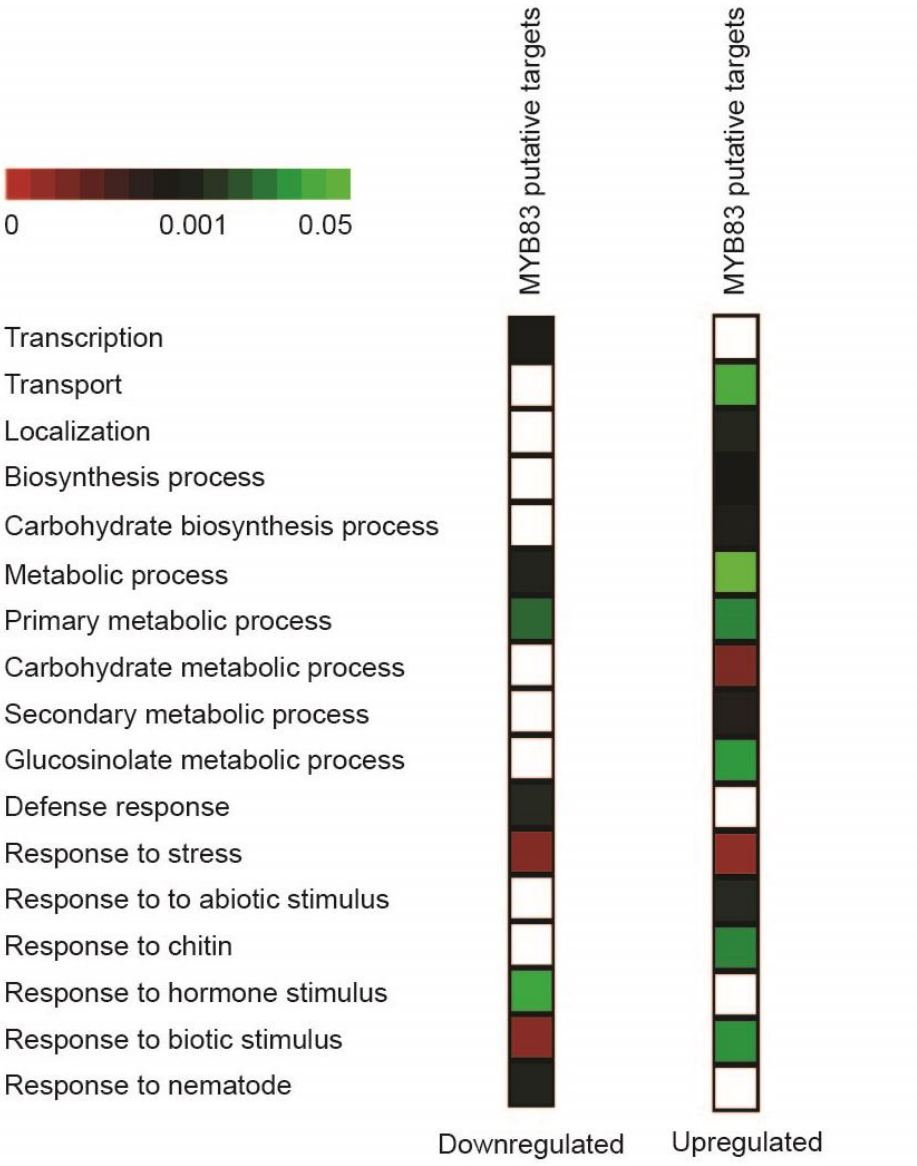

Figure 4-10. Gene Ontology classification and enrichment analyses of the putative direct targets of MYB83.

Enrichment analyses of upregulated and downregulated genes were performed separately using Fisher's exact test and Bonferroni multi-test correction with a significance cut-off $P < 0.05$.

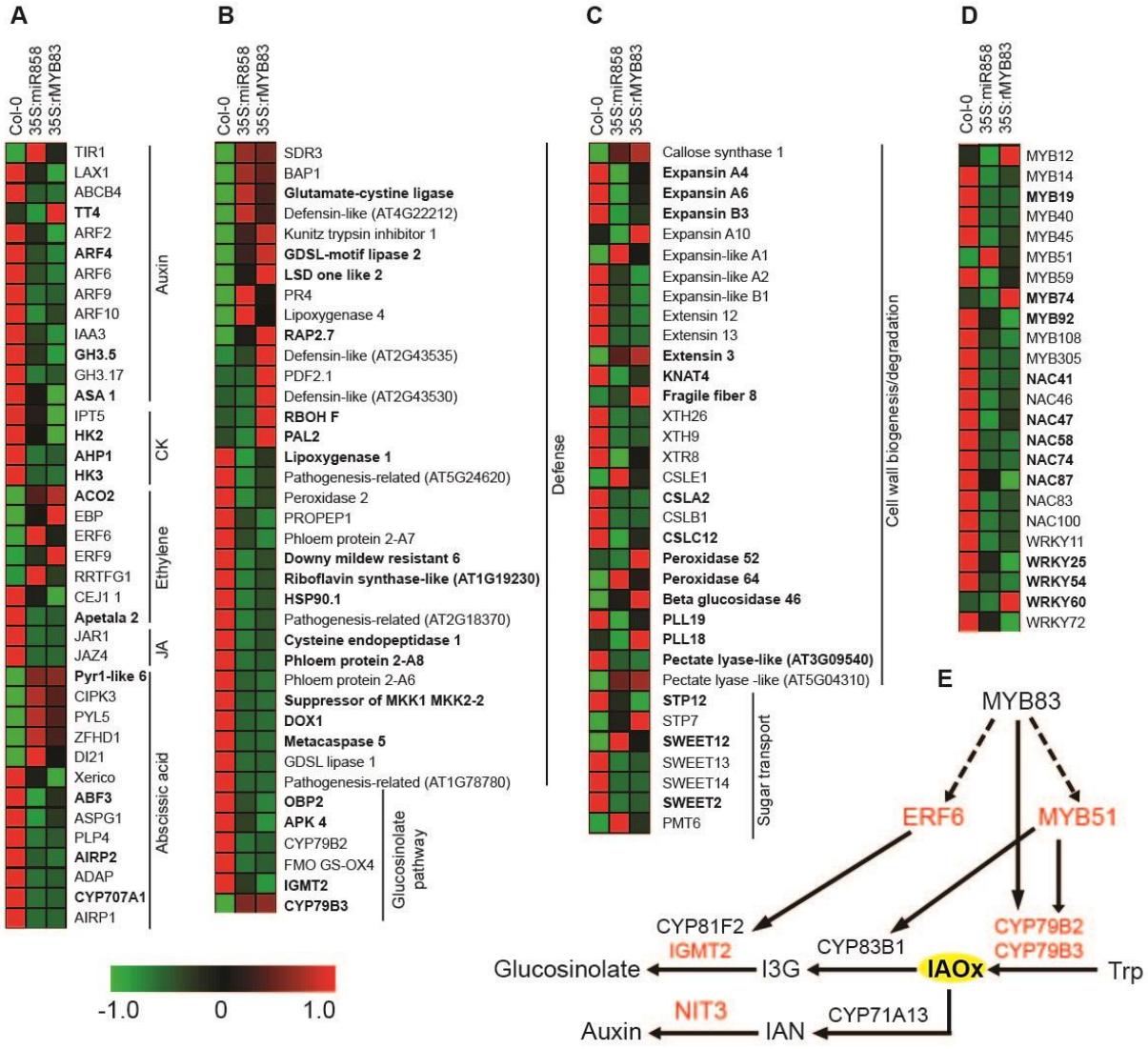

Figure 4-11. Differential expression patterns of a set of MYB83-regulated genes involved in key biological processes associated with nematode parasitism.

The RKPM values of the selected MYB83-regulated genes overlapping with the syncytium DEGs were row-wise normalized using Z score and used to construct the heat maps. Shown are genes involved in hormone signaling pathways (A), defense response (B), cell wall modification and sugar transport (C), transcriptional control (D), and glucosinolate biosynthesis (E).

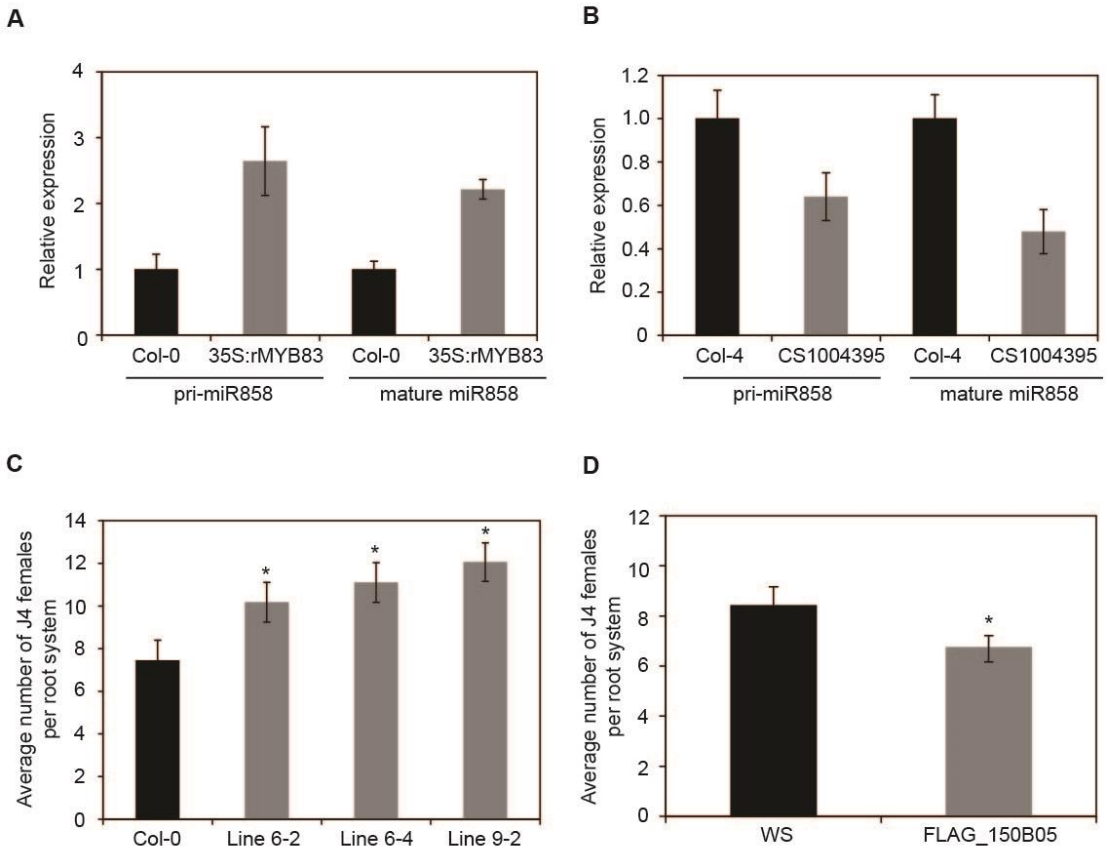

Figure 4-12. miR858/MYB83 regulatory loop involves MYB12.

A) and (B) MYB83 positively regulates the expression of miR858. The expression levels of primary and mature miR858 transcripts were quantified in the roots of two-week-old *rMYB83* overexpression plants (A) as well as the *myb83* mutant line CS1004395 (B) relative to the wild-type Col-0 or Col-4 plants, respectively using qPCR. Shown are relative expression values obtained from three biological samples ± SE. (C) and (D) MYB12 phenocopied the effects of MYB83 on plant susceptibility to *H. schachtii*. Three independent transgenic lines overexpression *35S:rMYB12* construct increased susceptibility to *H. schachtii* compared with the wild-type Col-0 plants (C), whereas the *myb12* mutant line FLAG_150B05 showed reduced susceptibility compared with the wild-type Ws plants (D). Shown are average numbers of J4 females per root system ± SE (n =20) at three weeks post inoculation. Asterisks indicate statistically significant differences from the corresponding wild-type plants at P value less than 0.05.

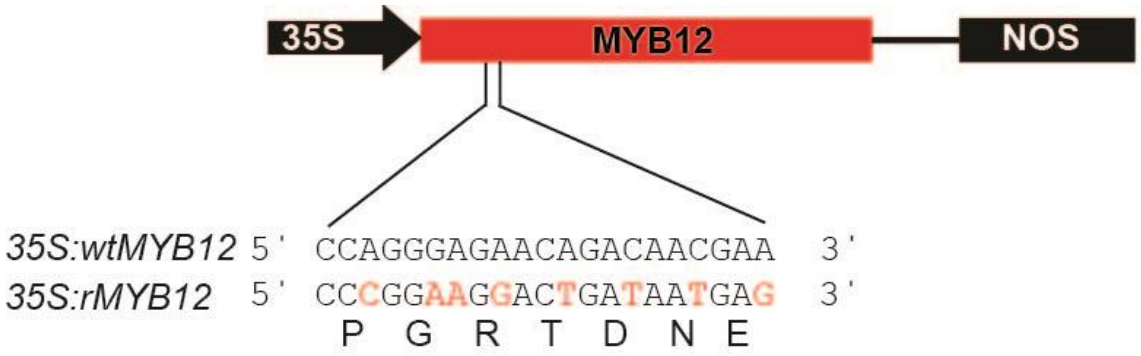

Figure 4-13. Schematic representation showing the construction of a miR858-resistant variant of *MYB12* (*rMYB12*) by introducing synonymous mutations to the miR858 binding site in the *MYB12* coding sequence.

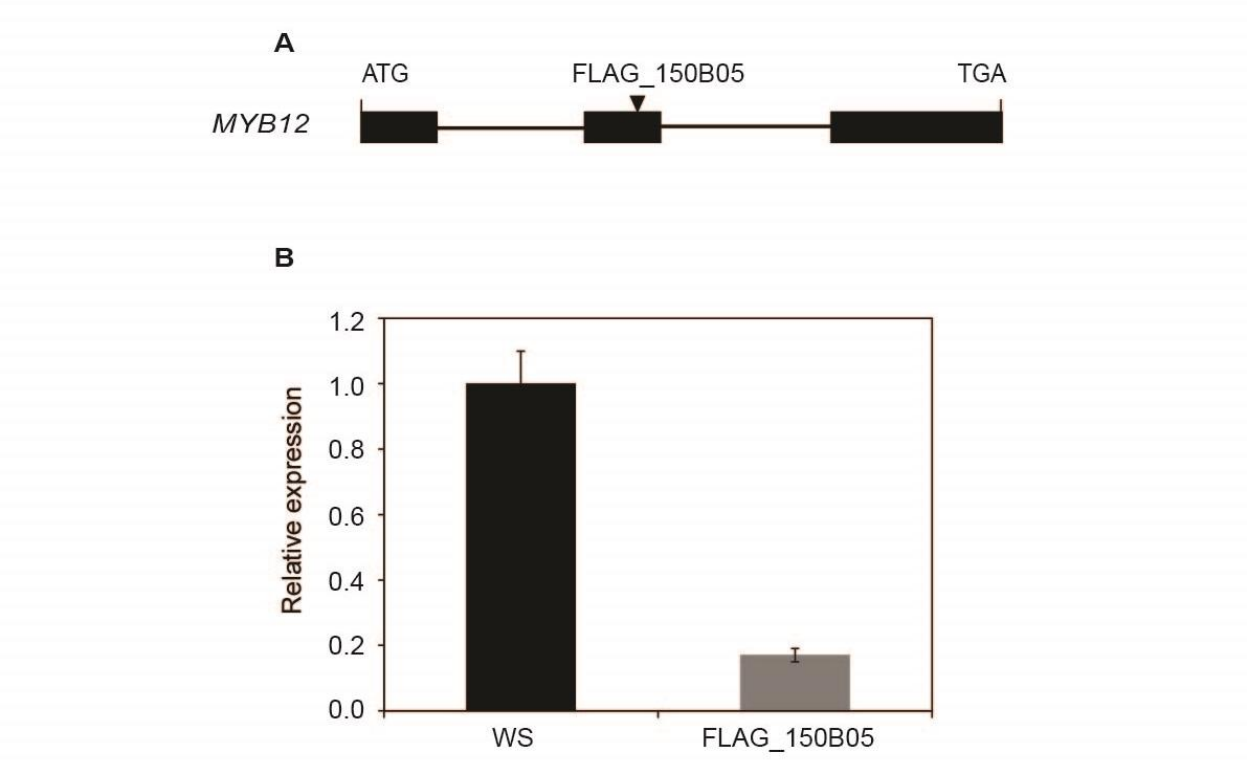

Figure 4-14. Characterization of the *MYB12* T-DNA mutant line (FLAG_150B05).

(A) Schematic representation of T-DNA insertion site in the *MYB12* mutant. (B) *MYB12* expression level in the mutant relative to the wild-type WS plants. *MYB12* expression level was quantified in two-week-old plants using qPCR and *Actin8* as internal reference control. Shown are averages of three biological samples ± SE.

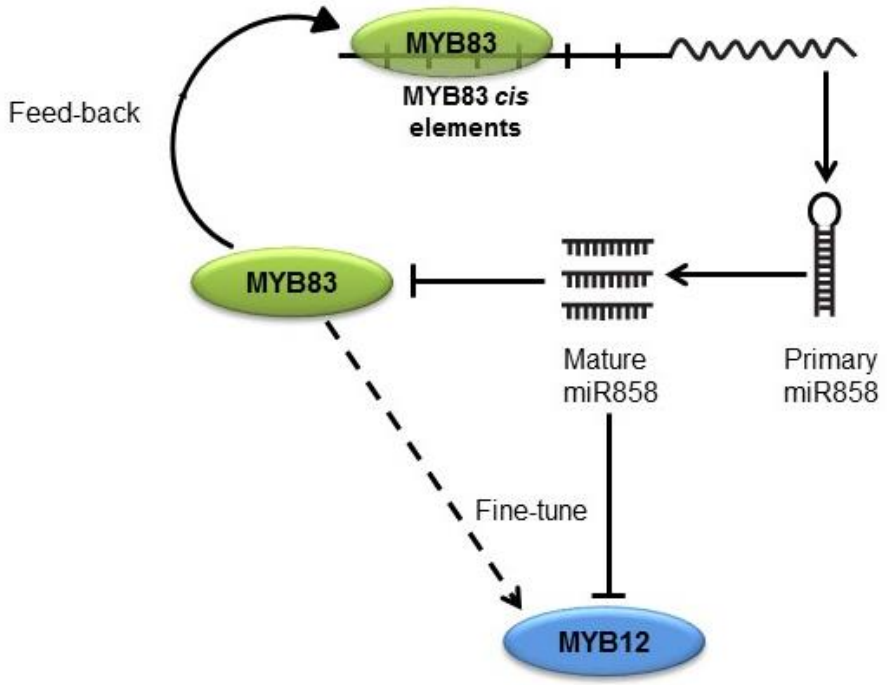

Figure 4-15. Model for miR858–MYB83 interaction

Our results indicate that miR858 and *MYB83* expression are connected through a feedback circuit in which miR858 regulates the expression of *MYB83* and responds to its expression levels. This regulatory mechanism ensures proper expression levels of more than a thousand of MYB83-regulated genes in the *H. schachtii*-induced syncytium. This fine-tuning mechanism appears to include MYB12, which was oppositely regulated by miR858 and MYB83, providing additional layer of tight control over gene expression.

Chapter 5

GROWTH REGULTING FACTOR 1 and 3: Key transcriptional regulators mediating the balanced trade-off between plant growth and stress responses

Abstract

Growth-regulating factors (GRFs) regulate various aspects of plant growth and development as well as responses to biotic and abiotic stress stimuli. However, the mechanisms through which these transcription factors regulate these biological processes remain largely unknown. In this study, we performed chromatin immunoprecipitation followed by sequencing (ChIP-seq) and RNA sequencing (RNA-seq) analysis of transgenic Arabidopsis lines expressing GFP-tagged GRF1 and GRF3 to identify genes that are directly regulated by GRF1 and GRF3. Specific and common cis-binding motifs of GRF1 and GRF3 were identified, revealing the mechanism underlying their functional redundancy. Comparison of the direct targets of GRF1 and GRF3, and their regulated genes revealed common as well as unique functions. Our result also showed that direct targets of GRF1 and GRF3 are associated with cell cycle regulation, various developmental processes particularly reproductive organ identity, and pollen and root development. In addition, we also identified that GRF1 and GRF3 directly bind to a large number of genes associated with abscisic acid, salt tolerance and defense response. Together, our results establish GRF1 and GRF3 as key transcriptional regulators mediating the balanced trade-off between plant growth and stress responses.

1. Introduction

GROWTH REGULATING FACTORs (GRFs) regulate a wide range of growth and developmental processes in plants. This transcription factor family contains 9 members in Arabidopsis, 13 in rice and 26 in soybean (Omidbakhshfard et al., 2015). GRF1 from rice was the first identified GRF which was determined to be one of the genes activated in response to gibberellins (van der Knaap et al., 2000). GRF genes have not been reported from species other than embryophytes suggesting that GRFs are embryophytes-specific transcription factors (Hoe Kim and Tsukaya, 2015; Omidbakhshfard et al., 2015). This transcription factor contains highly conserved QLQ and WRC domains in the N-terminus and a highly variable C-terminal domain. QLQ domain mediates the interaction of GRFs with GRF-interaction factors (GIFs), while WRC acts as DNA binding domain (Kim and Kende, 2004; Horiguchi et al., 2005; Osnato et al., 2010; Kim et al., 2012; Kuijt et al., 2014). The C-terminal end of GRF proteins is highly variable. Transactivation assay using yeast two-hybrid screens showed that the C-terminal domain is essential for transactivation activity (Kim and Kende, 2004). GRFs with short C-terminus sequences displayed no transactivation activities (Choi et al., 2004; Liu et al., 2014).

In Arabidopsis, seven of the nine GRF genes contain the miR396 binding site and hence are post-transcriptionally regulated by miR396 (Jones-Rhoades and Bartel, 2004). The miR396-GRFs regulatory module has been shown to regulate various aspects of plant growth and development, including leaf, stem and root development, floral development, and reproductive competence as well as defense responses (van der Knaap et al., 2000; Kim et al., 2003; Rodriguez et al., 2010; Hewezi et al., 2012; Kim et al., 2012; Baucher et al., 2013; Casadevall et al., 2013; Bao et al., 2014). miR396 overexpression-mediated GRF down-regulation induced abnormal floral organ development, demonstrating the function of miR396-GRF system in flower development (Liang et al., 2014). In addition, various transcription factors such as APETALA1 (AP1), AP2, SEPALLATA3 and SCHLAFMUTZE that regulate transition from shoot apical meristem (SAM) to flowering and floral meristem identity also regulate the expression of various GRFs (Yant et al., 2010; Pajoro et al., 2014). Hewezi et al. (2012) reported the requirement of a balanced expression of miR396-GRF1/3 for optimal root growth in Arabidopsis. They showed that overexpression of either miR396 or the miR396-resistant variants of GRF1 or GRF3 produced shorter roots compared to the wild type plants. Furthermore, a

functional role of GRFs in cell expansion and cell proliferation has been demonstrated (Kim et al., 2003; Kim and Kende, 2004; Rodriguez et al., 2010; Debernardi et al., 2014).

GRFs function in a redundant fashion (Kim et al., 2003; Rodriguez et al., 2010; Hewezi et al., 2012). For example, Arabidopsis single mutants of GRF1, GRF2 or GRF3 did not show obvious morphological irregularities, whereas double mutant combinations of these three GRFs showed small and narrow leave phenotypes. This phenotype was even more distinct in the *grf1grf2grf3* triple mutant (Kim et al., 2003). These results demonstrate overlapping function of GRFs in leaf development.

Hewezi et al. (2012) reported that miR396 and its target genes GRF1 and GRF3 play vital roles in controlling the transition from syncytium initiation/formation phase to maintenance stages during *H. schachtii* parasitism of Arabidopsis. It has been shown *H. schachtii* induced miR396 downregulation with concurrent increase in the expression of its target genes GRF1 and 3 during the early stage of syncytium development that would allow redifferentiation of root cells into syncytium cell-type. After completion of the syncytium formation stage, the expression of miR396 is activated resulting in upregulation of GRF1 and 3 during the syncytia maintenance stage. This study also revealed that miR396-GRF1/3 regulatory module regulates 44% of the the syncytium differentially expressed genes (7,225 genes) (Szakasits et al., 2009), suggesting pivotal roles of this regulatory system in the reprogramming of the root cells into new feeding structure. Global gene expression analysis of root tissues of transgenic plants overexpressing GRF1 or GRF3 showed enrichment of genes with functions associated with developmental pathways and defense signaling (Liu et al., 2014).

Unlike most animals, plants are sessile and have complex defense system against various pathogens. Under normal condition, the energetically costly inducible defense system is repressed that would allow investment of metabolic input and energy in growth and development. In response to pathogen attack, plants defense signaling is activated. As a result, plant metabolic inputs are temporarily diverted to plant defense response instead of the predetermined growth and development programs (Huot et al., 2014; Lozano-Durán and Zipfel, 2015). However, the underlying mechanisms that regulate the trade-off between plant growth and defense response remain largely unknown. However, recent studies have provided novel

insight into the mechanisms that may bring about the balance between plant growth and defense signaling (Fan et al., 2014; Lozano-Durán and Zipfel, 2015). Given that GRF1 and GRF3 are involved in diverse plant developmental processes and plant responses against various stresses, it is possible that GRF1 and GRF3 may coordinate the balance between plant growth and defense signaling (Hewezi et al., 2012; Kim et al., 2012; Liu et al., 2014).

Although previous studies have strongly indicated the role of GRF1 and GRF3 in various aspects of plant developmental processes including plant responses to biotic and abiotic stresses, the downstream targets of GRF1 and GRF3 are not known. In this study, we identified genome-wide binding sites and genes regulated by these two transcription factors. We discovered the specific and the shared cis-binding elements of GRF1 and GRF3 and revealed the mechanism of their functional redundancy. Our result showed that GRF1 and GRF3 primarily target genes associated with various aspects of plant development, salt tolerance and defense responses. In addition, our result also showed that GRF1 and GRF3 directly target various master regulators of growth and defense.

2. Results

2.1 Identification of the binding sites of GRF1 and GRF3

To identify the genome-wide binding sites of GRF1 and GRF3 transcription factors, we performed ChIP-seq analysis of transgenic plant expressing GFP-tagged GRF1 or GRF3 in the *grf1/grf2/grf3* triple mutant background. Transgenic plant expressing 35S:GFP was used as a negative control. We found that more than 98% of the called peaks (binding sites) of both GRF1 and GRF3 was in the non-coding region. For GRF1, we identified a total of 730 binding sites (Table 5-1). More than 50 % of these binding sites were located in gene promoters; 1000 bp upstream of the transcription start site (TSS). The remaining peaks were located in the intergenic region (32.3%), transcription termination site (TSS, 8.7%), intron (5.7%), and coding region (1.8%). The untranslated regions (UTRs) contained less than 1% of GRF1 binding sites (Figure 5-1A). Likewise, a total of 1189 binding sites were identified for GRF3 (Table 5-1). Majority of the identified GRF3 binding peaks were in the gene promoters (37.7%) and intergenic regions (35.9%) (Figure 5-1B).

Genes were considered as the direct targets of GRF1 or 3 only if the binding sites were located in gene promoters in at least two out of the three biological replications. Using this criterion, we identified 359 direct targets of GRF1 and 417 of GRF3. Comparison of the direct targets of GRF1 and GRF3 showed that 47 genes were common between both data sets. The binding peaks of the identified direct targets of GRF1 and GRF3 were located predominantly within 500 bp upstream of TSS (Figure 5-1C and D).

2.2 Identification of GRF1 and GRF3 binding motif

We used RSAT peak-motifs (Thomas-Chollier et al., 2012) to find the over-represented motif in 250 bp flanking the summit of each peak. For GRF1 two binding motifs (AAACCCtaa and tACTCGAcc) were identified (Figure 5-2A and C). The AAACCCtaa and tACTCGAcc binding motifs were found in 53% and 79% of the gene promoters (1000 bp upstream of translation start site) targeted by GRF1, respectively.

Interestingly, the majority of these gene promoters contain the motif within 500-bp upstream of the translation start site (Figure 5-2B and D). Similarly, we identified two motifs associated with GRF3 binding sites. Intriguingly, one of these motifs (tACTCGAcc) was common for both GRF1 and 3 (Figure 5-2E). This motif occurred in 65% of the gene promoters targeted by GRF3. The other motif (aaGAAGAAg) (Figure 5-2G) occurred in 18% of the gene promoters targeted by GRF3. These motifs were also located mainly within 500 bp upstream of translation start site of the identified GRF3 target genes (Figure 5-2F and H).

Further analysis showed that 133 of the GRF1 target genes contained only the GRF1 specific motif AAACCCtaa, suggesting that these genes are uniquely regulated by GRF1. Also, motif analysis indicated that 193 of the GRF1 target genes can be regulated by GRF1 and/or GRF3 because they contained the common tACTCGAcc motif (Table 5-2). Similarly, 226 of the direct targets of GRF3 contained only the GRF3 specific motif aaGAAGAAg, suggesting that these genes are uniquely regulated by GRF3. However, 71 of the GRF3 target genes contained the common motif and, hence can be regulated by GRF1 and/or GRF3 (Table 5-2). This result suggests that GRF1 and GRF3 may regulate the same genes by binding to the common motif. In addition, it also suggests that GRF1 functions predominantly by binding with AAACCCtaa and GRF3 functions predominantly by binding with aaGAAGAAg.

2.3 Functional categorization of direct targets of GRF1 and GRF3

We observed several genes associated with cell cycle regulation and cytoskeleton organization as the direct targets of GRF1 and GRF3 (Table 5-4). In addition, in agreement with the GO enrichment analysis of the DEGs of GRF1 and GRF3, we observed several genes associated with various plant development processes, hormones, abiotic stresses, and defense responses.

2.3.1 Embryogenesis

GRF1 and GRF3 targeted several genes associated with embryogenesis. Auxin plays vital role in embryo development and patterning. We identified direct targets of GRF1 and GRF3 that regulate auxin level in the developing embryo. For example, *JAGGED LATERAL ORGAN* (*JLO*) and *HANABA TARANU* (*HAN*) which are direct targets of GRF1 and GRF3, respectively, modulate PIN family proteins to regulate auxin transport for proper embryo development (Borghi et al., 2007; Nawy et al., 2010). In addition, *JLO* also activates *SHOOTMERISTEMLESS* (*STM*) and *KNAT1;* both play vital role in embryo development (Borghi et al., 2007; Bureau and Simon, 2008). In addition, *DORNRÖSCHEN* (*DRN*) and *MATERNAL EFFECT EMBRYO ARREST 26* (*MEE26*), direct targets of GRF3, and *CELLULOSE SYNTHASE LIKE 7* (*CSLA07*) which is targeted by both GRF1 and GRF3 are also involved in embryo patterning (Goubet et al., 2003; Cole et al., 2009; Kinoshita et al., 2010).

2.3.2 Flower development

Among the direct targets of GRF1 or GRF3 we identified *HUA ENHANCER 2* (*HEN2*) and *SPLAYED* (*SYD*), which play key function in floral organ identity. *HEN2* and *SYD* are essential for proper expression of the floral homeotic genes B and C (Western et al., 2002; Wu et al., 2012). In addition, other direct targets of GRF1 and GRF3 encode functions essential for flower development including *HAN*, *PEROXIDASE 53* (*PRX53*) and *JLO* (Zhao et al., 2004; Jin et al., 2011; Rast and Simon, 2012).

The identification of the direct targets of GRF1 and GRF3 revealed their implication in anther and pollen development. Various genes such as *bHLH091*, *OVERLY TOLERANT TO SALT 1* (*OTS1*), *CYP98A8*, *CYP98A9*, *FIMBRIN5* (*FIM5*), *ARABIDOPSIS TRANSMEMBRANE PROTEIN 18* (*TMEM18*) and *CSLA07* that are necessary for proper growth and function of the

anther and/or pollen were among the direct targets of GRF1 (Figure 5-3). Similarly, GRF3 also binds to the promoter of various genes associated with pollen development that include *IRREGULAR POLLEN EXINE1* (*IPE1*), *SISTER CHROMATID COHESION 1 PROTEIN 3* (*SYN3*), *CSLA07*, *ROP-INTERACTIVE CRIB MOTIF-CONTAINING PROTEIN 2* (*RIC2*), *MYB33* and *ANXUR2* (*ANX2*) (Figure 5-3). *OTS1* regulates stamen growth to synchronize with pistil growth to ensure fertilization (Campanaro et al., 2016). *bHLH091* and *MYB33* are necessary for the normal male fertility and anther development in Arabidopsis (Millar and Gubler, 2005; Zhu et al., 2015). *IPE1* regulates the development of anther cuticle and pollen exine that serve as protective barriers for pollen (Chen et al., 2016) while *CYP98A8* and *CYP98A9* regulate pollen wall patterning (Xu et al., 2014). *FIM5*, *TMEM18*, *RIC2* and *CSLA07* regulate pollen germination and pollen tube growth (Goubet et al., 2003; Dou et al., 2016; Zhang et al., 2016). *ANX2* controls rupturing of pollen tube tip appropriately to release the sperm cell for fertilization (Miyazaki et al., 2009). In addition to stamen growth, *OTS1* is also involved in flowering time regulation (Sadanandom et al., 2015). In this context, GRF3 also binds to the promoter of *LIGHT-REGULATED WD2* (*LWD2*), which functions in conjugation with *LWD1* for photoperiodic flowering control (Wu et al., 2008).

2.3.3 Root development

Among the identified GRF1 target genes associated with root development were *MORPHOGENESIS OF ROOT HAIR 6* (*MRH6*), *ECTOPIC ROOT HAIR 3* (*ERH3*) and *RGF1 INSENSITIVE 1* (*RGFR1*). Also, GRF3 directly targets a number of genes involved in various aspects of root development including *SHORT AND SWOLLEN ROOT 1* (*SSR1*), Z*INC FINGER PROTEIN 5* (*ZFP5*) and *PROLINE-RICH EXTENSIN-LIKE RECEPTOR KINASE 4* (*PERK4*) (Figure 5-3). *PERK4*, *RGFR1* and *SSR1* regulate primary root growth. *RGFR1* directly interacts with root meristem growth factor (RGF) and maintain gradients of *PLETHORA 1* (*PLT1*) and *PLT2* to ensure proper growth and development of primary root (Shinohara et al., 2016). *SSR1* controls the primary root growth by regulating the activity of PIN family proteins (Zhang et al., 2015). *MRH6* and *ZFP5* play important role in root hair development (An et al., 2012; Bruex et al., 2012).

2.4 Phytohormones related genes as the direct targets of GRF1 and GRF3

Among the phytohormone associated genes, GRF1 and GRF3 directly target significant number of genes with functions related to ABA. The ABA biosynthesis gene *NINE-CIS-EPOXYCAROTENOID DIOXYGENASE 5* (*NCED5*) and the regulator of ABA production *PALE CRESS* (*PAC*) were identified as direct targets of GRF1 and GRF3, respectively. PERK4 that functions in early stage of abscisic acid signaling by disrupting Ca^{++} homeostasis (Bai et al., 2009) was identified as the direct target of GRF3. Similarly, GRF3 also binds to the promoter of *PYR1-LIKE 13* (*PYL13*), a receptor of ABA. Additionally, *UDP-GLUCOSYL TRANSFERASE 71B6* (*UGT71B6*), which maintains ABA homeostasis was found to be the direct target of GRF3. *PLANT U-BOX 19* (*PUB19*) and *LIPID PHOSPHATE PHOSPHATASE 2* (*LPP2*), the negative regulators of ABA signaling, were direct targets of GRF1 and GRF3, respectively. A number of ABA-responsive genes were also among the direct targets of GRF1 or GRF3, including *RAF10*, *FIBRILLIN* (*FIB*), *INOSITOL-POLYPHOSPHATE 5-PHOSPHATASE 13* (*5PTASE13*) and *RESPONSIVE TO ABSCISIC ACID 28* (*ATRAB28*) (Figure 5-4).

In addition, we noted that GRF1 and GRF3 directly targeted several other genes associated with phytohormone biosynthesis and signaling. For example, GRF1 binds to the promoter of *ALLENE OXIDE CYCLASE 4* (*AOC4*), an enzyme that catalyzes JA biosynthesis as well as *ETO1-LIKE 1* (*EOL1*), a negative regulator of ethylene biosynthesis gene. GRF1 also directly binds to the promoter of the type-B *Arabidopsis RESPONSE REGULATOR 2* (*ARR2*), a key transcriptional factor regulating the expression of cytokinin primary response genes (Kim et al., 2012).

Similarly, GRF3 binds to the promoters of *NITRILASE 1* (*NIT1*) and *ISOPENTENYLTRANSFERASE 4* (*IPT4*), both encoding key enzymes that catalyze the biosynthesis of auxin and cytokinin, respectively. In addition, GRF3 targets *ICS2*, which participates with *ICS1* to the biosynthesis of SA (Garcion et al., 2008). Our analysis also showed that GRF3 directly targets *PIN2 PROMOTER BINDING PROTEIN 1* (*PPP1*) that regulates the expression of auxin transport protein particularly PIN1 and PIN2 (Benjamins et al., 2016). GRF1 and GRF3 also bind to the promoter of *JLO*, *SSR1* and *DRN*, which are known to modulate the activity of PIN family proteins and hence auxin transport. In addition, both GRF1 and GRF3

directly bind to the promoter of *BR-RELATED ACYLTRANSFERASE1* (*BAT1*), which regulate the endogenous level of brassinosteroids (Table 5-5).

2.5 GRF1 and GRF3 targets are associated with abiotic stresses

Careful exanimation of direct targets of GRF1 and GRF3 revealed that both transcription factors bind directly to the promoter regions of several genes associated with abscisic acid signaling. We discovered that GRF1 and GRF3 bind to the promoter of genes associated with salt, drought, or cold stresses (Figure 5-4). Salt tolerance genes were particularly enriched among the direct target genes of GRF1 and GRF3. For instance, GRF1 binds to the promoter of various salt tolerance genes, including *UB-LIKE PROTEASE 1D* (*ULP1D*), *5PTASE13, SALT OVERLY SENSITIVE 3* (*SOS3*) and *TGN-LOCALIZED SYP41 INTERACTING PROTEIN* (*TNO1*). Overexpression of these genes enhances plant tolerance to salt (Conti et al., 2008; Kaye et al., 2011; Kim and Bassham, 2011; Ye et al., 2013). We also found that GRF3 directly targets various genes that enhances plant tolerance to salt stress that include, for example, AT1G13930, *GLYCINE-RICH DOMAIN PROTEINS* 2 (AtGRDP2), *BASIC TRANSCRIPTION FACTOR 3* (*BTF3*), *HARDY* (*HRD*), and *SOS3* (Du et al., 2008; Abogadallah et al., 2011; Ortega-Amaro et al., 2014; Wang et al., 2014). Together, these findings indicate that GRF1 and GRF3 participate in the regulation of plant response to salt stress.

2.6 GRF1 and GRF3 target defense response genes

In response to wounding, plant induces defense responses similar to those that are triggered against pathogen infection. Two wounding-responsive genes, *PRX53* and *5PTASE13,* were identified as direct targets of GRF1 and/or GRF3 (Jin et al., 2011; Kaye et al., 2011). One of the identified targets of GRF1 was *AVRPPHB SUSCEPTIBLE 1* (*PBS1*), which acts as a cue for the activation of key plant defense response gene *RESISTANT TO P. SYRINGAE 5* (Qi et al., 2013). Similarly, *RIN2* was identified as the target of GRF3, which form a complex with *RPM1* to activate plant defense response (Kawasaki et al., 2005). Several genes that enhance plant basal defense response were identified as direct targets of GRF1 and/or GRF3 (Figure 5-5). This included various plant defensins, plant defensin-like proteins, and pathogenesis related (PR) proteins. Another target of GRF1 associated with plant basal defense was *ATPFA-DSP4,* which negatively regulates plant defense by suppressing the production and accumulation of H_2O_2

during bacterial infection (He et al., 2012). *RR2* and *BCS1* were also identified as direct targets of GRF1, and these genes are involved in SA-mediated defense response. *RR2* binds to SA responsive factor *TGA1A-RELATED GENE 3* (*TGA3*) and regulates SA signaling to enhance plant resistance (Choi et al., 2010). Overexpression of *BCS1* induced constitutive accumulation of SA and activation of cell death genes (Zhang et al., 2014). Several other genes such as *DELTA-VPE* and development and cell death (DCD) domain proteins that are involved in cell deaths (Nakaune et al., 2005; Tenhaken et al., 2005) were also among the direct targets of GRF1 and GRF3.

In addition, GRF1 and GRF3 were found to bind to the promoter of *SPY* and *HBI1,* respectively and these genes are known to regulate plant development as well as plant defenses (Wu et al., 2012; Fan et al., 2014; Johnson et al., 2015). Systemic acquired resistance (SAR) is a resistance against broad spectrum pathogens upon localized infection with pathogen. One of the direct targets of GRF3 is *EARLI1,* which is required for SAR. It has been shown that *earli1-1* loss-of-function plants are compromised in SAR responses to a virulent strain of *Pseudomonas syringae* (Cecchini et al., 2015). These results indicate that GRF1 and GRF3 regulate different aspects of defense responses.

2.7 Differentially expressed genes in GRF1 and GRF3

We performed RNA-seq analysis of 35S:GRF1 and 35S:GRF3 plants as wells as and the *grf1grf2grf3* triple mutant. We observed that 4012 genes were differentially expressed in 35S:GRF1. Among the 4012 differentially expressed genes (DEGs), 2124 genes were up-regulated and 1888 genes were down-regulated (Table 5-6). Similarly, we identified 4128 DEGs in 35S:GRF3. Among the DEGs in 35S:GRF3, 2324 genes were upregulated and 1804 genes were down-regulated. Comparison of the DEGs in 35S:GRF1 and 35S:GRF3 showed that 2605 genes were common between the two data sets (Figure 5-6A). This finding further confirm the redundant function of these two transcription factors. Comparison of the GRF1 DEGs with GRF1 direct target showed that 22% (79 out of 359) direct targets were differentially expressed. Out of these 79 genes, 35 genes were upregulated and the remaining 44 were downregulated. Similarly, 20% (83 out of 417) of the GRF3 direct targets overlapped with the DEGs. Out of these 83 genes, 47 genes were upregulated and the remaining 36 genes were downregulated.

These findings indicate that GRF1 and GRF3 can function as *trans*-activators as well as trans-repressors to a similar extent.

3. Discussion

Previous studies have revealed roles for GRFs in various developmental processes including response to abiotic and biotic stress (Omidbakhshfard et al., 2015). However, the downstream target genes that these transcription factors directly regulate remain unknown. In this study, we identified genome-wide binding sites and genes regulated by GRF1 and GRF3 transcription factor to understand the regulatory functions of GRF1 and GRF3. We observed a significant overlap between the identified direct targets of GRF1 and GRF3 with the DEGs in GRF1 and GRF3. Previous studies have shown redundant functions of GRF1 and GRF3 for various biological processes (Kim et al., 2003; Rodriguez et al., 2010). However, the underlying mechanism mediating the functional redundancy between GRFs was not clear. Our study provides unprecedented mechanistic understanding of the functional redundancy of GRF1 and GRF3. We discovered that GRF1 and GRF3 share a common cis-binding motif through which a common set of target genes can be simultaneously regulated. We also discovered a unique DNA binding motif for each of these two transcription factors that would allow GRF1 and GRF3 to regulate their target genes in a specific manner.

Our RNA-seq analysis revealed that about 20% of the identified targets were differentially expressed in the GRF1 and GRF3 overexpression plants. This finding can be explained by the fact that many of these targets are expressed in specific tissues and organs that were not included in our tissue samples; the floral organs for instance. In addition, several target genes of GRF1 and GRF3 are known to be regulated by biotic and abiotic stresses. Thus, developmentally- and stress-regulated genes cannot be identified in the 2-week-old plants used for RNA-seq analysis. Recent studies also showed small overlaps between the direct targets of various transcription factors and the DEGs (Sun et al., 2015; Birkenbihl et al., 2016) Also, our RNA-seq analysis revealed that GRF1 and GRF3 have dual functions acting as transcriptional activators or repressors. The *trans*-repression functions of GRF1 and GRF3 can be mediated through physical association with transrepressors. In this context, QLQ domain of the GRFs mediates protein-protein interactions (Hoe Kim and Tsukaya, 2015) and may play a role in this process.

Plants respond to biotic and abiotic stimuli by adjusting their developmental program. Enhanced plant defense responses against the stress are generally associated with inhibition of plant growth and development. Our results provide intriguing evidence for the involvement of GRF1 and GRF3 in coordinating the stress responses, and developmental and reproductive traits. It is tempting to speculate that in the absence of pathogen attack, GRF1/3 can repress their target genes that are associated with salicylic acid-mediated defense response such as *RR2* and *BCS1* or other defense-related genes allowing investment of energy for growth. Likewise, in response to pathogen attack, GRF1/3 may inhibit their direct targets that regulate growth and development but activate defense-associated direct targets. In line with our finding that GRF1/3 directly regulate genes that are associated with abscisic acid biosynthesis, reception, and negative regulation, GRF1/3 can mediate the balance between plant growth and abiotic stress through the abscisic acid signaling pathway. This would allow GRF1/3 to act as a switch to activate or repress abscisic acid signaling, which is known to function in response to abiotic stress. Apart from this, GRF1/3 directly target genes that are known to simultaneously regulate plant growth and defense. For example, *SYD* is involved in plant development processes such as flower and leaf development (Wu et al., 2012; Vercruyssen et al., 2014). Johnson et al. (2015) reported that *SYD* regulates plant immunity by maintaining proper level of *SNC1*. *snc1* (*suppressor of npr1, constitutive 1*) gain-of-function mutation displayed constitutive defense response with severe developmental defects (Zhang et al., 2003). Similarly, GRF3 targets *HBI1,* which also mediates the trade-off between plant growth and defense response. *HBI1* has been identified as a negative regulator of plant immunity, and in response to plant pathogen the expression of this gene is inhibited resulting in increased plant immunity and reduced plant growth (Fan et al., 2014). Collectively, these results point to a role of GRF1/3 in mediating the balance between plant growth and defense responses.

Another interesting finding of this study is that GRF1 binds to its own promoter, presumably to control its own transcription level, through regulatory feedback loop. This finding is in line with previous finding reported by Hewezi and Baum (2012). Considering its vital role in various biological processes, the feedback loop is necessary for stabilizing its own transcript abundance to maintain homeostasis. Alternatively, the feedback mechanism may allow GRF1 to either increase or reduce its expression to prioritize growth over defense or vice-versa. We also found that GRF1 binds to the promoter of the GRF7. GRF7 has been identified as a negative regulator

of abscisic acid signaling associated with drought and salinity stress (Kim et al., 2012). In addition to directly regulating abscisic acid signaling and abiotic stress, this result suggests an addition level of regulation for GRF1 in the regulation of abscisic acid-mediated abiotic stress.

It has been shown that that GRF1 and GRF3 play key role in the differentiation of infected root cells into feeding structures for the beet cyst nematode *H. schachtii*. Syncytium formation involves the activity of several cell cycle-related genes (de Almeida Engler et al., 1999) . Interestingly, we observed that various genes associated with cell cycle regulation were directly targeted by GRF1 and/or GRF3. Of particular interest is MAD1, which forms a complex with MAD2 to inhibit premature exit from cell division (Ding et al., 2012). MAD1 has been shown to play a vital role in regulating endoreduplication (Bao et al., 2014), a hallmark characteristic of syncytium formation. Endoreduplication is a form of incomplete cell cycle where mitotic phase is inhibited, and this cellular process stimulates the metabolic activity of syncytial cells to deliver sufficient nutrients for nematode development (de Almeida Engler and Gheysen, 2013; Kyndt et al., 2013). More importantly, CCS52A was also identified as a direct target of both GRF1 and GRF3. CCS52A regulates the transition from mitotic to endoreduplication cycle and has also been demonstrated to play key role in switching mitotic to endocycle during syncytium development (de Almeida Engler et al., 2012). Thus, it is tempting to suggest that regulation of MAD1/MAD2 complex formation and CCS52A activity by GRF1/3 may contribute to syncytium etiology by controlling the endoreduplication cell cycle.

GRF1 and GRF3 may impact syncytium formation and development by regulating cytoskeleton organization. It has recently been shown that depolymerization of actin cytoskeleton and microtubules occur during the susceptible plant-nematode interactions (Kyndt et al., 2013), a finding that points to a role of the cytoskeleton organization genes during plant-cyst nematode interaction. Strikingly, we found that GRF1 and GRF3 bind to the promoter of several cytoskeleton organization genes, including *ECTOPIC ROOT HAIR 3*, *MICROTUBULE-ASSOCIATED PROTEIN 18* (*MAP18*), *MAP70-2*, *ACTIN DEPOLYMERIZING FACTOR 6* (*ADF6*), and *NIMA-RELATED KINASE 4* (*NEK4*) as well as various genes encoding actin-binding proteins. The functions of these genes in cytoskeleton rearrangement have been established (Engler Jde et al., 2010; Kyndt et al., 2013). In addition, several genes targeted by

GRF1 or GRF3 and involved in defense response may also contribute to the functions of these transcription factors in shaping plant-nematode interactions.

Finally, it may be important to mention that GRF1 and GRF3 directly bind to the promoter of genes that mediate the trade-off between plant growth and defense including SYD and HBI1 (Zhang et al., 2003; Wu et al., 2012; Fan et al., 2014). Interestingly, our RNA-seq data revealed that upregulated genes in the GRF1/3 overexpression plants were enriched in abiotic stress-related genes, whereas downregulated genes were enriched in plant developmental process-related genes. Though this interesting finding is consistent with the well-known antagonistic relationship between stress responses and plant growth and development, it also provides additional support for the involvement of GRF1/3 in mediating the trade-off between plant growth and stress signaling.

4. Material and methods

4.1 Plant materials and growth conditions

For the construction of transgenic lines, Arabidopsis triple mutant *grf1grf2grf3* in Wassilewskija (WS) background was used (Kim et al., 2003). Seeds were sterilized using commercial bleach (2.8% sodium hypochlorite) followed by four washes with sterilized double distilled water. Plants were grown under long day conditions at 24°C under 16-h-light/8-h-dark conditions.

4.2 Plasmid construction

35S:GRF1-GFP construct was generated by amplifying the GRF1 coding sequence using gene specific primers with attB1.1 and attB2.1 sites overhang in the forward and reverse primers, respectively and cloned into pDONR221 using Gateway BP-reaction (Invitrogen). The gene was then cloned into the binary vector pGWB551 using Gateway LR-reaction (Invitrogen). Similarly, the 35S:GRF3-GFP construct was generated by amplifying the coding sequence of GRF3 using gene specific primers with EcoRI and HindIII restriction sites overhang in forward and reverse primers, respectively. The amplified products were digested, purified, and cloned into the corresponding restriction sites in the binary vector pEGAD. All the constructs were verified by sequencing.

4.3 *Generation of Transgenic Plants*

The binary vectors containing GFP-tagged GRF1 and GRF3, and the empty vector pGWB551 (35S:GFP) were transformed into *Agrobacterium tumefaciens* strain C58 by freeze-thaw method and used to transform the *grf1grf2grf3* triple mutant by floral dip method (Clough and Bent, 1998). Transgenic T1 lines overexpressing the GRF1:GFP fusion or GFP alone were identified by screening T1 seeds on hygromycin (25µg/ml) containing MS medium. Transgenic T1 lines overexpressing the GRF3:GFP fusion were identified by spraying 10-day-old T1 plants by BASTA (glufosinate ammonium, DuPont) at a concentration of 120µg/ml.

4.4 ChIP, library preparation and sequencing

35S:GRF1-GFP, 35S:GRF3-GFP and 35S:GFP transgenic plants were grown in MS medium with three independent replications per line at 24°C under 16-h-light/8-h-dark conditions. Two-week-old whole plant tissues were harvested from these 9 samples. Proteins were covalently crosslinked to DNA using 1% formaldehyde solution under vacuum for 25 minutes. Nuclei were isolated and lysed, and the chromatin was sheared using focused ultrasonicator (Covaris M220) with the following setting: Duty cycle 10%, intensity peak incident power 75 watt and cycles per burst 200 for 10 minutes. This resulted in chromatin fragments of about 400 bp. Sonicated DNA was immunoprecipitated using 10 µl anti-GFP antibody (5 mg/ml, Abcam). After immunoprecipitation, immune complexes were bound to Protein A agarose beads (GE Healthcare) and washed several times and then eluted in 250 µL elution buffer containing 1% SDS, 0.1M NaHCO3. Then, crosslinking was reversed by adding NaCl (20 ul of 5 M) to the elution and incubating the samples at 65°C overnight. DNA was purified following phenol-chloroform extraction method and finally the DNA was re-suspended in 20 µL of water.

The purified DNA was used for library preparation. ChIP-seq library was prepared using NEBNext Ultra II DNA Library Prep Kit (NEB E7645, Illumina) following manufacturer's instructions. The 9 libraries were barcoded, pooled together, and sequenced using HiSeq 3000 system with 150 bp pair-end reads.

4.5 ChIP-seq data analysis

Quality of the sequenced data was evaluated using FastQC (http://www.bioinformatics.babraham.ac.uk/projects/fastqc/) and the low-quality reads were

trimmed using Trimmomatic (Bolger et al., 2014). Reads were then mapped to the Arabidopsis reference genome (TAIR10) using Bowtie2 (Langmead and Salzberg, 2012). Binding peaks were called using MACS1.4 (Feng et al., 2012). Peak calling was performed separately for each of the three biological replications. Peaks identified in at least two replications were considered for downstream analysis. The RSAT (Regulatory Sequence Analysis Tools) suite was used to identify the cis-binding motifs in the non-redundant binding sites of GRF1 and GRF3 (Thomas-Chollier et al., 2012).

4.6 RNA-seq library preparation

Three independent replications of 35S:GRF1-GFP, 35S:GRF3-GFP, and *grf1grf2grf3* plants were grown in MS plates using a randomized complete-block design. Two weeks after planting, whole plant tissues were collected, frozen in liquid nitrogen and grounded into fine powder. mRNA was isolated from 20 mg tissue using magnetic mRNA isolation kit (NEB) following manufacturer's protocol. RNA-seq libraries were prepared with approximately 250 ng of mRNA using NEBnext mRNA library prep master mix (NEB) following manufacturer's protocol. The 12 RNA-seq libraries were barcoded, pooled together and sequenced using HiSeq 3000 system with 150 bp pair-end reads.

4.7 RNA-seq data analysis

FastQC (http://www.bioinformatics.babraham.ac.uk/projects/fastqc/) was used to determine the quality of the sequencing reads. Low quality reads were trimmed using Trimmomatic (Bolger et al., 2014). After trimming, high quality reads were mapped to the *Arabidopsis* reference genome (TAIR10) using TopHat v2.0.14 (Trapnell et al., 2009). Number of reads mapped uniquely to each annotated Arabidopsis gene were counted using HTSeq (Anders et al., 2015). The count data were normalized and the differentially expressed genes (DEGs) were determined using the R package DESeq2 (Love et al., 2014). A false discovery rate of less than 0.05 was used to identify the DEGs. GO term categorization and enrichment analysis of the DEGs were perfomed using AgriGO database (Du et al., 2010) with Fisher statistical test and Bonferroni adjustment at significance level of 0.05.

References

Abogadallah GM, Nada RM, Malinowski R, Quick P (2011) Overexpression of HARDY, an AP2/ERF gene from Arabidopsis, improves drought and salt tolerance by reducing transpiration and sodium uptake in transgenic *Trifolium alexandrinum* L. Planta **233:** 1265-1276

An L, Zhou Z, Sun L, Yan A, Xi W, Yu N, Cai W, Chen X, Yu H, Schiefelbein J, Gan Y (2012) A zinc finger protein gene ZFP5 integrates phytohormone signaling to control root hair development in Arabidopsis. Plant J **72:** 474-490

Anders S, Pyl PT, Huber W (2015) HTSeq-a Python framework to work with high-throughput sequencing data. Bioinformatics **31:** 166-169

Bai L, Zhang G, Zhou Y, Zhang Z, Wang W, Du Y, Wu Z, Song CP (2009) Plasma membrane-associated proline-rich extensin-like receptor kinase 4, a novel regulator of Ca signalling, is required for abscisic acid responses in *Arabidopsis thaliana*. Plant J **60:** 314-327

Bao M, Bian H, Zha Y, Li F, Sun Y, Bai B, Chen Z, Wang J, Zhu M, Han N (2014) miR396a-mediated basic helix-loop-helix transcription factor bHLH74 repression acts as a regulator for root growth in Arabidopsis seedlings. Plant Cell Physiol **55:** 1343-1353

Bao Z, Zhang N, Hua J (2014) Endopolyploidization and flowering time are antagonistically regulated by checkpoint component MAD1 and immunity modulator MOS1. Nat Commun **5:** 5628

Baucher M, Moussawi J, Vandeputte OM, Monteyne D, Mol A, Perez-Morga D, El Jaziri M (2013) A role for the miR396/GRF network in specification of organ type during flower development, as supported by ectopic expression of *Populus trichocarpa* miR396c in transgenic tobacco. Plant Biol **15:** 892-898

Benjamins R, Barbez E, Ortbauer M, Terpstra I, Lucyshyn D, Moulinier-Anzola J, Khan MA, Leitner J, Malenica N, Butt H, Korbei B, Scheres B, Kleine-Vehn J, Luschnig C (2016) PPP1, a plant-specific regulator of transcription controls Arabidopsis development and PIN expression. Sci Rep **6:** 32196

Birkenbihl RP, Kracher B, Somssich IE (2016) Induced genome-wide binding of three Arabidopsis WRKY transcription factors during early MAMP-triggered immunity. Plant Cell **doi: http://dx.doi.org/10.1105/tpc.16.00681**

Bolger AM, Lohse M, Usadel B (2014) Trimmomatic: a flexible trimmer for Illumina sequence data. Bioinformatics **30:** 2114-2120

Borghi L, Bureau M, Simon R (2007) Arabidopsis JAGGED LATERAL ORGANS is expressed in boundaries and coordinates KNOX and PIN activity. Plant Cell **19:** 1795-1808

Bruex A, Kainkaryam RM, Wieckowski Y, Kang YH, Bernhardt C, Xia Y, Zheng X, Wang JY, Lee MM, Benfey P, Woolf PJ, Schiefelbein J (2012) A gene regulatory network for root epidermis cell differentiation in Arabidopsis. PLoS Genet **8:** e1002446

Bureau M, Simon R (2008) JLO regulates embryo patterning and organ initiation by controlling auxin transport. Plant Signal Behav **3:** 145-147

Campanaro A, Battaglia R, Galbiati M, Sadanandom A, Tonelli C, Conti L (2016) SUMO proteases OTS1 and 2 control filament elongation through a DELLA-dependent mechanism. Plant Reprod **29:** 287-290

Casadevall R, Rodriguez RE, Debernardi JM, Palatnik JF, Casati P (2013) Repression of growth regulating factors by the microRNA396 inhibits cell proliferation by UV-B radiation in Arabidopsis leaves. Plant Cell **25:** 3570-3583

Cecchini NM, Steffes K, Schlappi MR, Gifford AN, Greenberg JT (2015) Arabidopsis AZI1 family proteins mediate signal mobilization for systemic defence priming. Nat Commun **6:** 7658

Chen X, Zhang H, Sun H, Luo H, Zhao L, Dong Z, Yan S, Zhao C, Liu R, Xu C (2016) IRREGULAR POLLEN EXINE1 is a novel factor in anther cuticle and pollen exine formation. Plant Physiol**:** pp. 00629.02016

Choi D, Kim JH, Kende H (2004) Whole genome analysis of the OsGRF gene family encoding plant-specific putative transcription activators in rice (*Oryza sativa* L.). Plant Cell Physiol **45:** 897-904

Choi J, Huh SU, Kojima M, Sakakibara H, Paek KH, Hwang I (2010) The cytokinin-activated transcription factor ARR2 promotes plant immunity via TGA3/NPR1-dependent salicylic acid signaling in Arabidopsis. Dev Cell **19:** 284-295

Clough SJ, Bent AF (1998) Floral dip: a simplified method for Agrobacterium-mediated transformation of *Arabidopsis thaliana*. Plant J **16:** 735-743

Cole M, Chandler J, Weijers D, Jacobs B, Comelli P, Werr W (2009) DORNRÖSCHEN is a direct target of the auxin response factor MONOPTEROS in the Arabidopsis embryo. Development **136:** 1643-1651

Conti L, Price G, O'Donnell E, Schwessinger B, Dominy P, Sadanandom A (2008) Small ubiquitin-like modifier proteases OVERLY TOLERANT TO SALT1 and -2 regulate salt stress responses in Arabidopsis. Plant Cell **20:** 2894-2908

de Almeida Engler J, De Vleesschauwer V, Burssens S, Celenza JL, Inzé D, Van Montagu M, Engler G, Gheysen G (1999) Molecular markers and cell cycle inhibitors show the importance of cell cycle progression in nematode-induced galls and syncytia. Plant Cell **11:** 793-807

de Almeida Engler J, Gheysen G (2013) Nematode-induced endoreduplication in plant host cells: why and how? Mol Plant Microbe Interact **26:** 17-24

de Almeida Engler J, Kyndt T, Vieira P, Van Cappelle E, Boudolf V, Sanchez V, Escobar C, De Veylder L, Engler G, Abad P (2012) CCS52 and DEL1 genes are key components of the endocycle in nematode-induced feeding sites. Plant J **72:** 185-198

Debernardi JM, Mecchia MA, Vercruyssen L, Smaczniak C, Kaufmann K, Inze D, Rodriguez RE, Palatnik JF (2014) Post-transcriptional control of GRF transcription factors by microRNA miR396 and GIF co-activator affects leaf size and longevity. Plant J **79:** 413-426

Ding D, Muthuswamy S, Meier I (2012) Functional interaction between the Arabidopsis orthologs of spindle assembly checkpoint proteins MAD1 and MAD2 and the nucleoporin NUA. Plant Mol Biol **79:** 203-216

Dou XY, Yang KZ, Ma ZX, Chen LQ, Zhang XQ, Bai JR, Ye D (2016) AtTMEM18 plays important roles in pollen tube and vegetative growth in Arabidopsis. J Integr Plant Biol **58:** 679-692

Du J, Huang YP, Xi J, Cao MJ, Ni WS, Chen X, Zhu JK, Oliver DJ, Xiang CB (2008) Functional gene-mining for salt-tolerance genes with the power of Arabidopsis. Plant J **56:** 653-664

Du Z, Zhou X, Ling Y, Zhang Z, Su Z (2010) agriGO: a GO analysis toolkit for the agricultural community. Nucleic acids Res **38:** W64-70

Engler Jde A, Rodiuc N, Smertenko A, Abad P (2010) Plant actin cytoskeleton re-modeling by plant parasitic nematodes. Plant Signal Behav **5:** 213-217

Fan M, Bai MY, Kim JG, Wang TN, Oh E, Chen L, Park CH, Son SH, Kim SK, Mudgett MB, Wang ZY (2014) The bHLH transcription factor HBI1 mediates the trade-off between growth and pathogen-associated molecular pattern-triggered immunity in Arabidopsis. Plant Cell **26:** 828-841

Feng J, Liu T, Qin B, Zhang Y, Liu XS (2012) Identifying ChIP-seq enrichment using MACS. Nat Protoc **7:** 1728-1740

Garcion C, Lohmann A, Lamodiere E, Catinot J, Buchala A, Doermann P, Metraux JP (2008) Characterization and biological function of the ISOCHORISMATE SYNTHASE2 gene of Arabidopsis. Plant Physiol **147:** 1279-1287

Goubet F, Misrahi A, Park SK, Zhang ZN, Twell D, Dupree P (2003) AtCSLA7, a cellulose synthase-like putative glycosyltransferase, is important for pollen tube growth and embryogenesis in Arabidopsis. Plant Physiol **131:** 547-557

He H, Su J, Shu S, Zhang Y, Ao Y, Liu B, Feng D, Wang J, Wang H (2012) Two homologous putative protein tyrosine phosphatases, OsPFA-DSP2 and AtPFA-DSP4, negatively regulate the pathogen response in transgenic plants. Plos One **7:** e34995

Hewezi T, Maier TR, Nettleton D, Baum TJ (2012) The Arabidopsis microRNA396-GRF1/GRF3 regulatory module acts as a developmental regulator in the reprogramming of root cells during cyst nematode infection. Plant Physiol **159:** 321-335

Hoe Kim J, Tsukaya H (2015) Regulation of plant growth and development by the GROWTH-REGULATING FACTOR and GRF-INTERACTING FACTOR duo. J Exp Bot **66:** 6093-6107

Horiguchi G, Kim GT, Tsukaya H (2005) The transcription factor AtGRF5 and the transcription coactivator AN3 regulate cell proliferation in leaf primordia of *Arabidopsis thaliana*. Plant J **43:** 68-78

Huot B, Yao J, Montgomery BL, He SY (2014) Growth–defense tradeoffs in plants: a balancing act to optimize fitness. Mol Plant **7:** 1267-1287

Jin J, Hewezi T, Baum TJ (2011) Arabidopsis peroxidase AtPRX53 influences cell elongation and susceptibility to *Heterodera schachtii*. Plant Signal Behav **6:** 1778-1786

Johnson KC, Xia S, Feng X, Li X (2015) The chromatin remodeler SPLAYED negatively regulates SNC1-mediated immunity. Plant Cell Physiol **56:** 1616-1623

Jones-Rhoades MW, Bartel DP (2004) Computational identification of plant microRNAs and their targets, including a stress-induced miRNA. Mol Cell **14:** 787-799

Kawasaki T, Nam J, Boyes DC, Holt BF, 3rd, Hubert DA, Wiig A, Dangl JL (2005) A duplicated pair of Arabidopsis RING-finger E3 ligases contribute to the RPM1- and RPS2-mediated hypersensitive response. Plant J **44:** 258-270

Kaye Y, Golani Y, Singer Y, Leshem Y, Cohen G, Ercetin M, Gillaspy G, Levine A (2011) Inositol polyphosphate 5-phosphatase7 regulates the production of reactive oxygen species and salt tolerance in Arabidopsis. Plant Physiol **157:** 229-241

Kim J-S, Mizoi J, Kidokoro S, Maruyama K, Nakajima J, Nakashima K, Mitsuda N, Takiguchi Y, Ohme-Takagi M, Kondou Y (2012) Arabidopsis GROWTH-REGULATING FACTOR7 functions as a transcriptional repressor of abscisic acid–and osmotic stress–responsive genes, including DREB2A. Plant Cell **24:** 3393-3405

Kim JH, Choi D, Kende H (2003) The AtGRF family of putative transcription factors is involved in leaf and cotyledon growth in Arabidopsis. Plant J **36:** 94-104

Kim JH, Kende H (2004) A transcriptional coactivator, AtGIF1, is involved in regulating leaf growth and morphology in Arabidopsis. Proc Natl Acad Sci USA **101:** 13374-13379

Kim S-J, Bassham DC (2011) TNO1 is involved in salt tolerance and vacuolar trafficking in Arabidopsis. Plant Physiol **156:** 514-526

Kinoshita N, Berr A, Belin C, Chappuis R, Nishizawa NK, Lopez-Molina L (2010) Identification of growth insensitive to ABA3 (gia3), a recessive mutation affecting ABA Signaling for the control of early post-germination growth in *Arabidopsis thaliana*. Plant Cell Physiol **51:** 239-251

Kuijt SJ, Greco R, Agalou A, Shao J, CJ't Hoen C, Övernäs E, Osnato M, Curiale S, Meynard D, van Gulik R (2014) Interaction between the GROWTH-REGULATING FACTOR and KNOTTED1-LIKE HOMEOBOX families of transcription factors. Plant Physiol **164:** 1952-1966

Kyndt T, Vieira P, Gheysen G, de Almeida-Engler J (2013) Nematode feeding sites: unique organs in plant roots. Planta **238:** 807-818

Langmead B, Salzberg SL (2012) Fast gapped-read alignment with Bowtie 2. Nat Methods **9:** 357-359

Liang G, He H, Li Y, Wang F, Yu D (2014) Molecular mechanism of microRNA396 mediating pistil development in Arabidopsis. Plant Physiol **164:** 249-258

Liu H, Guo S, Xu Y, Li C, Zhang Z, Zhang D, Xu S, Zhang C, Chong K (2014) OsmiR396d-regulated OsGRFs function in floral organogenesis in rice through binding to their targets OsJMJ706 and OsCR4. Plant Physiol **165:** 160-174

Liu J, Rice JH, Chen N, Baum TJ, Hewezi T (2014) Synchronization of developmental processes and defense signaling by growth regulating transcription factors. Plos One **9:** e98477

Love MI, Huber W, Anders S (2014) Moderated estimation of fold change and dispersion for RNA-seq data with DESeq2. Genome Biol **15:** 550

Lozano-Durán R, Zipfel C (2015) Trade-off between growth and immunity: role of brassinosteroids. Trends Plant Sci **20:** 12-19

Millar AA, Gubler F (2005) The Arabidopsis GAMYB-like genes, MYB33 and MYB65, are microRNA-regulated genes that redundantly facilitate anther development. Plant Cell **17:** 705-721

Miyazaki S, Murata T, Sakurai-Ozato N, Kubo M, Demura T, Fukuda H, Hasebe M (2009) ANXUR1 and 2, sister genes to FERONIA/SIRENE, are male factors for coordinated fertilization. Curr Biol **19:** 1327-1331

Nakaune S, Yamada K, Kondo M, Kato T, Tabata S, Nishimura M, Hara-Nishimura I (2005) A vacuolar processing enzyme, δVPE, is involved in seed coat formation at the early stage of seed development. Plant Cell **17:** 876-887

Nawy T, Bayer M, Mravec J, Friml J, Birnbaum KD, Lukowitz W (2010) The GATA factor HANABA TARANU is required to position the proembryo boundary in the early Arabidopsis embryo. Dev Cell **19:** 103-113

Omidbakhshfard MA, Proost S, Fujikura U, Mueller-Roeber B (2015) Growth-regulating factors (GRFs): a small transcription factor family with important functions in plant biology. Mol Plant **8:** 998-1010

Ortega-Amaro MA, Rodriguez-Hernandez AA, Rodriguez-Kessler M, Hernandez-Lucero E, Rosales-Mendoza S, Ibanez-Salazar A, Delgado-Sanchez P, Jimenez-Bremont JF (2014) Overexpression of AtGRDP2, a novel glycine-rich domain protein, accelerates plant growth and improves stress tolerance. Front Plant Sci **5:** 782

Osnato M, Stile MR, Wang Y, Meynard D, Curiale S, Guiderdoni E, Liu Y, Horner DS, Ouwerkerk PB, Pozzi C (2010) Cross talk between the KNOX and ethylene pathways is mediated by intron-binding transcription factors in barley. Plant Physiol **154:** 1616-1632

Pajoro A, Madrigal P, Muino JM, Matus JT, Jin J, Mecchia MA, Debernardi JM, Palatnik JF, Balazadeh S, Arif M, O'Maoileidigh DS, Wellmer F, Krajewski P, Riechmann JL, Angenent GC, Kaufmann K (2014) Dynamics of chromatin accessibility and gene regulation by MADS-domain transcription factors in flower development. Genome Biol **15:** R41

Qi D, Dubiella U, Kim SH, Sloss DI, Dowen RH, Dixon JE, Innes R (2013) Recognition of the protein Kknase PBS1 by the disease resistance protein RPS5 is dependent on S-acylation and an exposed loop in PBS1. Plant Physiol**:** pp. 113.227686

Rast MI, Simon R (2012) Arabidopsis JAGGED LATERAL ORGANS acts with ASYMMETRIC LEAVES2 to coordinate KNOX and PIN expression in shoot and root meristems. Plant Cell **24:** 2917-2933

Rodriguez RE, Mecchia MA, Debernardi JM, Schommer C, Weigel D, Palatnik JF (2010) Control of cell proliferation in *Arabidopsis thaliana* by microRNA miR396. Development **137:** 103-112

Sadanandom A, Adam E, Orosa B, Viczian A, Klose C, Zhang C, Josse EM, Kozma-Bognar L, Nagy F (2015) SUMOylation of phytochrome-B negatively regulates light-induced signaling in Arabidopsis thaliana. Proc Natl Acad Sci USA **112:** 11108-11113

Shinohara H, Mori A, Yasue N, Sumida K, Matsubayashi Y (2016) Identification of three LRR-RKs involved in perception of root meristem growth factor in Arabidopsis. Proc Natl Acad Sci USA **113:** 3897-3902

Sun T, Zhang Y, Li Y, Zhang Q, Ding Y, Zhang Y (2015) ChIP-seq reveals broad roles of SARD1 and CBP60g in regulating plant immunity. Nat Commun **6:** 10159

Szakasits D, Heinen P, Wieczorek K, Hofmann J, Wagner F, Kreil DP, Sykacek P, Grundler FM, Bohlmann H (2009) The transcriptome of syncytia induced by the cyst nematode *Heterodera schachtii* in Arabidopsis roots. Plant J **57:** 771-784

Tenhaken R, Doerks T, Bork P (2005) DCD - a novel plant specific domain in proteins involved in development and programmed cell death. BMC Bioinformatics **6:** 169

Thomas-Chollier M, Herrmann C, Defrance M, Sand O, Thieffry D, van Helden J (2012) RSAT peak-motifs: motif analysis in full-size ChIP-seq datasets. Nucleic acids Res **40:** e31

Trapnell C, Pachter L, Salzberg SL (2009) TopHat: discovering splice junctions with RNA-Seq. Bioinformatics **25:** 1105-1111

van der Knaap E, Kim JH, Kende H (2000) A novel gibberellin-induced gene from rice and its potential regulatory role in stem growth. Plant Physiol **122:** 695-704

Vercruyssen L, Verkest A, Gonzalez N, Heyndrickx KS, Eeckhout D, Han SK, Jegu T, Archacki R, Van Leene J, Andriankaja M, De Bodt S, Abeel T, Coppens F, Dhondt S, De Milde L, Vermeersch M, Maleux K, Gevaert K, Jerzmanowski A, Benhamed M, Wagner D, Vandepoele K, De Jaeger G, Inze D (2014) ANGUSTIFOLIA3 binds to SWI/SNF chromatin remodeling complexes to regulate transcription during Arabidopsis leaf development. Plant Cell **26:** 210-229

Wang W, Xu M, Wang Y, Jamil M (2014) Basal transcription factor 3 plays an important role in seed germination and seedling growth of rice. Biomed Res Int **2014:** 465739

Western TL, Cheng Y, Liu J, Chen X (2002) HUA ENHANCER2, a putative DExH-box RNA helicase, maintains homeotic B and C gene expression in Arabidopsis. Development **129:** 1569-1581

Wu JF, Wang Y, Wu SH (2008) Two new clock proteins, LWD1 and LWD2, regulate Arabidopsis photoperiodic flowering. Plant Physiol **148:** 948-959

Wu MF, Sang Y, Bezhani S, Yamaguchi N, Han SK, Li Z, Su Y, Slewinski TL, Wagner D (2012) SWI2/SNF2 chromatin remodeling ATPases overcome polycomb repression and control floral organ identity with the LEAFY and SEPALLATA3 transcription factors. Proc Natl Acad Sci USA **109:** 3576-3581

Xu J, Ding Z, Vizcay-Barrena G, Shi J, Liang W, Yuan Z, Werck-Reichhart D, Schreiber L, Wilson ZA, Zhang D (2014) ABORTED MICROSPORES acts as a master regulator of pollen wall formation in Arabidopsis. Plant Cell **26:** 1544-1556

Yant L, Mathieu J, Dinh TT, Ott F, Lanz C, Wollmann H, Chen X, Schmid M (2010) Orchestration of the floral transition and floral development in Arabidopsis by the bifunctional transcription factor APETALA2. Plant Cell **22:** 2156-2170

Ye J, Zhang W, Guo Y (2013) Arabidopsis SOS3 plays an important role in salt tolerance by mediating calcium-dependent microfilament reorganization. Plant Cell Rep **32:** 139-148

Zhang B, Van Aken O, Thatcher L, De Clercq I, Duncan O, Law SR, Murcha MW, van der Merwe M, Seifi HS, Carrie C, Cazzonelli C, Radomiljac J, Hofte M, Singh KB, Van Breusegem F, Whelan J (2014) The mitochondrial outer membrane AAA ATPase AtOM66 affects cell death and pathogen resistance in *Arabidopsis thaliana*. Plant J **80:** 709-727

Zhang M, Wang C, Lin Q, Liu A, Wang T, Feng X, Liu J, Han H, Ma Y, Bonea D, Zhao R, Hua X (2015) A tetratricopeptide repeat domain-containing protein SSR1 located in mitochondria is involved in root development and auxin polar transport in Arabidopsis. Plant J **83:** 582-599

Zhang M, Zhang RH, Qu XL, Huang SJ (2016) Arabidopsis FIM5 decorates apical actin filaments and regulates their organization in the pollen tube. J Exp Bot **67:** 3407-3417

Zhang Y, Goritschnig S, Dong X, Li X (2003) A gain-of-function mutation in a plant disease resistance gene leads to constitutive activation of downstream signal transduction pathways in suppressor of npr1-1, constitutive 1. Plant Cell **15:** 2636-2646

Zhao Y, Medrano L, Ohashi K, Fletcher JC, Yu H, Sakai H, Meyerowitz EM (2004) HANABA TARANU is a GATA transcription factor that regulates shoot apical meristem and flower development in Arabidopsis. Plant Cell **16:** 2586-2600

Zhu EG, You CJ, Wang SS, Cui J, Niu BX, Wang YX, Qi J, Ma H, Chang F (2015) The DYT1-interacting proteins bHLH010, bHLH089 and bHLH091 are redundantly required for Arabidopsis anther development and transcriptome. Plant J **83:** 976-990

Appendix

Table 5-1. Numbers of binding peaks and target genes of GRF1 and GRF3

TFs	Binding sites	Binding sites in the promoter	Promoter associated target genes
GRF1	730	369	359
GRF3	1189	539	417

Table 5-2. Occurrence of the identified motifs in GRF1 or GRF3 target genes

Motif	GRF1	GRF3
AAACCCtaa	133	0
aaGAAGAAg	0	226
tACTCGAcc	41	28
AAACCCtaa and tACTCGAcc	152	0
aaGAAGAAg and tACTCGAcc	0	43

Table 5-3. Number of differentially expressed genes identified in GRF1 and GRF3 overexpression lines

	Up-regulated	Down-regulated	Total
GRF1	2124	1888	4012
GRF3	2324	1804	4128

Table 5-4. Selected GRF1 and GRF3 direct target genes associated with cell cycle regulation and cytoskeleton organization.

Gene ID	Gene Name
Cell cycle regulation	
GRF1	
AT3G59550	SYN3
AT2G04660	APC2
AT4G11920	CCS52A2
AT1G80350	ERH3a
AT2G34860	EDA3
AT2G26760	CYCB1;4
AT4G35620	CYCB2;2
AT5G49880	MAD1
GRF3	
AT2G40360	ATPEP1
AT4G11920	CCS52A2
AT4G33260	CDC20.2
AT3G63280	NEK4
AT3G46580	MBD5
Cytoskeleton organization	
GRF1	
AT5G44610	MAP18
AT1G24764	MAP70-2
AT2G31200	ADF6
AT3G32400	Actin-binding FH2
AT5G58160	Actin-binding
GRF3	
AT5G07650	Actin-binding FH2
AT1G80245	Spc97/Spc98

Table 5-5. Selected GRF1 and GRF3 direct target genes associated with different phytohormones. Genes associated with abscisic acid are not included in this table.

Gene ID	Gene Name	Biological function
GRF1		
AT4G38825	SAUR13	Auxin
AT4G31910	BAT1	BR homeostasis
AT4G16110	RR2	Cytokinin regulator
AT4G02680	EOL1	ET biosynthesis
AT1G13280	AOC4	JA biosynthesis
GRF3		
AT3G44310	NIT1	Auxin biosynthesis
AT5G20810	SAUR70	Auxin response
AT1G43950	ARF23	Auxin signaling
AT1G21430	YUCCA11	Auxin response
AT5G08720	PPP1	Regulate PIN1 and PIN2
AT4G31910	BAT1	Brassinosteroids homeostasis
AT4G24650	IPT4	Cytokinin biosynthesis
AT1G18870	ICS2	SA biosynthesis

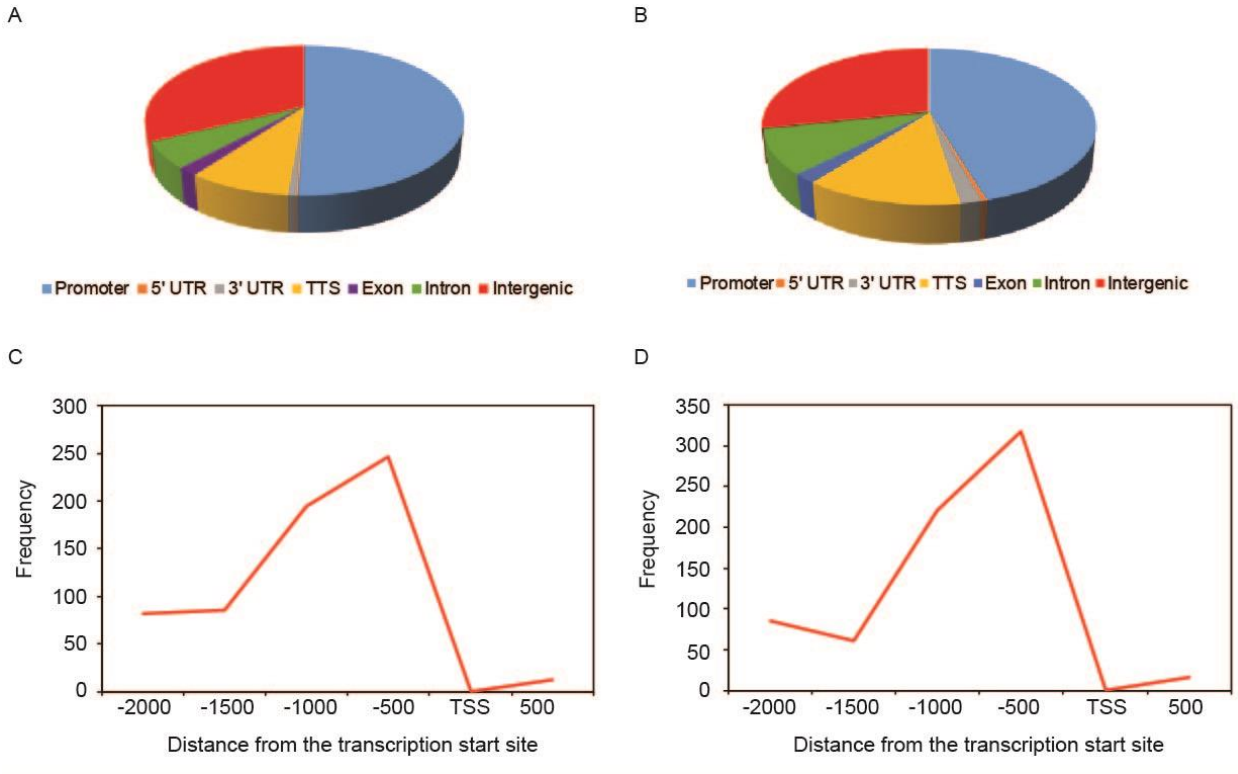

Figure 5-1. Distribution of GRF1 and GRF3 binding sites in the Arabidopsis genome.

Distribution of binding peaks of GRF1 (A) and GRF3 (B) in different annotated genomic features. Frequency of binding peaks of GRF1 (C) and GRF3 (D) in the gene promoters (2kb upstream of transcription start site (TSS).

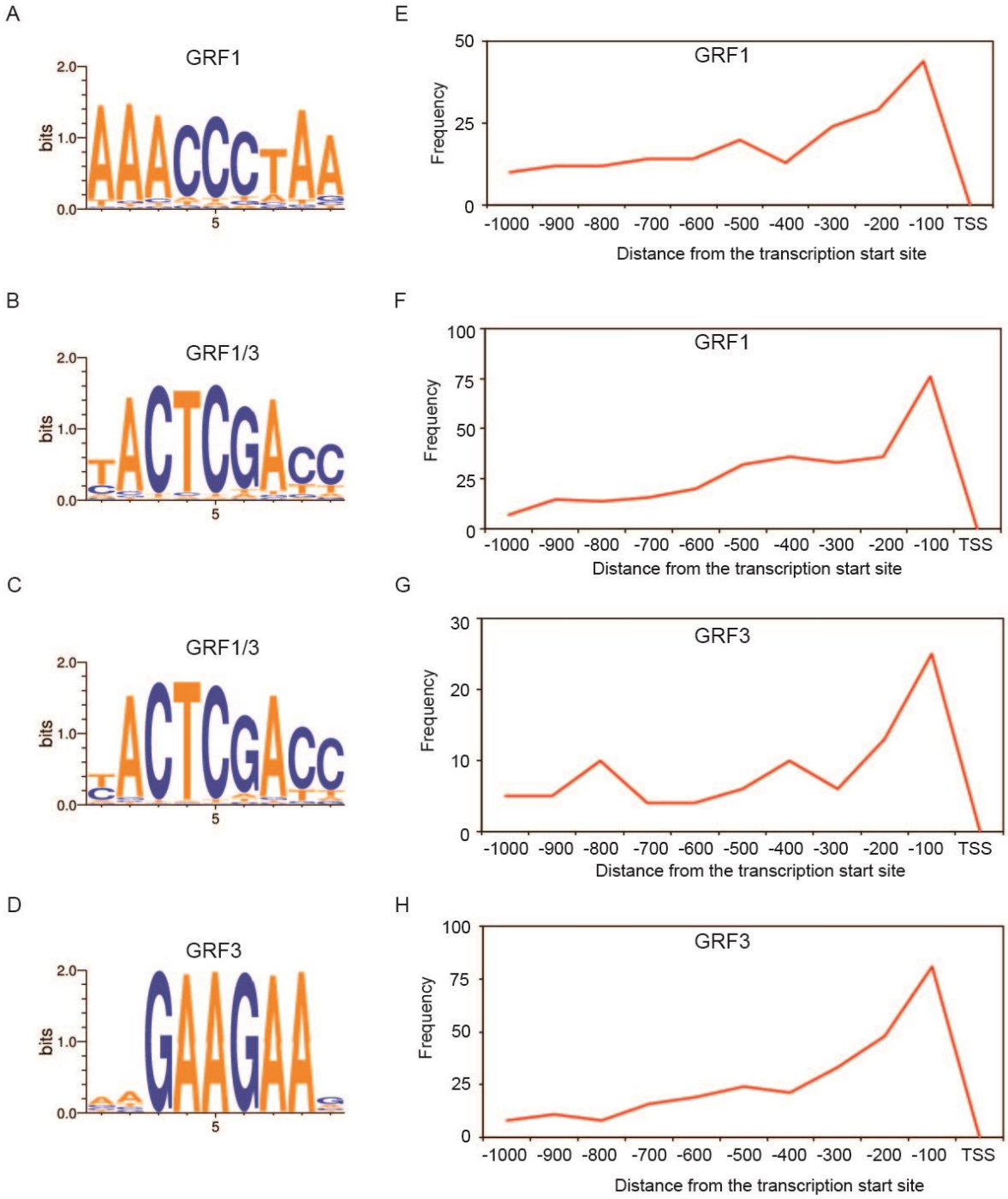

Figure 5-2. Identification of GRF1 and GRF3 binding motifs.

A to D, Sequence logos of the identified GRF1 and GRF3 binding motifs. E to H, frequency of the identified motifs in the gene promoters with respect to the TSS. target genes.

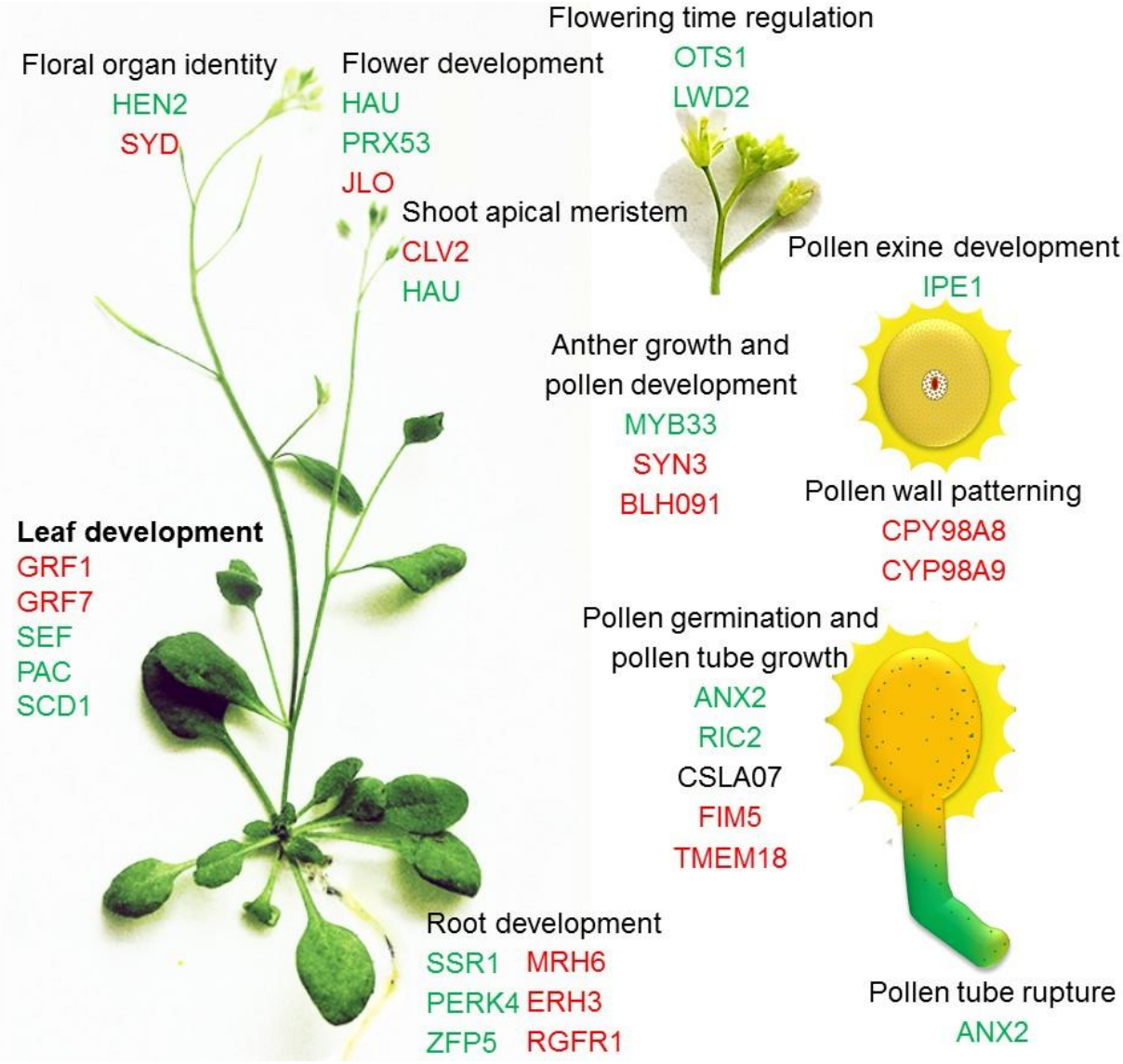

Figure 5-3. Schematic representation of GRF1 and GRF3 targets genes that are associated with various development processes.

Genes highlighed in red and green represent direct target of GRF1 and GRF3, respectively. Genes highlighted in black are direct targets of both GRF1 and GRF3.

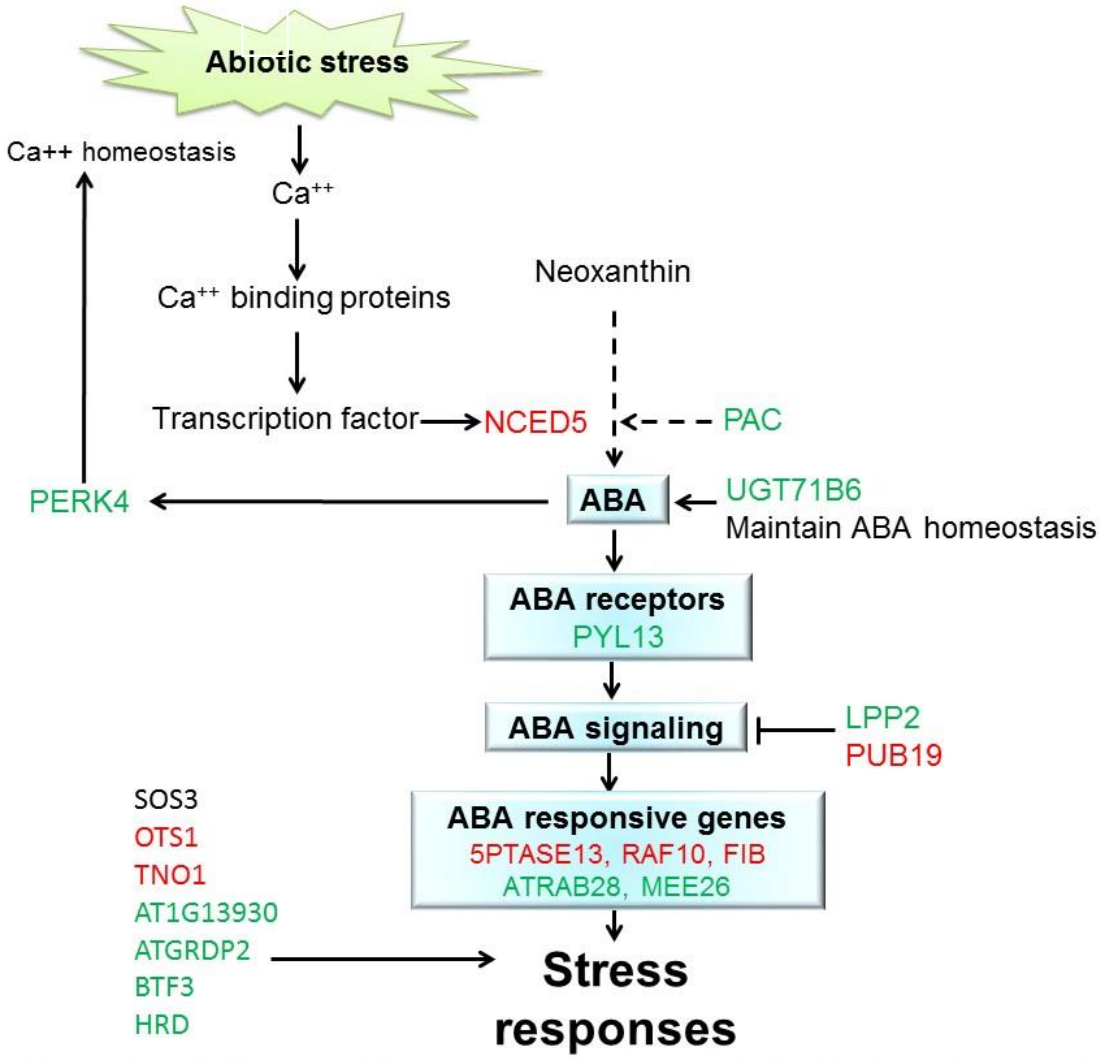

Figure 5-4. Schematic representation of GRF1 and GRF3 target genes that are associated with abscisic acid (ABA) pathway and abiotic stress responses.
GRF1 and GRF3 may regulate abiotic stress through ABA signaling pathways. They also target genes that positively regulate salt tolerance. Genes that are in red and green are the direct target of GRF1 and GRF3 respectively. Genes that are in black is targeted by both GRF1 and GRF3.

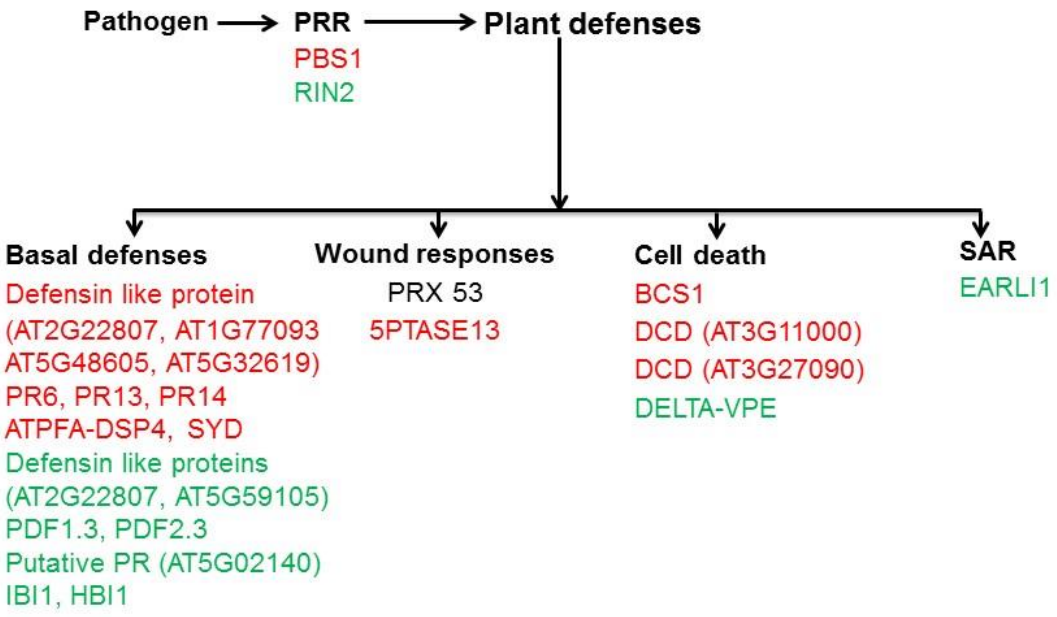

Figure 5-5. Schematic representation of GRF1 and GRF3 target genes that are associated with defense responses.

GRF1 and GRF3 targets genes that are involved in basal defense, wound response, cell death and systemic acquired resistance (SAR). Genes that are in red and green are the direct target of GRF1 and GRF3 respectively. Genes that are in black is targeted by both GRF1 and GRF3.

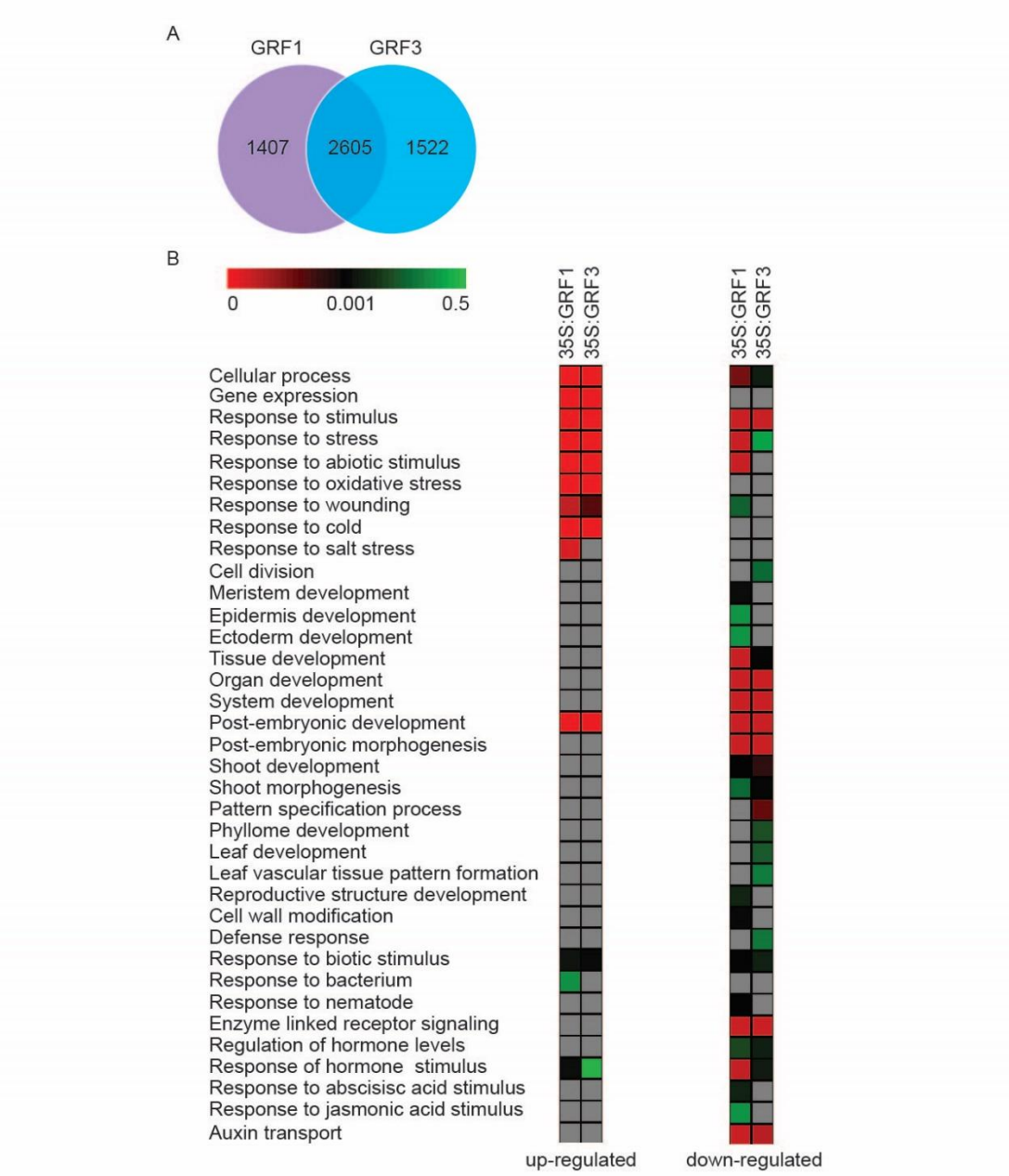

Figure 5-6. Functional classification and gene ontology analysis of the differentially expressed genes (DEGs) identified in GRF1 and GRF3 overexpression lines.

A) Venn diagram showing overlap between the DEGs in GRF1 and GRF3, B, Gene ontology enrichment analysis of up-regulated and down-regulated genes identified in GRF1 and GRF3 overexpression plants.

Chapter 6
Conclusions

Conclusions

Cyst nematodes are one of the most devastating root parasites that induce feeding site known as syncytium. The successful establishment of syncytium determines the compatibility of the interactions between host plants and the nematodes. Therefore, understanding syncytium ontogeny would help exploit the vulnerability of the feeding site to engineer plant resistant to cyst nematodes. There is an accumulating body of evidence pointing into the crucial role of phytohormones particularly auxin and ethylene, and microRNAs in syncytium ontogeny. The aim of this dissertation research was to explore the roles of phytohormones, miR858-MYB83 regulatory module, and miR396–targeted transcription factors GRF1/3 in *H. schachtii* parasitism of Arabidopsis. Previous studies have shown that components of auxin signaling pathway play vital roles in syncytium formation and development. To elucidate the possible interlinks between ARFs and Aux/IAAs in mediating auxin signaling during plant-nematode interaction, we constructed a protein-protein interaction map of 19 ARFs and 29 Aux/IAAs. In addition, we also located the interacting protein pairs to specific gene co-expression networks to define tissue specificity of each interacting Aux/IAA-ARF combination. Altogether, we identified a total of 213 interacting pairs, from which 79 interactions were previously unknown. ARF4-8 and 19 were found to interact with almost all Aux/IAA and formed the central hubs of the co-expression network. These results provide the foundation to further explore the biological importance of ARF-Aux/IAA associations for the morphogenesis and development of various plant tissues and organs including cyst nematode-induced syncytium.

Regarding the ethylene signaling components, we found that ethylene receptor ETR1, and EIN3/EIL1 positively regulate Arabidopsis susceptibility to *H. schachtii.* In spite of being the negative regulator (ETR1) and positive regulators (EIN3 and EIL1) of ethylene signaling, Arabidopsis mutants of ETR1 and EIN3/EIL1 both displayed enhanced resistance to *H. schachtii* suggesting that ETR1 and EIN3/EIL1 regulate Arabidopsis susceptibility to *H. schachtii* using distinct pathways. Our result showed that the receiver domain of ETR1 plays vital role in ETR1-mediated susceptibility to *H. schachtii*, as point mutations in the phosphorylation site and various positions thereafter in the ETR1 receiver domain significantly affected Arabidopsis susceptibility to *H. schachtii*. The receiver domain particularly γ loop and the C-terminal tail are predicted to be involved in protein-protein interactions. Therefore, it can be hypothesized that ETR1 mediates Arabidopsis susceptibility to *H. schachtii* independently of ethylene signaling by interacting with

not yet identified proteins. On the other hand, EIN3/EIL1 was found to negatively regulate the expression of *SID2,* an enzyme that encodes ICS1 that catalyzes salicylic acid biosynthesis, during *H. schachtii* infection of Arabidopsis. In line with this, increased resistance of *ein3-1/eil1* was eliminated from *ein3-1/eil1-1/sid2-2* that showed nematode susceptibility similar to *sid2-2*. This result suggested that EIN3/EIL1 mediate Arabidopsis susceptibility to *H. schachtii* via SID2, an enzyme that catalyze biosynthesis of salicylic acid. Quantification of various PR genes showed enhanced expression of PR1 in the mutant of EIN3/EIL1 under *H. schachtii* infected but no change in PR1 expression was observed in SID2 or triple mutant of EIN3, EIL1 and SID2. This result suggested that enhanced expression of salicylic acid-induced *PR1* is responsible for enhanced resistance of *ein3-1/eil1-1* to *H. schachtii*. This result also suggests a crosstalk between ethylene and salicylic acid during Arabidopsis-*H. schachtii* interactions.

During syncytium formation, infected root cells undergo massive transcriptome reprograming that guides these cells into specific cell fate. In this context, miRNA genes have been shown to play key regulatory roles. In this study, the potential regulatory roles of miR858/MYB83 module and the miR396-targeted genes GRF1 and GRF3 transcription factors in syncytium development and nematode parasitism were explored. Promoter activity assays and gene expression analyses revealed a role of miR858 in post-transcriptional regulation of MYB83 during *H. schachtii* infection. Manipulating the expression of miR858 and MYB83 through gain- and loss-of-function approaches significantly altered Arabidopsis response to nematode infection. RNA-seq analysis of miR858 and MYB83 overexpression plants revealed that genes that impact syncytium initiation and development such as those related to plant defense, cell wall biosynthesis, sugar transport, phytohormone signaling were regulated. We also found that miR858-mediated silencing of MYB83 is tightly regulated through a feedback loop that is likely to be important for fine-tuning the expression levels of MYB83-regulated genes in the *H. schachtii*–induced syncytium.

Previously, GRF1 and GRF3 have been demonstrated to regulate unexceptionally higher number of genes that are differentially expressed in the syncytium. In this study, we identified genome-wide binding sites of GRF1 and GRF3 using ChIP-seq approach. We discovered unique and common cis-binding motifs for GRF1 and GRF3 and revealed the underlying mechanism for their functional redundancy. Consistent with this finding we found significant overlaps between the direct targets of GRF1 and GRF3 as well as the differentially expressed genes. The direct

targets of GRF1 and GRF3 were associated with various developmental processes such as embryogenesis, floral organ identity, flower development, flowering time regulation, root development etc. In addition, we also observed that these two transcription factors bind to the promoter of various abiotic stress related genes. Remarkably, we found that GRF1 and GRF3 directly target genes associated cellular processes and molecular functions that play key roles in the development of cyst nematode-induced syncytium, including cycle regulation, cytoskeleton organization, phytohormone biosynthesis and signaling, and defense responses. Our results also point to a role of GRF1/3 in mediating the balance between plant growth and development.

In short, the findings of this dissertation provide new insights into the role of phytohormones and microRNA in Arabidopsis-*H. schachtii* interaction. While the results of this thesis contribute to advance our understanding of the molecular mechanisms controlling nematode parasitism of host plants, this study also identified several potential avenues to engineer nematode-resistant crops. ETR1 plays vital role in regulating plant susceptibility to various plant pathogens including cyst nematodes. We have identified that point mutations in the specific sites of the ETR1 receiver domain can enhance plant resistance to cyst nematode. Identification of these sites in the ETR1 receiver domain of other crop plants and introducing site specific mutations in crop plants by using CRISPR-CAS9 system, for example, will be useful in generating nematode-resistant genotypes. Nowadays, plant scientists are effectively using RNA interference technology involving miRNA to engineer superior crop plants by manipulating desirable and undesirable genes. In this context, we have identified that miR858 is a positive regulator of plant resistance to cyst nematode. miRNAs are evolutionary conserved across monocot and eudicot plants. Therefore, miR858 can be targeted for engineering cyst-nematode resistant plants. Our results indicate that GRF1 and GRF3 may mediate the balance between plant growth and defense response. This finding is of great importance for developing strategies to enhance plant growth and defense simultaneously. For example, tissue-specific manipulation of GRF1/3 in roots to prioritize defense over development to generate plants resistant to cyst nematodes without affecting aboveground plant development. In addition, our ARF-Aux/IAA co-expression network reveals tissue specificity of interacting ARF-Aux/IAA proteins that will be useful to explore the biological significance of ARF-Aux/IAA associations in plant morphogenesis and development.

Vita

The author was born on July 1983 as the son of Mr. Jagannath Piya and Mrs. Jaumaya Piya in Bandipur-6 Tanahun, Nepal. He obtained his Bachelor Degree in Agricultural Science majoring in Plant Breeding from Tribhuvan University, Institute of Agriculture and Animal Science, Rampur, Chitwan in 2007 and obtained his Master degree from South Dakota State University in Biology in 2013. He started his Doctor of Philosophy program in the Department of Plant Sciences at the University of Tennessee, Knoxville, under the direction of Dr. Tarek Hewezi in spring 2014. His dissertation research focused on understanding the role of hormonal and signaling pathways in plant-cyst nematode interaction.

For this dissertation research, he was financially supported by University of Tennessee, Institute of Agriculture (UTIA) and National Science Foundation (Award #: 1145053).